Investigation on [*S*,*S*]-EDDS biosynthesis and its applications

Investigation on [*S,S*]-EDDS biosynthesis and its applications

Dissertation

der Mathematisch-Naturwissenschaftlichen Fakultät

der Eberhard Karls Universität Tübingen

zur Erlangung des Grades eines

Doktors der Naturwissenschaften

(Dr. rer. nat.)

vorgelegt von

Naybel Hernández Pérez

aus Havanna, Kuba

Tübingen

2023

Gedruckt mit Genehmigung der Mathematisch-Naturwissenschaftlichen Fakultät der Eberhard Karls Universität Tübingen

Tag der mündlichen Qualifikation:	20.06.2023
Dekan:	Prof. Dr. Thilo Stehle
1. Berichterstatter:	Apl. Prof. Dr. Evi Stegmann
2. Berichterstatter:	Prof. Dr. Wolfgang Wohlleben

Acknowledgments

I would like to express my deepest gratitude to the individuals who have played an important role in making this thesis possible. First of all, I would like to thank my first supervisor, Evi Stegmann, for her invaluable guidance and support throughout my entire PhD journey. I am truly fortunate to have received such exceptional supervision, I simply could not have asked for better supervision and support than I have received over the past few years. I would also like to extend my sincere thanks to my second supervisor, Wolfgang Wohlleben, for his unwavering support and remarkable expertise. His guidance has enabled me to critically evaluate my work. I am grateful for the opportunity to learn from him and benefit from his wealth of knowledge.

I consider myself incredibly fortunate to have pursued a doctoral degree at the University of Tübingen. The Stegmann Lab, in particular, has provided an exceptional working environment, and I am grateful for the invaluable experiences and opportunities it has afforded me.

I would also like to express my gratitude to the GRK 1708: "Molecular Principles of Bacterial Survival Strategies" for their financial support, which has been instrumental in the realization of this research.

I am very thankful to all the people who have been part of this journey. To Dardan, Elisa, Erik, Sehee, Alena, Jens, Demi and Sigrid, I extend my deepest appreciation for being exceptional coworkers. They have created a vibrant and inspiring atmosphere in the lab, which has greatly contributed to my growth and success. I would also like to thank my students, Leonie, Laura, Nico, and Luca, for their valuable assistance in conducting various experiments. Their commitment and contributions have been invaluable to the overall outcomes of this research.

I am also grateful to my cooperation partners, Sandra Lopez Rayo from the Autonome University of Madrid, Daniel Petras, and Chambers Hughes, for their successful teamwork. Their collaboration has enriched this work.

Special appreciation goes to Andi for his assistance with the HPLC analysis and all the discussions we have had. I would also like to express my gratitude to Günter for generously sharing his time, knowledge, and insights during our discussions on important experiments. To our dedicated secretary, Aysun, I extend my biggest thanks for her unwavering support and exceptional organizational skills. Her contribution has been invaluable in managing crucial tasks. I am also grateful to Thomas Härtner for his prompt and reliable assistance whenever I needed it.

To my friends, I extend my deepest gratitude for their support and help throughout this journey. Their encouragement and companionship have made the challenges more manageable and the successes more meaningful.

Of course, this thesis would not have been possible without the love and support of my family. I want to thank my mother-in-law, Ina, and her husband, Norbert, for making it possible for me to come to Germany and pursue my PhD. To my father-in-law, Uli, and his wife, Ingrid, I am grateful for their unwavering support. Special thanks go to my mother, Moraima, and my sister Noalys, for being my pillars of strength, providing unconditional love and support. Without them, I would not have been able to embark on this journey in Germany. Last but certainly not least, I want to express my deepest thanks to my husband, Jonas, for his extensive support, unwavering belief in me, and for always pushing me to be strong. His love and constant presence in my life have been a constant source of inspiration and motivation.

To all of you, thank you.

Contents

Abbreviations

A.	*Amycolatopsis*
ABC	ATP-binding cassette
APCA	aminopolycarboxylic acid
EDDS	ethylendiaminedisuccinic acid
EDTA	ethylendiaminetetraacetic acid
NAD^+/ NADH	nicotinamide adenine dinucleotide
$NADP^+$/NADPH	nicotinamide adenine dinucleotide phosphate
Pi	inorganic phosphate
HPLC	high performance liquid chromatography
L-DAPP	L-diaminopropionic acid
Zur	zinc uptake regulator
E.	*Escherichia*
PCR	Polymerase chain reaction
S. aureaus	Staphylococcus aureus
E. coli	*Escherichia coli*
LC-MS	Liquid chromatography and tandem mass spectrometry
NCBI	National Center for Biotechnology Information
Ni-NTA	Nickel-nitrilotriacetic acid
OD	Optical density
WT	wild type
Fmoc-Cl	9-fuorenylmethyl chloroformate

Zusammenfassung

Zink ist ein essentielles Spurenelement für Bakterien und spielt eine wichtige Rolle bei vielen physiologischen Prozessen, einschließlich der DNA-Replikation und des Stoffwechsels. Bakterien haben verschiedene Mechanismen entwickelt, um Zink aus der Umwelt zu gewinnen, z. B. durch die Produktion von Zinkophoren. Ein Beispiel ist das Zinkophor [*S,S*]-EDDS, das von *Amycolatopsis japonicum* produziert wird. [*S,S*]-EDDS ist ein Isomer des in der Industrie häufig genutzten Ethylendiamintetraacetats (EDTA). Im Gegensatz zu EDTA ist [*S,S*]-EDDS jedoch biologisch abbaubar, was es zu einer vielversprechenden Alternative mit einem günstigen Umweltprofil macht. Neben der Anwendung in verschiedenen industriellen Prozessen, ist [*S,S*]-EDDS auch für die Landwirtschaft interessant. Diese beiden Aspekte wurden in der vorliegenden Arbeit untersucht.

(i) [*S,S*]-EDDS hat seine Wirksamkeit als Fe^{2+}- und Zn^{2+}- Düngemittel gezeigt, aber seine kurze Abbauzeit begrenzt seine langfristige Wirkung. Ein vielversprechender Ansatz zur Überwindung dieser Einschränkung ist die Verwendung des [*S,S*]-EDDS-Produzenten *A. japonicum* als Biodünger. Eine kontinuierliche Produktion von [*S,S*]-EDDS im Boden würde die wiederholte Ausbringung von [*S,S*]-EDDS überflüssig machen. Versuche mit *Phaseolus vulgaris* cv. Black pole auf kalkhaltigem Boden zeigten jedoch, dass *A. japonicum* nicht zu einer Verbesserung des Pflanzenwachstums oder der Spurenelementkonzentration führte.

(ii) Für den Einsatz von [*S,S*]-EDDS als Chelatbildner in verschiedenen industriellen Anwendungen muss die Ausbeute an [*S,S*]-EDDS in *A. japonicum* verbessert werden. Eine Voraussetzung dafür ist das Verständnis der Biosynthese von [*S,S*]-EDDS. Mit Hilfe eines breiten Methodenspektrums (biochemische, genetische und Markierungsstudien) konnte bestätigt werden, dass L-Asparaginsäure und Oxalessigsäure Vorstufen der [*S,S*]-EDDS-Biosynthese sind. Darüber hinaus wurde ((S)-2-Amino-2-Carboxyethyl)-L-Asparaginsäure (ACEAA) erstmals als Biosynthese-Zwischenprodukt identifiziert. Weiterhin konnte gezeigt werden, dass die

zuvor vermutete Vorstufe L-Diaminopropionsäure (L-DAPP) nicht an der Biosynthese beteiligt ist, was auf einen neuen Weg der [*S,S*]-EDDS-Biosynthese hinweist. Zur weiteren Optimierung der [*S,S*]-EDDS-Ausbeute wurden genetische Strategien eingesetzt, um den Stoffwechselfluss auf die gewünschten Metaboliten umzulenken. Zur Priorisierung der Zielgene für das Metabolic Engineering wurde das Bioinformatik-Tool Secondary Metabolite Transcriptomic Pipeline (Sema-Trap) zur Sequenzbasierten Transkriptomanalyse eingesetzt. Dabei wurden $bldC_{\mathrm{Aj}}$, $lacI_{\mathrm{Aj}}$ und $glts_{\mathrm{Aj}}$ als Zielgene für das Engineering in *A. japonicum* identifiziert. Die Überexpression dieser Gene führte zu einer 3-fachen Erhöhung der [*S,S*]-EDDS-Produktion im Vergleich zum *A. japonicum* Wildtyp. Zusammengenommen bieten diese Ergebnisse Potential für weitere Schritte bei der Optimierung der [*S,S*]-EDDS-Produktion.

Summary

Zinc is a crucial trace element for bacteria and plays an essential role in several physiological processes, including DNA replication and metabolism. Bacteria have evolved various mechanisms to acquire zinc from the environment, such as the production of zincophores. One example is the zincophore [*S,S*]-EDDS produced by *Amycolatopsis japonicum*. [*S,S*]-EDDS is an isomer of ethylenediamine tetraacetate (EDTA), which is widely used in industry. However, unlike EDTA, [*S,S*]-EDDS is biodegradable, making it a promising alternative with a favorable environmental profile. Besides its application in various industrial processes, [*S,S*]-EDDS is also interesting for agriculture. These two aspects were investigated in the present work.

(i) [*S,S*]-EDDS has demonstrated efficacy as a Fe^{2+} and Zn^{2+} fertilizer, but its short degradation time limits its long-term impact. To overcome this limitation, a promising approach is to use the [*S,S*]-EDDS producer *A. japonicum* as a biofertilizer. Continuous production of [*S,S*]-EDDS would avoid the need for multiple applications of [*S,S*]-EDDS. The experiments carried out with *Phaseolus vulgaris* cv. Black pole in calcareous soil showed that the use of *A. japonicum* as a biofertilizer, however, did not lead to any improvement in plant growth or microelement concentration.

(ii) For the use of [*S,S*]-EDDS as a chelating agent in various industrial applications, the yield of [*S,S*]-EDDS in *A. japonicum* needs to be improved. A prerequisite for this is the understanding of the biosynthesis of [*S,S*]-EDDS. Using a wide range of methods (biochemistry, genetics, and labeling studies) it was confirmed that L-aspartic acid and oxaloacetic acid are precursors for [*S,S*]-EDDS biosynthesis. In addition, ((S)-2-amino-2-carboxyethyl)-L-aspartic acid (ACEAA) was identified for the first time as a biosynthetic intermediate. Furthermore, the results strongly indicated that the previously proposed precursor, L-diaminopropionic acid (L-DAPP), is not involved in the biosynthesis, suggesting a novel biosynthetic

pathway for [*S,S*]-EDDS. Genetic strategies were used to redirect the metabolic flux towards the desired metabolites to further optimize [S,S]-EDDS yields. To prioritize target genes for metabolic engineering, the bioinformatic tool Secondary Metabolite Transcriptomic Pipeline (Sema-Trap) was used for RNA-Seq-based transcriptome analysis. This identified $bldC_{\mathrm{Aj}}$, $lacI_{\mathrm{Aj}}$ and $glts_{\mathrm{Aj}}$ as target genes for engineering in *A. japonicum*. Overexpression of these genes resulted in a 3-fold increase in [*S,S*]-EDDS production compared to *A. japonicum* wild type. Taken together, these findings provide the potential for further progress in optimizing [*S,S*]-EDDS production.

List of Tables

List of Figures

Chapter 1

Introduction

1.1 The genus *Amycolatopsis*: A source for natural products with promising future

In 1986, the genus *Amycolatopsis* was officially recognized as a distinct group of nocardioform actinomycetes, with distinctive cell chemistry characteristics such as a type IV cell wall composition and the absence of mycolic acids (Lechevalier *et al.*, 1986). Currently (accessed on April 2023), the genus comprises 98 verified species and 5 subspecies (Parte *et al.*, 2020). *Amycolatopsis* has demonstrated exceptional versatility and utility in a wide range of industrial applications. Several species have exhibited tremendous potential for degrading the commonly used broad-spectrum herbicide ZJ0273 (Cai *et al.*, 2012), plastics such as poly(β-hydroxybutyrate)(PHB) and poly(e-caprolactone)(PCL) (Nishida and Tokiwa, 1993) and polylactic acid (PLA) (Pranamuda *et al.*, 1997). Additionally, *Amycolatopsis* has been found to be effective in heavy metal treatment (Albarracín *et al.*, 2008) and bioconversion, with examples including the production of wuxistatin and vanillin (Zhuge *et al.*, 2008)(Fleige *et al.*, 2013).

Bacteria of this genus have adapted to a wide range of environments. They exist in different soils in the presence of insects, lichens, plants, sponges, and marine sediments. They produce various secondary metabolites for their own benefit. Antibiotics produced by *Amycolatopsis* include vancomycin (McCormick *et al.*, 1955) and rifamycin (Sensi *et al.*, 1959), both having a long history of clinical use. This genus also produces several siderophores, natural products that act as high-affinity ferric iron chelators (Neilands, 1995). The siderophores include amychelin (Seyedsayamdost *et al.*, 2011), albachelin (Kodani *et al.*, 2015) and albisporachelin

(Wu *et al.*, 2018).

Amycolatopsis japonicum MG417-CF17, originally named *Amycolatopsis orientalis* (Goodfellow *et al.*, 1997) was not known to produce antimicrobial compounds for a long time. The strain's potential to produce various secondary metabolites was discovered through genome sequencing and bioinformatic analysis such as antiSMASH (Blin *et al.*, 2013). By constitutively expressing a pathway-specific regulator, the biosynthetic gene cluster (BGC) encoding the synthesis of the glycopeptide antibiotic ristomycin A was activated (Spohn *et al.*, 2014). Ristomycin A is used in the diagnosis of von Willenbrand syndrome. *A. japonicum* was also found to produce the polyene ECO-0501. ECO-0501 is biologically active against Gram-positive bacteria. The strain is also capable of synthesizing the siderophore amycolachrome (Cebulla, 1995). One of the promising compounds synthesized by *A. japonicum* is the aminopolycarboxylic acid (APCA) ethylenediamine-succinic acid ([*S,S*]-EDDS).

[*S,S*]-EDDS biosynthesis in *A. japonicum*

[*S,S*]-EDDS was first discovered as a natural product of *A. japonicum* in 1984 during a screening for phospholipase C inhibitors (Nishikiori *et al.*, 1984). It is an inhibitor of phospholipase C through the formation of complexes with zinc ions, a co-factor for the enzyme (Hough *et al.*, 1989). The synthesis of [S,S]-EDDS in *A. japonicum* is strongly inhibited by even trace amounts of zinc (Cebulla, 1995; Zwicker *et al.*, 1997; Spohn *et al.*, 2016). Therefore, in analogy to siderophores, which are only synthesized under iron-deficient conditions, it is suggested that *A. japonicum* uses [*S,S*]-EDDS as a zincophore to fulfil its Zn^{2+} requirements (Cebulla, 1995; Hantke, 2001). It is produced exclusively in the [*S,S*]-configuration (Nishikiori *et al.*, 1984). The production of [*S,S*]-EDDS has also been identified in other *Amycolatopsis* strains, including *Amycolatopsis lurida*, *Amycolatopsis decaplaina* and *Amycolatopsis alba*, suggesting that the ability to tolerate zinc deficiency by producing [*S,S*]-EDDS is likely an evolutionary adaptation in certain *Amycolatopsis* species (Spohn *et al.*, 2016)

Identifying the biosynthetic genes was achieved by exploiting the knowledge of zinc regulation of [*S,S*]-EDDS production (Spohn *et al.*, 2016). Since the global zinc uptake regulator (Zur) was known to control zinc uptake functions and zin-

cophore biosynthesis genes in several other bacteria, Spohn et al. searched for a global zinc uptake regulator in the *A. japonicum* genome, suggesting that this regulator causes zinc inhibition of [*S,S*]-EDDS production. Zur_{Aja}, a homologue of Zur regulators known from e.g. *Streptomyces coelicolor, Corynebacterium glutamicum* or *M. tuberculosis*, was identified. The *A. japonicum* genome was then screened for a DNA-binding motif of Zur_{Aja}. Among others, a Zur_{Aja} binding motif was found in the operon structure of *aesA-D*. Deletion of these genes confirmed their involvement in [*S,S*]-EDDS production (Spohn *et al.*, 2016). Specifically, *aesA-C* encode for enzymes involved in the biosynthesis of [*S,S*]-EDDS, while aesD encodes for a putative exporter (Spohn *et al.*, 2016). Notably, the assembly mechanism of [*S,S*]-EDDS remains distinct from the well-known Nonribosomal peptides (NRPS) or NRPS-independent siderophore (NIS) pathways known to catalyze ionophore synthesis.

Previous studies using stable isotope labeled L-aspartic acid (DL-4-^{13}C aspartic acid) demonstrated the incorporation of this amino acid into [S,S]-EDDS (Cebulla, 1995). Based on this result, a putative pathway for the biosynthesis of [*S,S*]-EDDS was postulated (Cebulla, 1995). The non-proteogenic amino acid L-diaminopropionic acid (L-DAPP) and L-serine were proposed as putative biosynthetic precursors. According to this pathway, either L-aspartate and L-serine with pyridoxal phosphate as a cofactor (pathway II) or 2,3- diaminopropionate and oxaloacetic acid (pathway I) undergo a reaction to form intermediate IM 1. Decarboxylation then occurs, leading to the formation of intermediate IM 2, followed by the addition of a molecule of oxaloacetic acid (OAA) to form the intermediate IM 3. Finally, reduction of the double bond results in the production formation of the final product [*S,S*]-EDDS (Cebulla, 1995) (Figure 1.1).

Based on the similarity of AesA-D to the staphyloferrin B biosynthetic proteins, a different biosynthetic pathway was postulated. In this hypothetical pathway, AesA and AesC use aspartic acid as amino donor to convert *O*-phosphoserine to L-DAPP, and OAA and L-DAPP are assembled through an unknown mechanism to form an imine intermediate. AesB is suggested to catalyze the next decarboxylation of the OAA-DAPP imine intermediate, leading to the formation of the diaminoethylene (Dae) moiety. Finally, a carbonyl reaction of the Dae-intermediate with a second OAA molecule, coupled with a reduction of the two double bonds, could lead to the functional [*S,S*]-EDDS (Spohn *et al.*, 2016) (Figure 1.2). To determine whether *O*-phosphoserine played a role in the biosynthetic pathway, addi-

tional investigations were carried out. In a recent study, a combination of gene deletion experiments and genetic engineering approaches led to the demonstration that *O*-phosphoserine was indeed a biosynthetic precursor (Edenhart *et al.*, 2020).

In both postulated pathways (Figure 1.1, 1.2), L-DAPP is considered as a putative precursor. L-DAPP is an intermediate in the biosynthesis of several secondary metabolites such as: viomycin, zwittermicin, capreomycin and poly (DL-diaminopropionic acid) (PDAP). In these cases, it is synthesized from L-ornithine and L-serine/*O*-acetylserine (Carter *et al.*, 1974) (Zhao *et al.*, 2008), (Xu *et al.*, 2015). L-DAPP is also a precursor required for the biosynthesis of staphyloferrin B, but in this case, it is synthesized from L-glutamic acid and *O*-phosphoserine (Beasley *et al.*, 2011).

An alternative biosynthetic pathway for [*S,S*]-EDDS has been proposed by (Wang *et al.*, 2022) (Figure 1.3), which involves a simplified three-step process. First, AesC catalyzes the formation of the first C-N bond by reacting L-aspartic acid with *O*-phosphoserine to produce 2-amino-2-carboxyethyl aspartic acid (ACEAA). Next, AesB decarboxylates ACEAA to produce the intermediate aminoethyl aspartic acid (AEAA). Finally, AesA catalyzes the formation of the second C-N bond to synthesize [*S,S*]-EDDS. Notably, this pathway does not involve L-DAPP as a precursor and proposes that there is a connection between the biosynthesis and degradation of [*S,S*]-EDDS, since it has been reported that microorganisms can degrade [*S,S*]-EDDS via an EDDS lyase, which produces AEAA as an intermediate (Poddar *et al.*, 2018). To date, experimental evidence has only confirmed the involvement of L-aspartic acid and *O*-phosphoserine as precursors in the [*S,S*]-EDDS biosynthetic pathway. However, none of the proposed hypothetical pathways have been conclusively established, as no intermediates have been identified, and there have been no successful attempts to reconstitute the pathway *in vitro*.

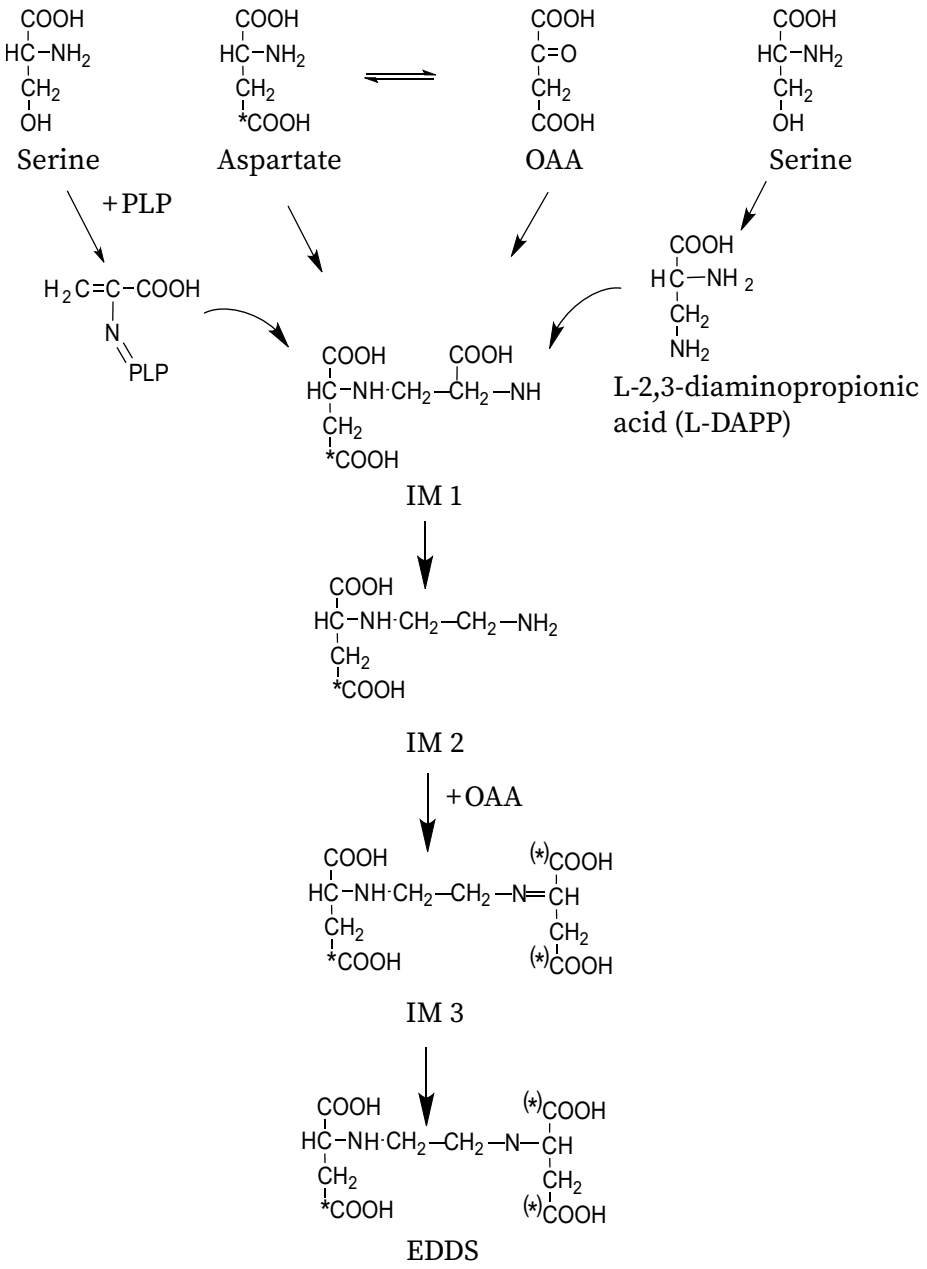

Figure 1.1. **[*S,S*]-EDDS biosynthetic pathway proposed by (Cebulla, 1995)**. IM: intermediate, OAA: oxaloacetic acid, PLP: pyridoxalphosphate, (*): ^{13}C labeling.

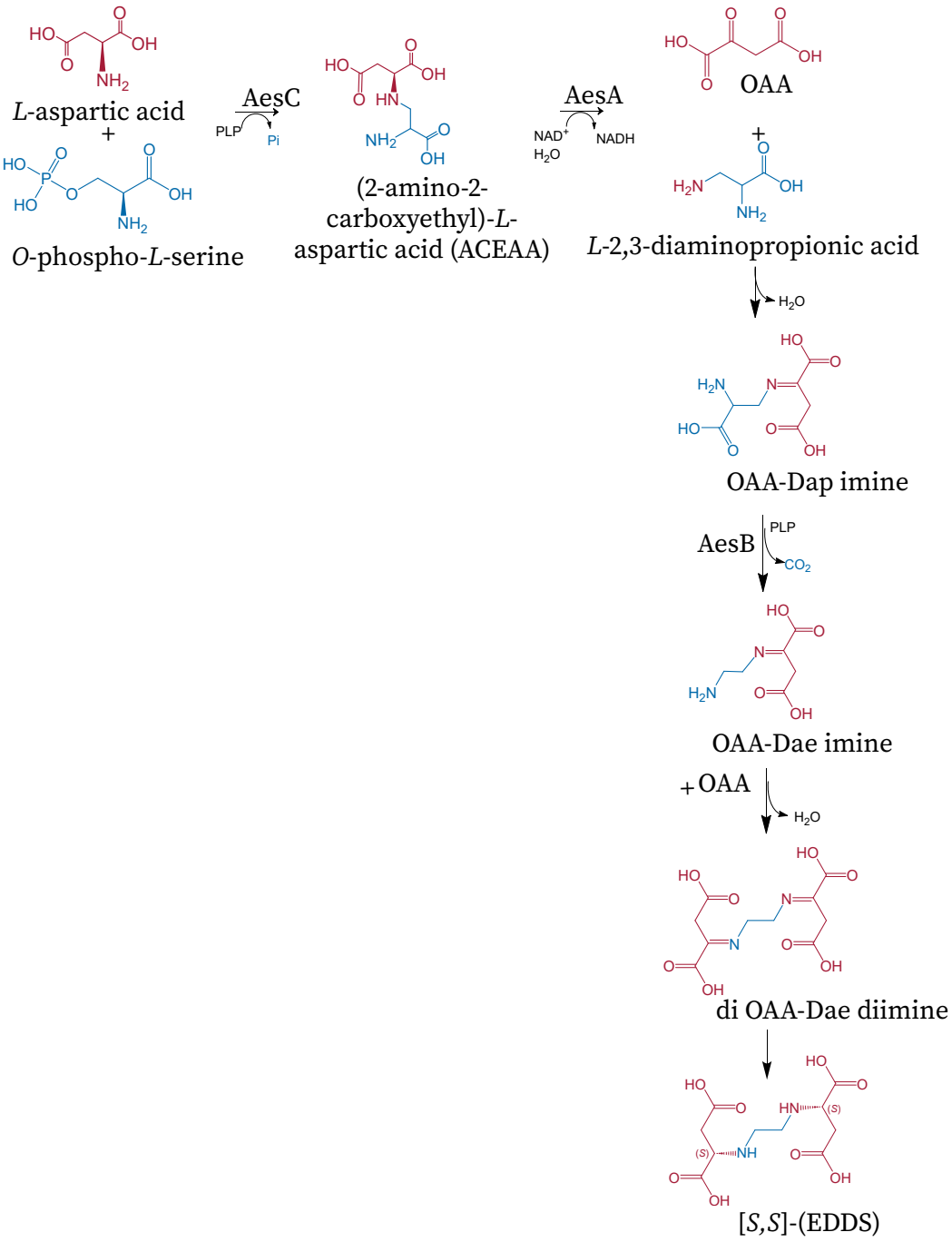

Figure 1.2. **[*S,S*]-EDDS biosynthetic pathway proposed by (Spohn *et al.*, 2016)** OAA: oxal acetic acid; Dae: diaminoethylene; AesA: putative ornithinine cyclodeaminase (Nicotinamide adenine dinucleotide (NAD^+) depending reaction; AesB: putative amino acid decarboxylase; AesC: putative cysteine synthase pyridoxalphosphate (PLP) depending reaction.

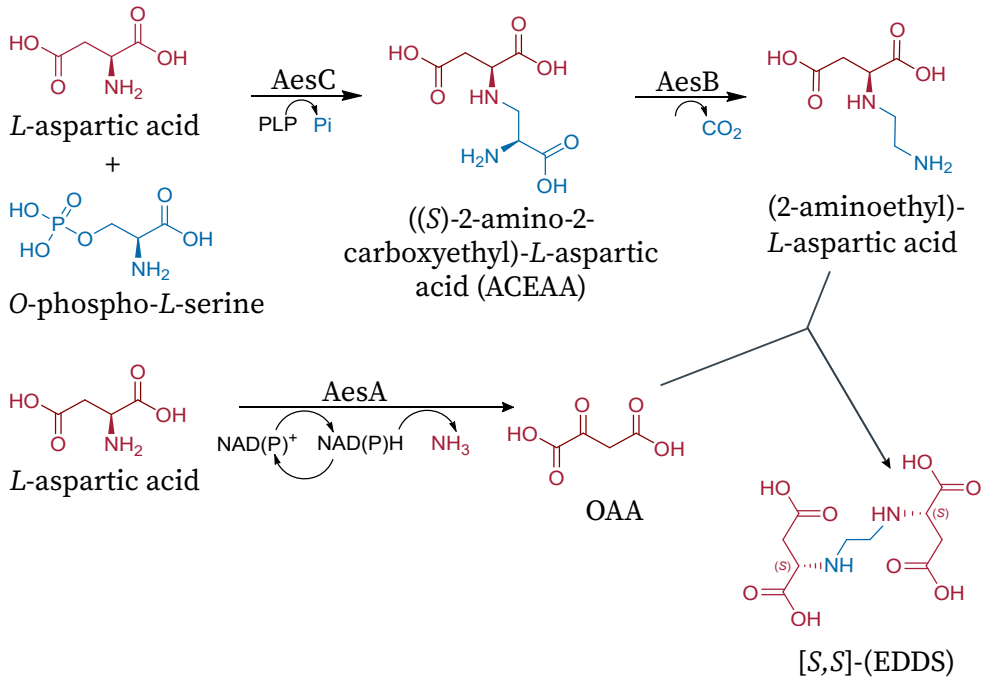

Figure 1.3. **[*S,S*]-EDDS biosynthetic pathway proposed by (Wang *et al.*, 2022).** OAA: oxalacetic acid; AesA: putativeornithine cyclodeaminase (Nicotinamide adenine dinucleotide (NAD^+) depending reaction; AesB: putative amino acid decarboxylase; AesC: putative cysteine synthase (pyridoxalphosphate (PLP) depending reaction.

1.2 Bacterial zinc acquisition and homeostasis

The production of [*S,S*]-EDDS in *A. japonicum* only occurs under zinc limitation, suggesting its function to acquire zinc in deficient situations. Zinc is a vital trace element in bacteria that plays a crucial role in a variety of physiological processes, including DNA replication (Schapiro *et al.*, 2003) and metabolism (Ramsaywak *et al.*, 2004). Zinc is essential for the correct structural and catalytic function of many enzymes, with an estimated 5-6 % of bacterial proteins using zinc as a cofactor (Blindauer, 2015). Additionally, zinc-binding can influence the dimerization of many bacterial DNA-binding proteins, particularly those interacting with inverted

repeats or palindromic DNA sequences (Blindauer, 2015). It is the second most abundant transition metal after iron (Outten and O'Halloran, 2001) and the second most utilized metal cofactor after magnesium (Andreini *et al.*, 2008). Zinc is stable in the Zn^{2+} oxidation state (Capdevila *et al.*, 2016). Recent research has focused on the role of Zn^{2+} in pathogenic bacteria (Veesenmeyer *et al.*, 2009), where efficient Zn^{2+} acquisition and increased Zn^{2+} tolerance are critical for host survival and overall pathogenicity (Ammendola *et al.*, 2007).

An excess of this metal can be toxic to cells if its concentration exceeds a certain threshold. Zn^{2+} is able to form more stable complexes with proteins than other essential metals (Irving and Williams, 1953), so when Zn^{2+} is present in excess in the cell, it binds to metalloproteins that are normally associated with other metals and impairs their function (a process known as mismetallation) (Foster *et al.*, 2014; Maret, 2019).

In order to maintain Zn^{2+}-homeostasis, bacteria possess several mechanisms including Zn^{2+}-uptake, export, intracellular sequestration, and transcription of specific genes regulated by Zn^{2+} transcription factors (Kandari *et al.*, 2021). Transcription factors are able to sense intracellular Zn^{2+} concentrations by binding to Zn^{2+} ions that are available in the cell (Choi and Bird, 2014). They can be divided into two main categories based on their role in preventing either zinc deficiency or excess/-toxicity. In cases of zinc excess, sensors induce the expression of genes encoding efflux, such as RND multi-drug efflux transporters (e.g. CzcABC), P-type ATPases (e.g. ZntA) and cation diffusion facilitator (CDF) family transporters (e.g. ZitB) (Patzer and Hantke, 2000). Periplasmic zinc excess can be buffered by metallo chaperones such as the "zinc resistance-associated protein" (ZraP) in some bacteria (Noll *et al.*, 1998). On the other hand, the expression of uptake transporters such as ABC transporters (e.g. ZnuABC) is induced at limited Zn^{2+} concentrations (Patzer and Hantke, 1998).

Most high-affinity zinc uptake systems are regulated by the zinc uptake regulator (Zur), a member of the ferric uptake regulator (Fur) family of proteins that is conserved across the major bacterial phyla (Hantke, 2005). Zur is a sensor of intracellular zinc levels and can be a repressor or activator of gene transcription. In the presence of zinc concentrations above 100 μM, Zur acts as a repressor when bound to Zn^{2+}, effectively repressing the expression of genes encoding high-affinity zinc importers (znuABC), zinc-free paralogues of ribosomal proteins (Shin *et al.*, 2007)

and also zincophores such as coelibactin and (Kallifidas *et al.*, 2010) and [S,S]-EDDS (Spohn *et al.*, 2016). In *Streptomyces coelicolor,* zinc-bound Zur induces expression of the *zitB* gene, encoding both zinc uptake and export (Choi *et al.*, 2017). Zn^{2+} deficiency (concentrations below 10 μM) causes dissociation of apo Zur from DNA, allowing derepression of targeted genes (Hantke, 2001).

1.3 Use of biofertilizers in agriculture

Zinc deficiency in plants can lead to reduced stress tolerance and chlorophyll synthesis. Visible symptoms of acute deficiency are leaf chlorosis, small deformed leaves and stunted growth (Robson, 1993). Zinc deficiency is a common problem in agriculture, particularly in crops grown on calcareous soils where Zn^{2+} solubility is reduced by increased calcium carbonate concentrations (Robson, 1993). Zinc-deficient soils are widespread and may contribute to human zinc deficiency, particularly in countries where diets are based on cereals (Sandstead, 2013). Given the projected growth of the world's population, it has been estimated that annual global agricultural production will need to increase by about 60 % between 2005/2007 and 2050 (Nikos Alexandratos and Jelle Bruinsma - FAO, 2012). As a result, there is an increasing need for innovative strategies that can support optimal crop performance and the development of economically important crops (Bindraban *et al.*, 2018).

The widespread use of chemical fertilizers in modern agriculture has resulted raised serious concerns. These non-biodegradable chemicals accumulate in the soil and pose a threat to the environment and human health. In addition, the overuse of chemical fertilizers has led to soil deterioration, air and water pollution, and greenhouse gas emissions (Bonner and Alavanja, 2017). To address these issues, microbial biofertilizers have emerged as a promising solution. Beneficial microbes play an important role in supporting plant growth by colonizing different plant systems, such as the epiphytic, endophytic, and rhizospheric systems. These microbes facilitate nutrient uptake from the surrounding plant environment and contribute to soil nutrient enrichment while suppressing soil-borne diseases (Kour *et al.*, 2020). Several bacterial species have been successfully implemented as biofertilizers (Fasusi *et al.*, 2021).

Plant-Growth-Promoting *Rhizobacterias* (PGPRs) belong to a type of beneficial

microbes that can promote plant growth through their own metabolic processes, such as phosphate solubilization, hormone production, nitrogen fixation, or by directly influencing the plant's metabolic pathways. This leads to increased uptake of water and minerals, enhanced root development, and increased enzymatic activity, contributing to plant growth (Pérez-Montaño *et al.*, 2014). PGPRs also support the actions of other beneficial microorganisms and help to suppress plant pathogens. Furthermore, many PGPRs produce siderophores, such as pyoverdine produced by *Pseudomonas fluorescens* C7, under iron-limiting conditions. Treatment of *Arabidopsis thaliana* plants with *Pseudomonas fluorescens* C7 has been shown to increase iron concentration in plant tissues, resulting in improved plant growth (Vansuyt *et al.*, 2007). The potential agricultural benefits of PGPRs in improving soil fertility and crop yield cannot be overstated, and their use offers a sustainable alternative to chemical fertilizers, which can have detrimental effects on the environment.

One such example is the chelating agent ethylenediaminetetraacetic acid (EDTA), which has been shown to optimize metal uptake in plants. However, EDTA is not retained or degraded by conventional wastewater treatment and is therefore released in large quantities into the aquatic environment, where it is difficult to degrade. The persistence of EDTA in the environment depends in particular on the stability of the complexes it forms with metals. Copper and iron are the most stable. In laboratory experiments where EDTA was applied to different types of soil, only 14 % degradation was observed after 20 days (Wen *et al.*, 2009). However, in plant experiments with high concentrations of EDTA, no EDTA degradation occurred after 40 days (Meers *et al.*, 2005). Therefore, an alternative compound that has the positive complexing properties, but is biodegradable, is required. Such an alternative is [*S,S*]-EDDS. It has been shown that it can be used as a fertilizer, since plants treated with [*S,S*]-EDDS-iron complexes took up as much iron as plants treated with EDTA-iron complexes. Thus, [*S,S*]-EDDS-iron complexes were as effective as EDTA-iron complexes in preventing chlorosis and improving soybean growth (López-Rayo *et al.*, 2019). In addition, in pot experiments, [*S,S*]-EDDS was more effective than EDTA in increasing the concentration of Cu^{2+} and Zn^{2+} in maize and beans. In comparison to EDTA, [S,S]-EDDS increased soluble Cu^{2+} and Zn^{2+} concentrations by a factor of about 192 and 8, respectively, especially in the first days after treatment (Luo *et al.*, 2006). Furthermore, the uptake of metal

ions mobilized by [*S,S*]-EDDS by plants is beneficial for the remediation of contaminated soils (Meers *et al.*, 2005). The mobilized heavy metals are taken up by the plants, which can then be harvested and incinerated to ensure safe disposal of the heavy metals. The main advantage of [*S,S*]-EDDS is its high biodegradability, which significantly reduces the environmental risk compared to EDTA. It is noteworthy that only the [*S,S*]-isomer of EDDS is readily biodegradable, but not the [*R,R*]-isomer and the meso-forms. After an initial lag period of 7-11 days, [*S,S*]-EDDS is completely degraded in various soil types with a half-life range of 3.8-7.5 days (Meers *et al.*, 2005; Tandy *et al.*, 2005; Edenhart *et al.*, 2020).

1.4 Industrial applications of [*S,S*]-EDDS

[*S,S*]-EDDS has been proven to be a functional equivalent EDTA, a chelating agent not only used in agriculture, but also in industrial and domestic applications. Due to EDTA ability to complex metals, it is used in several applications including pulp, paper and textile production, cleaning and laundry operations, soil remediation, food products, tanning processes, photography, wastes and effiuents treatment, pharmaceuticals, and cosmetics (Knepper, 2003; Nowack and VanBriesen, 2005). Only in the pulp and paper industry, where the major use of EDTA takes place, it was estimated that about 10,000-20,000 tons of EDTA were used per year (Jones and Williams, 2002). In the last decades, discussion about their environmental consequences has been raised. Since [*S,S*]-EDDS exhibits similar metal coordination chemistry as EDTA with comparable chelating properties (Whitburn *et al.*, 1999), but in contrast to EDTA, [*S,S*]-EDDS readily biodegradable until complete mineralization (Schowanek, 1997; Takahashi *et al.*, 1997) it is considered an alternative in many applications.

A chemical synthesis procedure has been reported for [*S,S*]-EDDS maleic acid, maleic anhydride, or fumaric acid with ethylenediamine (Kezerian and Ramsey, 1964). This procedure leads to the formation of a mixture of three isomers and low yield of [*S,S*]-EDDS, making it unsuitable for industrial purposes. Alternatively, single stereisomers of EDDS can be synthesized using 1,2-dibromoethane and L-aspartic acid in the presence of Cobalt (III) (Neal, J.A., and Rose, N.J., 1968). However, this method presents several drawbacks, such as the toxicity of 1,2-dibromoethane to humans and aquatic organisms, the production of toxic hydrogen bro-

mide during the reaction, which necessitates extensive removal and the requirement of a fossil reactant (charcoal), which is not a renewable resource. Innospec Inc. UK currently produces [*S,S*]-EDDS chemically using non-renewable fossil resources under the trade name ENVIOMET™. However, the high costs of producing the stereochemically [*S,S*]-configuration have limited its use.

The development of a biotechnological process for the production of [*S,S*]-EDDS has been the subject of many different approaches. A yield of approximately 20 g/L [*S,S*]-EDDS was achieved after 40 days of cultivation in a fed-batch fermentation by optimizing the synthetic medium with appropriate phosphate, nitrogen and carbon sources (Zwicker *et al.*, 1997). However, the industrial biotechnological production of [*S,S*]-EDDS was not possible, because the production was inhibited by ubiquitous low μM concentrations of zinc. In 2016, the first *A. japonicum* mutant was constructed by deleting the *zur* gene in *A. japonicum* (*A. japonicum* Δ*zur*). This mutant was able to bypass zinc regulation (Spohn *et al.*, 2016). The availability of this mutant provided the first opportunity to develop a biotechnological process. More recently, metabolic engineering approaches have been used to construct a zinc-deregulated overproducer strain. In this strain, the transcription level of [*S,S*]-EDDS was increased and the supply of the precursor *O*-phosphoserine was optimized. Zinc repression was removed by replacing the zinc-regulated promoter with a constitutive one. This *A. japonicum* strain OP2 allowed the production of 9.8 g/L within 135 hours of fermentation time (Edenhart *et al.*, 2020). The chemical properties of [S,S]-EDDS are impressive. However, the yield of [S,S]-EDDS needs to be increased in order to establish a cost-effective biotechnological production process that is economically viable for industrial applications. Further steps for successful engineering require a complete understanding of the biosynthetic pathway used by *A. japonicum* to produce [*S,S*]-EDDS.

1.5 Aim of the work

[*S,S*]-EDDS has great potential for various applications, especially in agriculture. Previous studies have shown that fertilization with Zn-[*S,S*]-EDDS can increase the Zn^{2+} concentration in plants. The main objective of this study is to evaluate the potential of an [*S,S*]-EDDS overproducing strain, *Amycolatopsis japonicum* SP44, as a continuous source of [*S,S*]-EDDS.

Despite the promising chemical properties of [*S,S*]-EDDS, the establishment of a biotechnological process for its production has not been profitable. For the development of such a process it is crucial to increase the yield of [*S,S*]-EDDS. Therefore, the second aim of this work is to decipher the biosynthetic pathway of [*S,S*]-EDDS, identify the precursors and understand the enzymatic processes. With this knowledge, targeted interventions in the biosynthesis can help to further increase the production yield of [*S,S*]-EDDS.

Chapter 2

Materials and methods

2.1 Materials

2.1.1 Antibiotics

Table 2.1. Antibiotics used in this study

Antibiotic	Stock concentration	Supplier
Ampicillin	150 μg/ml	Roth
Apramycin	100 μg/ml	Genaxxon
Chloramphenicol	25 μg/ml	Sigma-Aldrich
Hygromycin	100 μg/ml	Roth
Nalidixic acid	25 μg/ml	Roth

2.1.2 Chemicals, reagents and media

Table 2.2. Chemicals, reagents and media

Chemical	Supplier
Acrylamide/Bis-acrylamide (37.5:1)	Carl Roth
Agarose	Genaxxon
Ammonium persulfate (APS)	SERVA
Ampicillin (Amp) sodium salt	Roth
Apramycin	Genaxxon
Biotin	iba
Bromophenol blue sodium salt	SERVA
$CaCl_2$ x H_2O	Roth
Casamino acids	Becton, Dickinson and Company
Chloramphenicol (Cam)	Sigma-Aldrich
Coomassie Brilliant Blue G-250	Carl Roth
Copper sulphate	
DL-Diaminopropionic acid	Sigma Aldrich
Dimethylsulfoxid (DMSO)	Merck
Ethylenediamine-N,N'-disuccinic acid trisodium salt solution (EDDS)	Sigma Aldrich
Ethanol	Carl Roth
Ethylenediaminetetraacetic acid (EDTA)	Carl Roth
Ferric (III) citrate	Merck
Glucose	Carl Roth
Glycerol	Sigma Aldrich
Hydrochloric acid (HCl)	Fisher Chemical
Luria-Bertani (LB) broth	Sigma Aldrich
L-ornithine	Merck
L-prolin	AppliChem
L-aspartic acid	Merck
Malat	Merck
Malt Extract	Oxoid
Mannitol	Sigma Aldrich
Magnesium chloride x $6H_2O$ ($MgCl_2$)	Merck
Magnesium sulfate heptahydrate $MgSO_4$ x 7 H_2O	AppliChem
Potassium dihydrogen phosphate (KH_2PO_4)	Fisher Chemical
Sodium chloride (NaCl)	Merck
Sodium dodecyl sulfate (SDS)	SERVA
Sodium hydroxide (NaOH)	VWR Chemicals
Sodium phosphate dibasic (Na_2HPO_4)	Sigma-Aldrich
Pyridoxal-5'-phosphate (PLP)	Sigma Aldrich
Tetramethylethylenediamine (TEMED)	BioRad
Thiobarbituric acid (TBA)	SERVA

Table 2.2. Chemicals, reagents and media (continued)

Chemical	Supplier
Tris-(hydroxymethyl)-aminomethane (Tris)	Sigma Aldrich
Tryptic Soy Broth (TSB)	Becton, Dickinson and Company
Zinc sulfate ($ZnSO_4$)	Merck
α-ketoglutarate	Fluka
β-Mercaptoethanol	Merck
9-fluorenylmethyl chloroformate (Fmoc-Cl)	Sigma-Aldrich
Dansyl chloride	SigmaAldrich
NAD^+	Sigma Aldrich

2.1.3 Culture medium

Table 2.3. Media preparation

Medium	Preparation (1L)
Medium used for standard [*S,S*]-EDDS production	
M3, pH 7.5	20 g glycerol 20 g Soy flour
M7	8 g KH_2PO_4 12 g Na_2HPO_4 x $2H_2O$ 11.3 g sodium glutamate monohydrate 40 ml M7 Supplements 10 ml Ferric (III)-Citrate
M7 supplements (synthetic medium (SM))	625 g glycerol 30 g $MgSO_4$ x $7H_2O$ 0.24 g Ferric citrate in 40 ml ddH_2O
Medium used for [*S,S*]-EDDS in inverse labeling experiments with ^{13}C-glycerol	
M7	8 g KH_2PO_4 12 g Na_2HPO_4 x $2H_2O$ 3.2 g NH_4Cl 40 ml M7 Supplements 10 ml Ferric (III)-chloride
M7 supplements	30 g $MgSO_4$ x $7H_2O$ 0.31 g Ferric chloride in 50 ml ddH_2O

^{13}C-glycerol is added separately (625 g/l)

Table 2.4. Media preparation (continued)

Medium	Preparation. Continued (1L)
Medium used for [*S,S*]-EDDS in inverse labeling experiments with $^{15}NH_4Cl$	
M7	8 g KH_2PO_4 12 g Na_2HPO_4 x $2H_2O$ 40 ml M7 Supplements 10 ml Ferric (III)-chloride
M7 supplements	625 g glycerol 30 g $MgSO_4$ x $7H_2O$ 0.31 g Ferric chloride in 50 ml dd H_2O

$^{15}NH_4Cl$ is added separately (0.32 g in 100 ml)

Table 2.5. Bacterial strains and plasmids used in this study

Strains	Relevant properties	Reference
E. coli NovaBlue^{TM}	general cloning host	Novagen
E. coli ET12567	*F⁻ dam-13::Tn9, dcm-6 hsdM hsdR*	MacNeil *et al.* (1992)
E. coli Rosetta^{TM}(DE3)	*F- ompT hsdSB(rB- mB-) gal dcm (DE3) pRARE* (*Cam*^{R})	Novagen
A. japonicum MG417-CF17	[*S,S*]-EDDS producer, wild type	Nishikiori *et al.* (1984)
A. japonicum ΔEDDS	Δ*aesA-C*	Spohn *et al.* (2016)
A. japonicum Δ*zur*	*zur* gene inactivated	Spohn *et al.* (2016)
A. japonicum ΔEDDS (*aesA*)	constitutive SP44*, *Hyg*^{R}	Edenhart, unpublished
A. japonicum ΔEDDS (*aesB*)	constitutive SP44*, *Hyg*^{R}	Edenhart, unpublished
A. japonicum ΔEDDS (*aesC*)	*Hyg*^{R}	Edenhart, unpublished
A. japonicum ΔEDDS (*aesAB*)	constitutive SP44*, *Hyg*^{R}	Edenhart, unpublished
A. japonicum ΔEDDS (*aesAC*)	constitutive SP44*, *Hyg*^{R}	Edenhart, unpublished
A. japonicum ΔEDDS (*aesBC*)	constitutive SP44*, *Hyg*^{R}	Edenhart, unpublished
A. japonicum SP44*	constitutive SP44* promoter	Edenhart *et al.* (2020)
A. japonicum OP1	pSE_*aesA-D*	Edenhart *et al.* (2020)
A. japonicum OP2	pSE_*aesA-D*, pRM4-*serA-serC*	Edenhart *et al.* (2020)

Table 2.5. Bacterial strains and plasmids used in this study (continued)

Strains	Relevant properties	Reference
A. japonicum (*bldC*)	constitutive *ermEp**, *Apra*^{R}	Mungan *et al.* (2022)
A. japonicum (*lacI*)	constitutive *ermE*p*, *Apra*^{R}	Mungan *et al.* (2022)
A. japonicum (*glts*)	constitutive *ermEp**, *Apra*^{R}	Mungan *et al.* (2022)
A. japonicum (*bldC-lacI-glts*)	constitutive *ermEp**, *Apra*^{R}	Mungan *et al.* (2022)
LDAPP1	*A. japonicum* ΔEDDS::pRM4 AJAP_RS19040 -19050-*aesB* *Apra*^{R}	This study
LDAPP2	*A. japonicum* ΔEDDS:: AJAP_RS22275 -22260-*aesB* *Apra*^{R}	This study
plasmids		
pRM4	pSET152 *ermEp** derivate with artificial RBS, *Apra*^{R}	(Menges *et al.*, 2007)
pIJ10257	*ermEp**, ribosome binding site and multicloning site from pIJ8723 cloned into pMS81	(Hong *et al.*, 2005)
pUB307	RP1 derivative	(Flett *et al.*, 1997)
DHFR-*aesC*	*Amp*^{R}	This study
pGM1192	mCherry, aac(3)IV, tsr	Günther Muth, unpublished
pGM1192-*aesC*	*Apra*^{R}	This study
pDAPP1	*ermEp**, *Apra*^{R}	This study
pDAPP2	*ermEp**, *Apra*^{R}	This study

Hyg^{R} hygromycin resistance, *Apra*^{R} Apramycin resistance,
Cam^{R} Chloramphenicol resistance, *Amp*^{R} ampicillin resistance.

Table 2.6. List of oligonucleotides used in this study

Primer	Sequence (5'-3')
Primers used for amplification of the *A. japonicum asl* (AJAP_RS14075)	
Asl_{Aj}-BglII-F	AGATCTGTGAGCGGGAATGAGCAG
Asl_{Aj}-HindIII-R	AAGCTTTCAGCCGAGCCAGGTGCG
Primers used for amplification of the *A. japonicum aesC* (AJAP_RS08350) for *in vitro* AesC synthesis)	
$AesC_{Aj}$-DHFR-F	AGTACTGGATCCATGACGATCGTCCGGCGCGC
$AesC_{Aj}$-DHFR-R	CAGTCAAGCTTTCATCCGCCCACCGCCACC
Primers used for amplification of the *A. japonicum aesC* (AJAP_RS08350) codon optimized for *E. coli*	
AesC-codon_E.coli-F	GGATCCATGACCATTGTGCGTCGCG
AesC-codon_E.coli-R	AAGCTTTTAACCACCCACG
Primers used for amplification of the *A. japonicum bldC* (AJAP_RS36645)	
bldC_pRM4_F	CGACGGTATCGATAAGCTAGCCAGGGGA GGACCCAATGACCGCGACCATGGGCGGA
bldC_pRM4_R	GGGCTGCAGGAATTCGATATCAAGCTTAGA TCTCATCAGACCTTGCGAGCGGGCTCG
Primers used for amplification of the *A. japonicum lacI* (AJAP_RS11995)	
lacI_pRM4_F	GGGCTGCAGGAATTCGATATCAAGCTTAGA TCTCATCATGCGGGGTACTCCTGGGTCGATTCG
lacI_pRM4_R	CGACGGTATCGATAAGCTAGCCAGGGGAGG ACCCAATGTCGCTGGCGAAGGTGGCCC

Table 2.6. List of oligonucleotides used in this study (continued)

Primer	Sequence (5'-3')
Primers used for amplification of the *A. japonicum* glutamate synthase (*glts*) (AJAP_RS11230)	
GS_pRM4_F	CGACGGTATCGATA ACCCAGTGGCTGATCCGACGGGTTTCCTGAAGTACG
GS_pRM4_R	GGGCTGCAGGAATTCGATATCAAGCTTAGATC TCATCAGACCACCGCGAGCGGCA
Primers used for amplification of the *A. japonicum bldC-lacI-glts*	
bldC_F_assem_pRM4	CGACGGTATCGATAAGCTAGCCAGGGGAGGAC CCAATGACCGCGACCATGGGCGGAAGG
bldC_R_assem_pRM4	ACCTTCGCCAGCGACATTCAGACCTTG CGAGCGGGCTCGCT
lacI_F_assem_pRM4	CCCGCTCGCAAGGTCTGAATG TCGCTGGCGAAGGTGGCCCG
lacI_R_assem_pRM4	CCCGTCGGATCAGCCACTCATGCGG GGTACTCCTGGGTCGATTCGCG
GSsmall_F_assem_pRM4	CAGGAGTACCCCGCATGAGTGGCTG ATCCGACGGGTTTCCTGAAGTACGAC
GSsmall_R_assem_pRM4	GGGCTGCAGGAATTCGATATCAAGCTTAGA TCTCATCAGACCACCGCGAGCGGCAACG

Table 2.6. List of oligonucleotides used in this study (continued)

Primer	Sequence (5'-3')
RT primers used for amplification of *A. japonicum* gene fragments	
sigB-RT-F	CCTCAACGGAATCGGCAAGACG
sigB-RT-R	ATCAGGTCGAGCAGTGGCATCC
aesA-RT-F	TCTGCACAGCCTCGAACTCAC
aesA-RT-F	TTGGCGGTAGCTCGTCTTGAAC
aesB-RT-F	TGGTCCATCCGGCCACTTTC
aesB-RT-F	AAAGGAGGCCGTCGGGTTTG
aesC-RT-F	CATCCCGATCAGCACAACCATCC
aesC-RT-R	AAGATGATCGAGCCGACAGGTTC
aesD-RT-F	TCGCCGGTCCGATGATGTTC
aesD-RT-F	AGATGAAGGCGGCGTTGAG

Table 2.6. List of oligonucleotides used in this study (continued)

Primer	Sequence (5'-3')
Primers used for amplification of *A. japonicum dappA1-dappC1-aesB*	
AJAP_RS19040_F	GTATCGATAAGCTAGCCAGGGGAGGACCC AGTGCTCGCCACGATCGGGAACACTCCC
AJAP_RS19040_R	GTCGAACCAGCTCATTCAGGAGATGGTGGC CAGGGCGCG
AJAP_RS19050_F	GCCACCATCTCCTGAATGAGCTGGTTCGAC GTGGCCGACAGC
AJAP_RS19050_R	GTCGATCAGGTCCACTCAGCCGAGGTGGAC AACGGTACCGAGCC
AesB-19040-50_F	GTCCACCTCGGCTGAGTGGACCTGATCGA CACCCTGTCCCCGC
AesB-19040-50_R	GCAGGAATTCGATATCAAGCTTAGATCTC ATCATCGGATCTCCTGGATCGGGTGGTCGGT
Primers used for amplification of *A. japonicum dappA2-dappC2-aesB*	
AJAP_RS22260_F	GTATCGATAAGCTAGCCAGGGGAGGACCCA GTGAGCTGGTACAAGGGGGAGGGGAAG
AJAP_RS22260_R	CCACAGGTTTTCCATTCAGATCAAGACCAG TGAATTGTCAACGACCCGCG
AJAP_RS22275_F	CTGGTCTTGATCTGAATGGAAAACCTGTGG CTCGCCGACG
AJAP_RS22275_R	GTCGATCAGGTCCACTCACACGAGCTCCA GCGCCTGCC
aesB-22260-22275_F	CTGGAGCTCGTGTGAGTGG ACCCTGTCCCC
aesB-22260-22275_R	GCAGGAATTCGATATCAAGCTT AGATCTCATCATCGGATCTCCTGGATCGGGTGGTCG

2.2 Methods

2.2.1 Media and culture conditions

E. coli strains were grown in Luria broth (LB) medium (Sambrook *et al.*, 1989) at 37°C and were supplemented with antibiotics when required, to maintain plasmids. To maintain plasmid selection in ET12567 (pUB307), 50 μg ml^{-1} kanamycin, and 25 μg ml^{-1} chloramphenicol were added to maintain the selection of pUB307 and the dam - mutation, respectively. *A. japonicum* was grown in tryptic soy broth (TSB) or R5 medium (Kieser *et al.*, 2000).

Liquid cultures of *A. japonicum* strains in 100 ml volume were grown to detect [*S,S*]-EDDS production according to (Zwicker *et al.*, 1997; Spohn *et al.*, 2016). The optimized SM consisted of glycerol (25 g l^{-1}), $MgSO_4 \times 7\ H_2O$ (1.2 g l^{-1}), Ferric (III) citrate (60 mg l^{-1}), KH_2PO_4 (8 g l^{-1}), $Na_2HPO_4 \times 2\ H_2O$ (12 g l^{-1}) and sodium glutamate monohydrate (11.3 g l^{-1}), which was used as the nitrogen source. To grow the strains in a reduced 3 ml volume, 12-well microplates were used. The cultures were grown on a rotary shaker (120 r.p.m.) at 30°C. Precultures were grown in complex culture medium (glycerol (20 g l^{-1}); soybean meal (20 g l^{-1}) at pH 7.5) for 48 hours. A total of 150 μl of this pre-culture was used to inoculate 3 ml of SM. The cultures were grown for a further 72 hours before [*S,S*]-EDDS production test and analysis by RT-PCR.

2.2.2 Determination of *A. japonicum* growth in soil

The growth assay was performed in a sterile 12-well microplate. 1x 10^5 spores from *A. japonicum* WT, *A. japonicum* SP44 or *A. japonicum* ΔEDDS were inoculated into 1g of sterile soil (three times autoclaved). After one, two, three, and five days, *A. japonicum* strains were recovered from the soil by shaking the 1g of soil in 9 ml of sterile water and mixing for 10 min at room temperature. To determine colony-forming units (cfu), serial dilutions were prepared and plated onto mannitol soy flour agar plates (MS agar) (Kieser *et al.*, 2000). The plates were incubated at 30°C for 2-3 days, after which the number of cfu was counted. To determine spore counts, appropriate dilutions were selected and the number of spores was counted as spores/ml, taking into account the dilution factor.

2.2.3 RNA extraction from soil and reverse transcription (RT)-PCR analysis

Three grams of sterile soil samples in a sterile 6-well microplate were inoculated with 10^5 spores from *A. japonicum* WT, *A. japonicum* SP44 or *A. japonicum* ΔEDDS spores and incubated for three days at 30 °C. After three days, up to 2 g of soil was added to a 15 ml tube and total RNA isolation was performed using RNeasy Power Soil (Qiagen). To eliminate any DNA contamination, RNA preparations were treated with TURBO DNA-free (Invitrogen) following the instructions provided with the kit. To exclude DNA contamination, negative controls were carried out by using total RNA as the template for a PCR using the primer pair sigB-RT-F and sigB-RT-R. cDNA from 3 mg RNA was generated with random hexameric primers, reverse transcriptase, and cofactors (Fermentas). PCRs were performed according to (Spohn *et al.*, 2014) with the primers listed in (Table 2.6). PCRs were carried out under the following conditions: (1) an initial denaturation step (94 °C for 2 min); (2) 27 cycles of PCR, with 1 cycle consisting of denaturation (95 °C for 30 s), annealing (59°C for 30 s), and polymerization (72°C for 30 s); and (3) an additional polymerization step (72 °C for 1 min). Each PCR mixture (25 μl) contained a 1 μl aliquot of RT reaction product. As a positive control, cDNA was amplified from the major vegetative sigma factor (*sigB*) transcript, which is produced constitutively. The PCR products were analyzed by agarose gel electrophoresis (2 %).

2.2.4 Plant experiments

2.2.4.1 Seed germination

Seeds from green bean (*Phaseolus vulgaris* cv. Black pole) were disinfected by immersion in 500 ml of distilled water and 0.1 ml of sodium hypochlorite, shaked for 10 min, followed by two times washed with 500 ml deionized water for 10 min each. Then, they were placed in plastic trays (17 seed/tray aproximately) with 1 mM $CaSO_4$ wetted paper, covered, and kept in a germination chamber for 3 days at 28 °C in the dark.

2.2.4.2 Growth in hydroponics

After germination, plants were sown in plastic containers of 5 l with a 1/5 diluted nutrient solution (NS) for 6 days. The concentration of the diluted solution was: 0.2 mM $Ca(NO_3)$ 2x $4H_2O$; 0.18 mM KNO_3; 0.06 mM $MgSO_4$ x 7 H_2O; 0.02 mM KH_2PO_4; 7.0 μM NaCl; 2.0 μM H_3BO_3; 0.01 μM Na_2MoO μM_4 x $2H_2O$; 23.1 μM Na_2·EDTA; 0.5 μM M $MnSO_4$ x H2O; 0.2 μM $CuSO_4$ x $5H_2O$; 2 μM $ZnSO_4$ x $7H_2O$; 0.2 μM $NiCl_2$ x $6H_2O$; 0.2 μM $CoSO_4$·H2O; 1 μM Fe-HBED. pH was adjusted at 6,5 using KOH.

After these 6 days, the solution was changed by a full-strength nutrient solution without Zn^{2+} in order to induce the Zn^{2+} deficiency in plants for four days, when slight deficiency symptoms were observed. The concentration of the nutrient solution in this period was: 1.0 mM $Ca(NO_3)2$ x $4H_2O$; 0.9 mM KNO_3 ; 0.3 mM $MgSO_4$ x $7H_2O$; 0.1 mM KH_2PO_4; 35 μM NaCl; 10 μM H_3BO_3; 0.05 $NaMoO_4$·H_2O; 1.0 μM $MnSO_4$ x H_2O; 0.5 μM $CuSO_4$ x $5H_2O$; 0.1 μM $NiCl_2$ x $6H_2O$; 0.1 μM $CoSO_4$ x $7H_2O$; 50 μM Fe-HBED. Additionally, 0.1 g l^{-1} of $CaCO_3$ was added to each container in order to simulate alkaline conditions (pH of the nutrient solution was around 7.5).

2.2.4.3 Soil characteristics

Soil samples were sieved using 5 mm sieves. The pots were methacrylate tubes of 7 cm diameter and 16 cm length. Each pot was filled with 600 g of calcareous soil: calcareous sand mixture (70:30), covered with aluminum foil to prevent from light exposure and filled with distilled water until 100 % water holding capacity (WHC). Tubes had a cloth on the bottom, fastened with a rubber base to create subject. A petri plate was placed at the bottom to avoid and control water losses in case of leaching. The soil was a sandy clay soil from Picassent (Valencia, Spain) mixed with calcareous sand (975 g kg^{-1} $CaCO_3$, 1–3 mm size). The soil characteristics are shown in Table 2.7.

Table 2.7. Chemical characteristics of soils used in biological experiments.

Parameter	Information
Texture	Sandy loam
pH (H_2O)	7.9
pH (KCl)	7.4
EC (1:5 extract) (dS m-1)	0.2
OM (g kg-1)	9.2
N Kjeldahl (g kg-1)	0.30
$CaCO_3$ total (g kg-1)	380
$CaCO_3$ active (g kg-1)	89
Micronutrients (mg/kg) (Soltanpour and Schwab, 1977)	
Fe	5.3
Mn	4.5
Cu	1.0
Zn	3.0

2.2.4.4 Transplant to pots and application of treatments

After pre-growing, the plants were transplanted to pots (1 plant per pot) and a solution containing 0.1 g l^{-1} of $CaCO_3$ + 0.1 g l^{-1} of $NaHCO_3$ was added to maintain the 80 % WHC, instead of water. This solution containing $CaCO_3$ was used to simulate calcareous conditions and force the Zn^{2+} deficiency. One day after the plant transplanting to pots, the treatments were applied to the pots. The following treatments were assayed: (1) Positive control, [*S,S*]-EDDS (24 μmol / pot), (2) *A. japonicum* WT (5 x 10^8 CFU/ml), (3) *A. japonicum* SP44, a zinc-deregulated overproducer (5*10^8 CFU/ml), (4) *A. japonicum* ΔEDDS (5*10^8 CFU/ml) as negative control. Additional pots without anay treatment were included.

Pictures were taken over the whole experiment to compare visual aspect. Three samplings were done, at 7 days post treatments application (DPT), after 21 DPT and at 24 DPT. For that, plant shoots were cut 1 cm from soil, washed with a soap-solution (0.1 % Tween 80 , 0.1 M HCl), followed by 2 washes in distilled water. After washing, stems and leaves were separated and weighed (fresh weight). Finally, they were dried in an oven on paper bags at 65 °C to dry for three days. Then, they were kept in paper bags in a dry place at room temperature.

2.2.4.5 Measurement of chlorophyll development

The chlorophyll index was measured using the soil plant analysis development (SPAD) chlorophyll meter (Minolta, Osaka, Japan) every two days, with five measurements per plant level.

2.2.4.6 Analysis of samples

The sample analysis was performed as described by (López-Rayo *et al.*, 2019). At the specified sampling time, leaves and stems were separated and washed with 0.1 % (w/v) HCl and 0.01 % (w/v) non-ionic detergent solution (Tween 80) to remove any inorganic surface deposit and rinsed twice with ultrapure water, as described by (Álvarez-Fernández *et al.,* 2001). The samples were then dried in a forced air oven at 60 °C for 3 days, and weighed and analyzed for mineral concentration after dry digestion at 480 °C for 4 h and acid digestion with 1:1 diluted HCl for ash solubilization. The roots were carefully separated, washed and analyzed as described by (López-Rayo *et al.*, 2019)

2.2.5 Derivatization of [*S,S*]-EDDS with Fmoc-Cl

9-fuorenylmethyl chloroformate (Fmoc-Cl) was prepared by dissolving 12.9 mg in 5 ml of acetone to give a concentration of 10 mM. Derivatization of [*S,S*]-EDDS was also performed in 1M buffer borate pH 8.0. 100 μl of buffer borate were mixed with 0.5 μl of sample and 200μl of Fmoc-Cl. The mixture was incubated for 30 minutes at room temperature, as described by (Tandy *et al.*, 2005).

2.2.6 Derivatization with Fmoc-Cl of [*S,S*]-EDDS extracted from soil samples

The samples were treated with 10 mM EDTA buffer pH 11.5 to promote the chelation of metals with EDTA. The samples were incubated for 30 minutes at room temperature and then centrifuged. The supernatant was mixed with Fmoc-Cl for derivatization, as described in section 2.2.5.

2.2.7 Detection of [*S,S*]-EDDS from soil samples by HPLC-MS

10 g soil previously inoculated with *A. japonicum* strains or [*S,S*]-EDDS standard, were dissolved in sterile water, mixed for 1h, and incubated for 30 min in an ultrasonic bath. Samples were filtered and centrifuged. The soil water extracts were concentrated using the Genevac EZ-2 evaporating system until dry and dissolved in 1 ml of water. Next, the sample was mixed with 10 mM EDTA pH 11.5 and derivatized with Fmoc-Cl as described in Section 2.2.6.

2.2.8 [*S,S*]-EDDS production test

Liquid culture of *A. japonicum* WT and recombinant strains was performed in 100 ml volume to determine [*S,S*]-EDDS production according to (Spohn *et al.*, 2016). The optimized synthetic medium (SM) consisted of glycerol (25 g l^{-1}), $MgSO_4 \times 7$ H_2O (1.2 g l^{-1}), Ferric (III) citrate (60 mg l^{-1}), KH_2PO_4 (8 g l^{-1}), $Na_2HPO_4 \times 2$ H_2O (12 g l^{-1}) and sodium glutamate monohydrate (11.3 g l^{-1}), which was used as the nitrogen source. Pre-cultures were grown on a rotary shaker (120 rpm) at 29 °C in complex culture medium (glycerol (20 g l^{-1}); soybean meal (20 g l^{-1}) at pH 7.5) in 50 ml volume for 48 h. A total of 5 ml of this pre-culture was used to inoculate 95 ml of SM. The cultures were grown for further 96 h before the [*S,S*]-EDDS production was analyzed.

2.2.9 Detection of [*S,S*]-EDDS using HPLC–ESI-MS

Culture broths were prepared by centrifugation. 2.5 µl of the supernatants were analyzed by HPLC-ESI-MS using a Nucleosil 100-C18 column (3 μm, 100x2 mm with precolumn 10x2 mm (Dr. Maisch GmbH, Ammerbuch-Entringen, Germany), coupled to an ESI mass spectrometer (LC/MSD Ultra Trap System XCT 6330 (Agilent Technology, Waldbronn, Germany). Analysis was carried out at a flow rate of 0.4 ml/min with a solvent gradient of A = 0.1 % formic acid and B = 0,06 % formic acid in acetonitrile (gradient: t0=t5=0 % B, t10=t12=100 % B, post time 6 min. 0 %, 40°C. Electrospray ionization (alternating positive and negative ionization) in Ultra Scan mode, 100-800 m/z with a capillary voltage of 3.5 kV and a drying gas temperature of 350°C was used for LC-MS analysis. Detection of m/z values was conducted with Agilent Data Analysis for 6300 Series Ion Trap LC/MS version 6.1 (Bruker-Daltonik

GmbH).

2.2.10 Detection of [*S,S*]-EDDS (derivatized with Fmoc-Cl or Dansyl Chloride) by HPLC-ESI-MS

Culture broths were prepared by centrifugation. 2.5 µl of the supernatants were analyzed by HPLC-ESI-MS using a Nucleosil 100-C18 column (5 μm, 100x3 mm fitted with a precolumn 4x2 mm (Phenomenex, Aschaffenburg), coupled to an ESI mass spectrometer (LC/MSD Ultra Trap System XCT 6330 (Agilent Technology, Waldbronn, Germany). Analysis was carried out at a flow rate of 0.5 ml /min with gradient elution. Solvent A was 0.1 % formic acid and solvent B was 0.06 % formic acid in acetonitrile. Gradient elution was performed as follows: t0=10 % B, t15=t17=100 % B, post time 6 min. 10 % B, 40°C. Electrospray ionization (alternating positive and negative ionization) in Ultra Scan mode, 100-1500 m/z with a capillary voltage of 3.5 kV and a drying gas temperature of 350 °C was used for LC-MS analysis. Detection of m/z values was conducted with Agilent Data Analysis for 6300 Series Ion Trap LC/MS version 6.1 (Bruker-Daltonik GmbH).

2.2.11 Detection of [*S,S*]-EDDS biosynthesis using HPLC-DAD

For the detection of [*S,S*]-EDDS, 1 ml of sample was thoroughly mixed with 20 μl of $CuSO_4$ (100 mM) and once again centrifuged before using the supernatant for HPLC analysis. [*S,S*]-EDDS analyses were carried out on a HP1090M liquid chromatograph equipped with a thermostated autosampler, a diodenarray-detector and an HP Kayak XM 600 Workstation (Agilent). A total of 10 μl of samples were injected onto a Hypersil ODS column (125 × 4 mm, 3 μm) column and analyzed by isocratic elution with solvent A – acetonitrile (96:4, v/v) at a flow rate of 1 ml/min. Solvent A consisted of 20 mM phosphate buffer (pH 7.2) with 5 mM tetrabutyl ammonium hydrogen sulfate. UV detection was performed at 253 nm. For data analysis, Chemstation LC3D software Rev. A.08.03 was used. [*S,S*]-EDDS-Na_3 was used as standard.

2.2.12 Isolation and purification of [*S,S*]-EDDS from *A. japonicum* cultures

Isolation and purification of [*S,S*]-EDDS was conducted according to (Zwicker *et al.*, 1997).

2.2.13 Analytical instrumentation. Nuclear magnetic resonance (NMR)

^{13}C NMR spectra were recorded on a Bruker Avance II 400 MHz spectrometer at 100 MHz in deuterium oxide (D_2O). 181.4, 179.8, 60.6, 46.0, 41.1 ppm. ^{1}H-^{15}N HMBC spectra were recorded on a Bruker Avance II 400 MHz spectrometer at 400 MHz in (D_2O).

2.2.14 High resolution LC-MS

High-resolution LC-MS was recorded on an Agilent 1290 Infinity II using a Kinetex 1.7 µm C18 100 Å, 50 x 2.1 mm column, Bruker impact II mass spectrometer, and a flow rate of 0.5 mL/min. Used LC solvents were A: H_2O (0.1 % FA), B: MeCN (0.1 % FA). Standard conditions: Gradient 10-100 % B over 10 minutes, and hold 100 % B for 2 minutes.

2.2.15 Construction of the plasmid pGM1192-*asl*$_{Aj}$

For the construction of the plasmid pGM1192-*asl*$_{Aj}$, the *asl*$_{Aj}$ (AJAP_RS14075) sequence was amplified from *A. japonicum* using the primers Asl$_{Aj}$-BglII-F (F stands for forward primer) and Asl$_{Aj}$-BglII-R (R stands for reverse primer) (Table 2.6). The amplified fragment was cloned into the plasmid pGM1192 previously digested with the enzymes BamH1 and HindIII. The plasmid was sequenced to confirm its correctness. *E. coli* Nova Blue was transformed with pGM1192-*asl*$_{Aj}$ and finally, the plasmid was transferred to *E. coli* Rosetta (DE3) for the expression of *asl*$_{Aj}$.

2.2.16 Construction of the plasmid DHFR-*aesC* for cell-free protein expression

To construct the expression plasmid DHFR-*aesC* the *aesC* (AJAP_RS08350) gene of *A. japonicum* was amplified via PCR with the primer pairs AesC$_{Aj}$-DHFR-F and

$AesC_{Aj}$-DHFR-R (Table 2.6) using the pGM1192-*aesC* plasmid as template. The amplified fragment contained additionally the Strep-tagII sequence at the N-terminal, provided by the plasmid pGM1192. The amplified fragment of *aesC* was digested with ApoI and NdeI, while the DHFR plasmid was digested with EcoRI and ApoI. The purified digestion products were ligated and the resulting plasmid DHFR-*aesC* was used for the cell-free expression of *aesC* using the PURExpress *in vitro* protein synthesis, following the instructions of the suppliers.

2.2.17 Construction of pGM1192-*aesC*$_{Co}$

The optimized sequence for *aesC* expression in *E. coli* was obtained from BioCat in the plasmid pET-24a (+). This plasmid was used as template for the amplification of *aesC*$_{Co}$ via PCR with the primers AesC-codon_E.coli-F and AesC-codon_E.coli-R, which also creates overhangs with the enzymes BamH1 and HindIII. To introduce the amplified fragment into pGM1192, this plasmid was digested with BamH1 and HindIII. The plasmid pGM1192-*aesC*$_{Co}$ was sequenced to confirm the correctness of the inserts. *E. coli* Nova Blue was transformed with pGM1192-*aesC*$_{Co}$ and finally, the plasmid was transferred to *E. coli* Rosetta (DE3) for the expression of *aesC*$_{Co}$.

2.2.18 Construction of the plasmids pRM4-*bldC*, pRM4-*lacI*, pRM4-*glts* and pRM4-*bldC-lacI-glts*

To construct the overexpression plasmids, the putative *bldC* (AJAP_RS36645), the putative *lacI* (AJAP_RS11995) and glutamate synthase (*glts*)(AJA_RS11230) genes of *A. japonicum* were amplified via PCR with the primers listed in (Table 2.6) and purified using QIAquick gel extraction kit. The pRM4 vector, containing the constitutive promoter *ermEp**, was linearized with the restriction enzyme NdeI and purified. Using NEBuilder HiFi DNA Assembly cloning kit (NEB, catalog no.E2621S) the linearized pRM4 was ligated with each of the amplified genes. In addition the pRM4-*bldC-lacI-glts* was constructed containing all the three genes. The plasmids were independently transferred into *A. japonicum* WT via conjugation where it integrated via the ϕC31 att site into the chromosome (Stegmann *et al.*, 2001) resulting in the strains *A. japonicum* (*bldC*), *A. japonicum* (*lacI*), *A. japonicum* (*glts*) and *A. japonicum* (*bldC, lacI, glts*)

2.2.19 Construction of *A. japonicum* LDAPP1

To construct the plasmid pDAPP1, *dappA1* (AJAP_RS1950), *dappC1* (AJAP_RS1940) and *aesB* (AJAP_RS08345) were amplified using the primers listed in (Table 2.6) and cloned via NEBuilder HiFi DNA Assembly (New England BioLabs) into pRM4 under the control of the constitutive promoter *ermEp**. The resulting plasmid pDAPP1 was sequenced to verify its correctness and was transferred to *A. japonicum* ΔEDDS, generating the strain *A. japonicum* LDAPP1.

2.2.20 Construction of *A. japonicum* LDAPP2

To construct the plasmid pDAPP2, *dappA2* (AJAP_RS22275) *dappC2* (AJAP_RS22260) and *aesB* (AJAP_RS08345) were amplified using the primers listed in (Table 2.6) and cloned via NEBuilder HiFi DNA Assembly (New England BioLabs) into pRM4 under the control of the constitutive *ermEp**. The resulting plasmid pDAPP1 was sequenced to verify its correctness and transferred to *A. japonicum* ΔEDDS, generating the strain *A. japonicum* LDAPP2.

2.2.21 Protein purification

E. coli Rosetta (DE3) was used to express all the genes. All the primers and plasmids used for gene expression are shown in (Table2.6). Cells were cultivated in 10 ml LB medium containing the appropriate antibiotic, overnight at 37 °C 180 rpm. The next day, 5 ml of the pre-culture was used to inoculate the main culture in 300 ml LB without antibiotics. The cells were incubated at 37 °C until they reached exponential growth (OD_{600} 0.6-0.8). Followed the incubation time. Cells were harvested by centrifugation at 4000 g for 10 min at 4 °C, and disrupted by French Press in 20 ml of lysis buffer (50 mM Tris-HCl (pH 8.0), 100 mM NaCl, DNAse, and protease inhibitor cocktail). The cell lysates were centrifuged at 18,000 rpm for 30 min at 4 °C and the supernatants were filtered with a 0.22 μM filter. 5 ml Strep-Tactin®XT superflow (iba, Göttingen, Germany) columns were used to purify Strep-tagged proteins. The cell extracts were loaded into the columns, washed with wash buffer W (100 mM Tris-HCl pH 8 and 150 mM NaCl, 1mM EDTA) and eluted with elution buffer BXT (100 mM Tris-HCl pH 8.0, 150 mM NaCl, 1mM EDTA and 50 mM biotin). The buffer of all purified proteins was exchanged using Amicon™ Ultra-15 Cen-

trifugal Filter with the appropriate cut-off value. All purifications were verified via SDS-PAGE.

2.2.22 Measurment of argininosuccinate lyase activity

To determine the Asl_{Aj} activity, 10 μg of purified Asl_{Aj} were used for the enzymatic reaction. The reaction mixture contained 100 mM KH_2PO_4 buffer with 0.5 mM argininosuccinate (ASA) as substrate. The reaction was started through the addition of 10 μg ASL. Samples were taken at time 0 and after 1 and 3 hours. The fumarate formation was measured through the absorption at 240 nm in 96-well plates with a Tecan reader and by HPLC-MS.

[*S,S*]-EDDS/[*S,S*]-EDDS-Zn^{2+} degradation through ASL was also tested. The reaction mixture contained 100 mM 100 mM 100 mM KH_2PO_4 buffer and 0.2 mM or 0.5 mM [*S,S*]-EDDS. The reaction was started through the addition of 10 μg ASL. The control contained additionally 100 mM KH_2PO_4 buffer instead of ASL. Samples were taken after 0, 1, and 3 hours and inactivated for 10 minutes at 90°C.

2.2.23 Enzymatic reactions with the putative ornithine cyclodeaminase (AesA)

The absorption spectra of AesA were measured with a Tecan Spark spectrophotometer at a constant wavelength of 340 nm. The measurement period varied depending on the experiment. The measurement temperature was set at 29 °C, as these are the optimal cultivation conditions of actinomycetes. Tris-HCl (50 mM, pH 8.0) was used as a buffer. Substrates were pipetted into Greiner 96-well flat-bottom plates. The reactions were started by adding the cofactors NAD^+ or NADH. The reaction consisted of 1 μM of AesA, 200 μM of NAD^+, $NADP^+$ or NADH, 50 mM TRIS-HCl (pH 8.0) and 1 mM substrate (OAA, L-ornithine, L-DAPP, L-aspartic acid, L-alanine, and malate).

2.2.24 Feeding with naturally occurring precursors

A. japonicum WT was cultivated under EDDS production conditions, described previously in section 2.2.8. Cultures were fed with 5 mg/ml precursor at the beginning of the growth and then incubated for five days at 29°C. After this time, samples

were centrifuged at 5000 rpm. For the detection of [*S,S*]-EDDS, 1 ml of supernatant was mixed with 20 μl of $CuSO_4$ (100 mM) and once again centrifuged before using the supernatant for HPLC-DAD analysis.

2.2.25 Feeding with isotope-labeled precursors

For feeding studies, cultures of *A. japonicum* OP2 was cultvated in M7-medium as described above. The respective isotope-enriched precursors (i.e., 1,4-^{13}C-^{15}N-L-aspartic acid, ^{15}N-L-aspartic acid, ^{13}C5,^{15}N2-L-ornithine, Alpha-^{15}N and L-ornithine (5-^{15}N) were added to the main cultures at a final concentration of 5 mM or 10 mM denpending on the isotope labeled precursor. After 24 h of incubation time, culture supernatants were monitored via HPLC-MS.

2.2.26 Inverse labeling experiments using ^{13}C-glycerol

A. japonicum OP2 mycelia was added to SM-13 growth medium with no carbon source (three separate 0.5 ml culture). The ^{12}C-glycerol source was added to one culture, the ^{13}C-glycerol source to the second, and the ^{13}C-glycerol source plus 5 mM L-aspartic acid, L-ornithine or L-DAPP the last culture. Cultures were grown for four days, and then centrifuged at 4,800 rcf for ten minutes. The resulting supernatants were analyzed by HPLC-MS.

2.2.27 Inverse labeling experiments using $^{15}NH_4Cl$

A. japonicum OP2 mycelia was added to SM-13 growth medium with no nitrogen source (three separate 0.5 ml cultures). The ^{14}N-NH_4Cl source was added to one culture, the ^{15}N-NH_4Cl to the second, and the ^{15}N-NH_4Cl plus 5 mM L-aspartic acid, L-ornithine or L-DAPP the last culture. Cultures were grown for four days, and then centrifuged at 4,800 rcf for ten minutes. The resulting supernatants were analyzed by HPLC-MS.

2.2.28 Quantification and statistical analysis

Three biological replicates were analyzed for each mutant. For every mutant, one pre-culture was used. Three independent flasks that were inoculated with the same pre-culture under identical conditions were considered different biological

replicates. Every measured data point, as well as the mean and SD of the 3 replicates are shown in the graphs. GraphPad PRISM was used to perform paired Student's t tests to determine the statistical significance. Asterisks in the figures were used to symbolize the p value: One asterisk represents $p \leq 0.05$, two asterisks $p \leq 0.01$, three asterisks $p \leq 0.001$, and four asterisks $p \leq 0.0001$.

Chapter 3

Results and Discussion

3.1 Studying the feasibility of using *A. japonicum* as a biofertilizer

[*S,S*]-EDDS, has been shown to be an environmentally sustainable alternative to conventional synthetic chelating agents such as EDTA or o,o-EDDHA. Its effectiveness as a fertilizer has been demonstrated by increased Fe^{2+} and Zn^{2+} supply in susceptible plants (López-Rayo *et al.*, 2016, 2019). The highest Zn^{2+} concentration was observed 7 days after treatment of the plants with [*S,S*]-EDDS. At this time [*S,S*]-EDDS was still detectable in the soil. In long-term experiments (21 or 25 days after treatment), the concentration of the micronutrient was lower. This decrease in efficacy is correlated with the complete biodegradation of [*S,S*]-EDDS, which occurs after approximately 7-11 days (Tandy *et al.*, 2006). Based on this, we hypothesised that *A. japonicum* could be used directly as a biofertilizer. However, *A. japonicum* wild type (WT) synthesises [*S,S*]-EDDS only under zinc-deficient conditions ($Zn^{2+} \leq 2\ \mu M$) (Cebulla, 1995; Zwicker *et al.*, 1997; Spohn *et al.*, 2016). To avoid the inhibition of [*S,S*]-EDDS production in *A. japonicum* WT by the Zn^{2+} concentration present in the soil, a zinc-deregulated mutant was used.

Zinc-deregulated *A. japonicum* mutants (*A. japonicum* Δ*zur*, *A. japonicum* SP44, *A. japonicum* OPl, and *A. japonicum* OP2) capable of producing [*S,S*]-EDDS even in the presence of Zn^{2+} have been developed (Spohn *et al.*, 2016; Edenhart *et al.*, 2020). Among the available mutants, *A. japonicum* SP44 was selected for its ability to sporulate. This ability was not retained in the *A. japonicum* Δ*zur* mutant.

To explore the potential use of *A. japonicum* SP44 as a biofertilizer, experiments were conducted to determine its growth and its ability to produce [*S,S*]-EDDS in

soil. Furthermore, pot experiments under controlled conditions were conducted to examine how effective *A. japonicum* SP44 could be in improving Zn^{2+} uptake in black beans (*Phaseolus vulgaris* cv. Black pole) grown under zinc-deficient conditions. To simulate zinc-deficient conditions, calcareous soil was chosen (Table 2.7). Zinc deficiency is a widespread agricultural problem in this type of soil , especially in crops grown on calcareous soil where zinc fertilization is essential (Robson, 1993). The reason for zinc deficiency in this type of soil is the adsorption of the microelements on soil colloids or precipitation (Saeed and Fox, 1977).

The study included pots treated under five different conditions: (1) *A. japonicum* WT (negative control, zinc-regulated [*S,S*]-EDDS producer), (2) *A. japonicum* ΔEDDS (negative control, [*S,S*]-EDDS deletion mutant, unable to produce [*S,S*]-EDDS), (3) *A. japonicum* SP44 (zinc-deregulated [*S,S*]-EDDS overproducer), (4) commercially [*S,S*]-EDDS (positive control), and (5) control pots without any treatment. For each condition, five replicates were included for further statistical analysis. Microelement uptake in the plants was measured at 7, 21, and 25 days after treatment, and compared with the control group and with the direct application of [*S,S*]-EDDS. This comparison should help to understand the potential benefits of using *A. japonicum* as a biofertilizer.

3.1.1 Investigating the growth of *A. japonicum* in the soil

To assess the suitability of the soil type for supporting the growth of *A. japonicum* strains, l g of sterile calcareous soil was inoculated with 10^5 *A. japonicum* spores from and the colony-forming units (CFU) was monitored at different time points (Section 2.2.2). In order to maintain consistency with the experiments conducted with plants, a calcareous soil type, zinc-deficient (Table 2.7) was selected. In order to make the soil samples sterile, they had to be autoclaved three times before they could be inoculated with the spores of *A. japonicum*.

lt was found that *A. japonicum* WT, *A. japonicum* ΔEDDS and *A. japonicum* SP44 were able to grow in the used soil, thereby confirming that the soil was suitable for this type of experiment. The growth was characterized by an exponential phase observed between days one and three, followed by an early stationary phase that lasted until day five, the final time point of measurement. This result confirmed the growth of *A. japonicum* strains in a zinc-deficient calcareous soil (Figure 3.1).

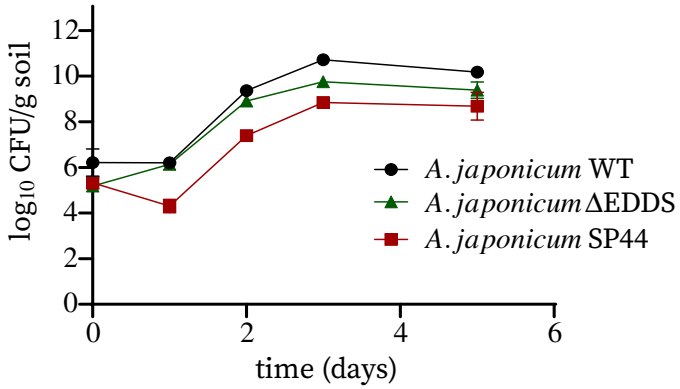

Figure 3.1. **Growth of *A. japonicum* WT and mutants in the soil**. Colony forming units (cfu) determined at different time points of *A. japonicum* WT and mutant´s growth in soil. 1 g of sterile soil was inoculated with 10^5 spores. The number of cfu was determined at every time point by counting the number of bacterial colonies on agar plates.

3.1.2 Assessing the production of [*S,S*]-EDDS by *A. japonicum* in a soil environment

While previous studies have evaluated the production of [*S,S*]-EDDS by *A. japonicum* under laboratory conditions, (Cebulla, 1995; Zwicker *et al.*, 1997; Spohn *et al.*, 2016; Edenhart *et al.*, 2020), information on its production in a soil environment is limited. To investigate this, two experiments were conducted: First, transcriptional analysis of [*S,S*]-EDDS biosynthetic genes (*aesA-D*) in soil through RNA isolation and RT-PCR, and second, detection of [*S,S*]-EDDS produced by *A. japonicum* SP44 in soil using HPLC-MS analysis.

3.1.2.1 Transcription analysis of [*S,S*]-EDDS genes in the soil

To analyze the expression of the [*S,S*]-EDDS biosynthetic gene duster (BGC) in soil, 10^5 spores of *A. japonicum* WT and mutants were used to inoculate three grams of sterile soil samples. After three days, total RNA was isolated from soil samples using RNAeasy power soil total RNA kit (Section 2.2.3) with an average yield of 15 μg and A260/280 ratio of 1.8 in all the samples. The RNA was used to produce

the corresponding cDNA. PCR was performed using cDNA as a template and the primers listed in (Table 2.6). The major sigma factor (*sigB)* of *A. japonicum* WT, which is constitutively expressed throughout growth, was used as a positive control. The negative control consisted of a sterile soil sample without bacterial inoculation and was treated under the same conditions during the RNA isolation and PCR. The transcriptional analysis revealed that the housekeeping gene, *sigB*, was expressed in all samples inoculated with bacteria. Expression of the [*S,S*]-EDDS genes was only observed in soil samples inoculated with *A. japonicum* SP44, the zinc-deregulated [*S,S*]-EDDS producer. In *A. japonicum* WT, expression of the *aes* genes could not be detected (Figure 3.2).

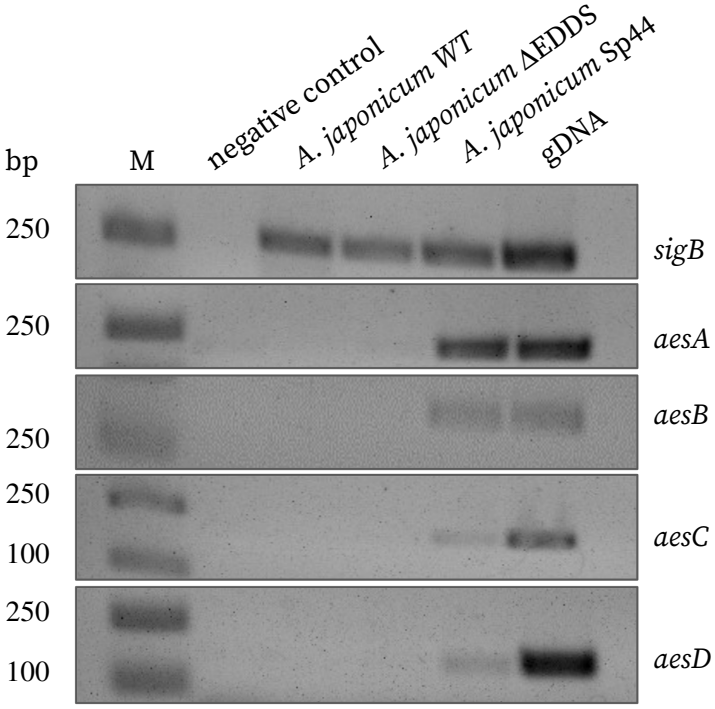

Figure 3.2. **Zinc-dependent transcription of the [*S,S*]-EDDS biosynthetic genes in *A. japonicum* strains grown in soil**. Sterile soil samples were inoculated with spores and incubated for 3 days. (M) marker. (Negative control) sterile soil sample. (*A. japonicum* WT) wild type strain, zinc-regulated [S,S]-EDDS produce. (*A. japonicum* ΔEDDS) [*S,S*]-EDDS deletion mutant. (*A. japonicum* SP44) zinc-deregulated [*S,S*]-EDDS overproducer. (gDNA) *A. japonicum* genome. (*sigB*) general stress-response sigma factor (housekeeping gene). *aes*A/B/C/D: [*S,S*]-EDDS biosynthetic genes.

3.1.2.2 Optimization of the analytical method for the detection of [*S,S*]-EDDS in soil samples

The establishment of a reliable method based on the derivatization of [*S,S*]-EDDS with 9-fluorenylmethyl chloroformate (Fmoc-Cl) before HPLC-MS analysis was essential for the detection of [*S,S*]-EDDS in soil samples. The process known as derivatization consists of the decoration of a natural product with a non-natural moiety using a derivatizing agent, to yield the highly fluorescent derivatives for HPLC analysis (Ho, 2005; Hughes, 2021). Fmoc-Cl has been used to derivatize amines primarily in aqueous media (Sastre Toraño and Guchelaar, 1998), and it was first introduced by (Carpino and Han, 1972) for the derivatization for primary and secondary amines. Although the method for the determination of [S,S]-EDDS in soil solution had previously been described by (Tandy *et al.*, 2005) it needed to be adapted to the HPLC-MS instrument used.

First, the method was tested using an [*S,S*]-EDDS standard in pure water. Therefore, 97.7 μM [*S,S*]-EDDS was derivatized with Fmoc-Cl in 1 M buffer borate pH 8.0 (described in detail in section 2.2.5). In positive mode, a peak with mass 515.1 *m/z* for Fmoc-[S,S] EDDS (single derivatized [*S,S*]-EDDS) was detected in the Based Peak Chromatogram (BPC) (Figure 3.3). To evaluate the analysis of [*S,S*]-EDDS from soil samples and determine the detection limit of this method with the available instruments, decreasing concentrations from 9.7 μM to 0.0097 μM of [*S,S*]-EDDS standard were applied to the soil. After re-extraction of [*S,S*]-EDDS, the samples were treated with EDTA buffer prior to derivatization in order to complex the metal present in the soil sample with EDTA, as metals present in the soil would form a complex with [*S,S*]-EDDS and thus prevent its Fmoc-Cl derivatization (Tandy *et al.*, 2005). The samples were analyzed by HPLC-MS. The HPLC-MS chromatogram revealed a peak with *m/z* 515.1 $[M+H]^+$, which corresponded to Fmoc-[*S,S*]-EDDS. However, this method was unable to detect low concentrations of the compound in the soil samples (Figure 3.4).

To verify the identity of the detected peak, EDTA buffer was treated with Fmoc-Cl as a control. Since both [*S,S*]-EDDS and EDTA have the same mass signal with *m/z* 293 $[M+H]^+$, it was essential to demonstrate that the detected peak was indeed Fmoc-[*S,S*]-EDDS and not Fmoc-EDTA. It was confirmed, as expected, that Fmoc-Cl did not derivatize EDTA (Figure S1) because EDTA contains tertiary amines instead

of secondary amines like [*S,S*]-EDDS (Ho, 2005).

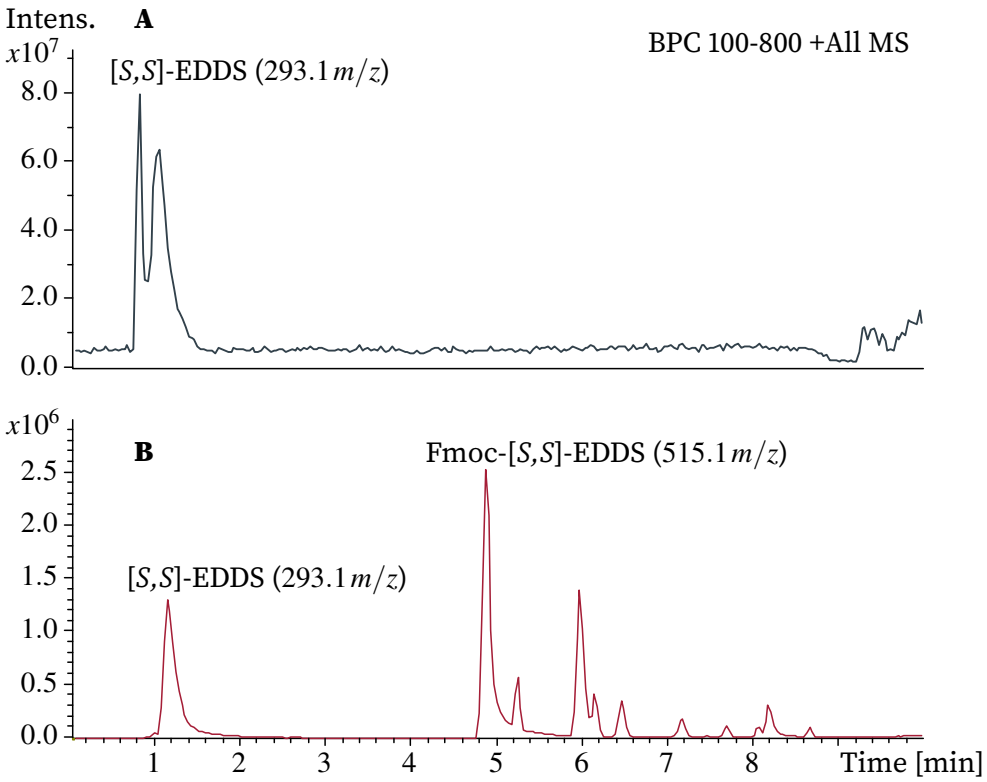

Figure 3.3. **HPLC-MS analysis of Fmoc-[*S,S*]-EDDS standard solution.** Base peak chromatograms (BPC) in positive mode of (A) 97.7 μM [*S,S*]-EDDS, (*m/z* 293.1 $[M+H]^+$). (B) 97.7 μM [*S,S*]-EDDS derivatized with Fmoc (Fmoc-[*S,S*]-EDDS) in borate buffer pH 8.0 (*m/z* 515.1 $[M+H]^+$). The peak *m/z* 293.1 $[M+H]^+$ corresponds to underivatized [*S,S*]-EDDS, and extra peaks are attributed to reaction side products.

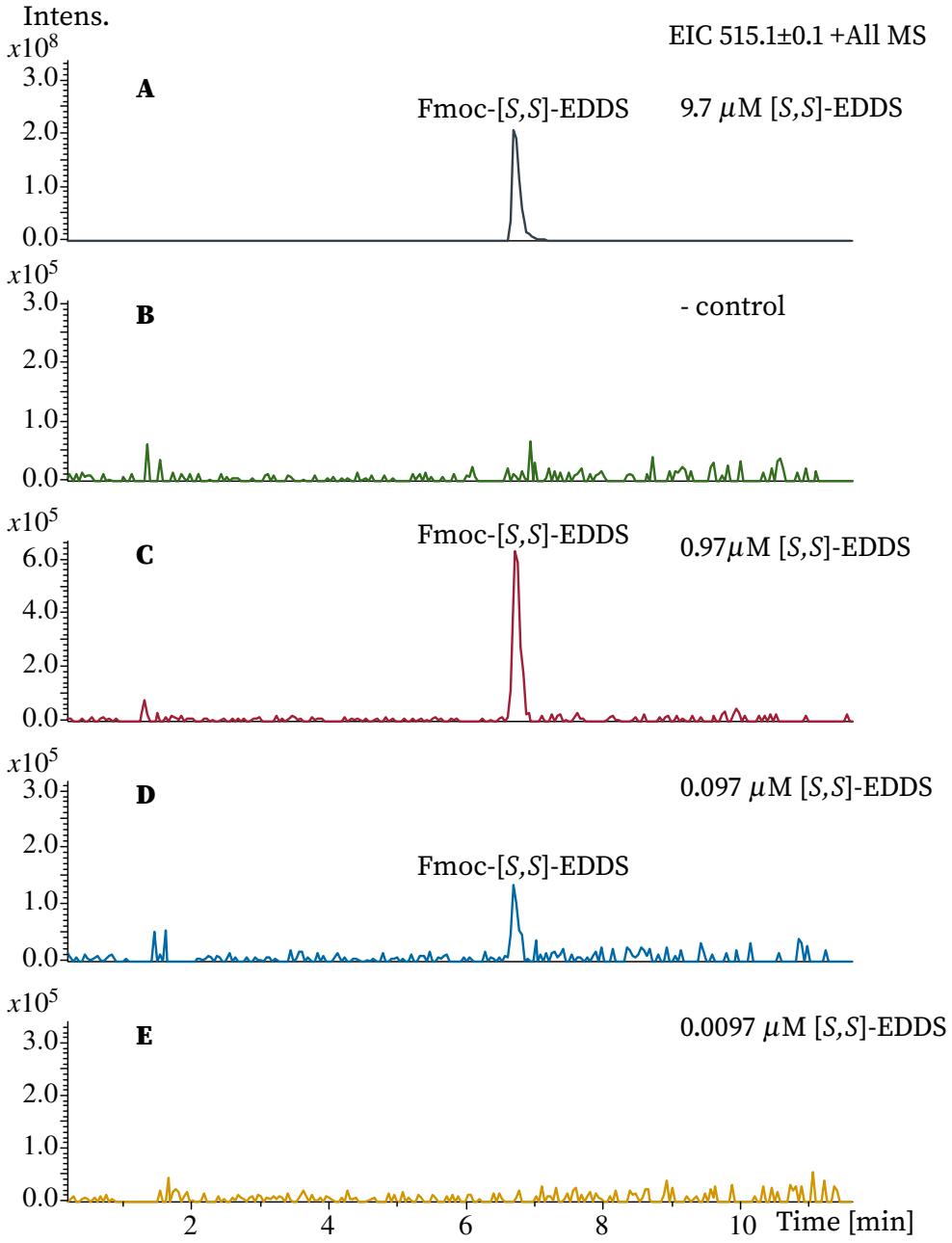

Figure 3.4. **HPLC-MS signals of decreasing concentrations of Fmoc-[*S,S*]-EDDS standard solutions applied to soil samples.** Soil extracts were pre-treated with EDTA buffer pH 11.5 before the derivatization with Fmoc-Cl in borate buffer pH 8.0. Extracted ion chromatograms (EIC) from soil extracts for Fmoc-[*S,S*]-EDDS *m/z* 515.1 $[M+H]^+$. (A) 9.7 µM [*S,S*]-EDDS. (B) negative control, sterile soil sample. (C) 0.97 µM [*S,S*]-EDDS. (D) 0.097 µM [*S,S*]-EDDS. (E) 0.0097 µM [*S,S*]-EDDS.

3.1.2.3 Detection of [*S,S*]-EDDS produced by *A. japonicum* in soil samples

To determine the production of [*S,S*]-EDDS by *A. japonicum* SP44 in soil, 10 g of three times sterilized calcareous soil was inoculated with 10^5 spores. The soil samples were inoculated for ten days at 29° C and every day, 1 ml sterile water was added to the samples to keep the humidity. Soil extracts were treated as described before, and analyzed by HPLC-MS. As controls, 10^5 spores from *A. japonicum* ΔEDDS ([*S,S*]-EDDS deletion mutant) and *A. japonicum* WT (unable to produce [*S,S*]-EDDS due to zinc concentrations in soil above 2 μM) were used. HPLC-MS results revealed a peak with the *m/z* value of 515.1 $[M+H]^+$, corresponding to Fmoc-[*S,S*]-EDDS only in the samples where the [*S,S*]-EDDS standard was applied. [*S,S*]-EDDS production was not detected in soil samples inoculated with *A. japonicum* WT, *A. japonicum* ΔEDDS, or *A. japonicum* SP44.

The method for the detection of [*S,S*]-EDDS from soil samples has been established. However, no [*S,S*]-EDDS was found to be produced by *A. japonicum* SP44 in soil (Figure 3.5).

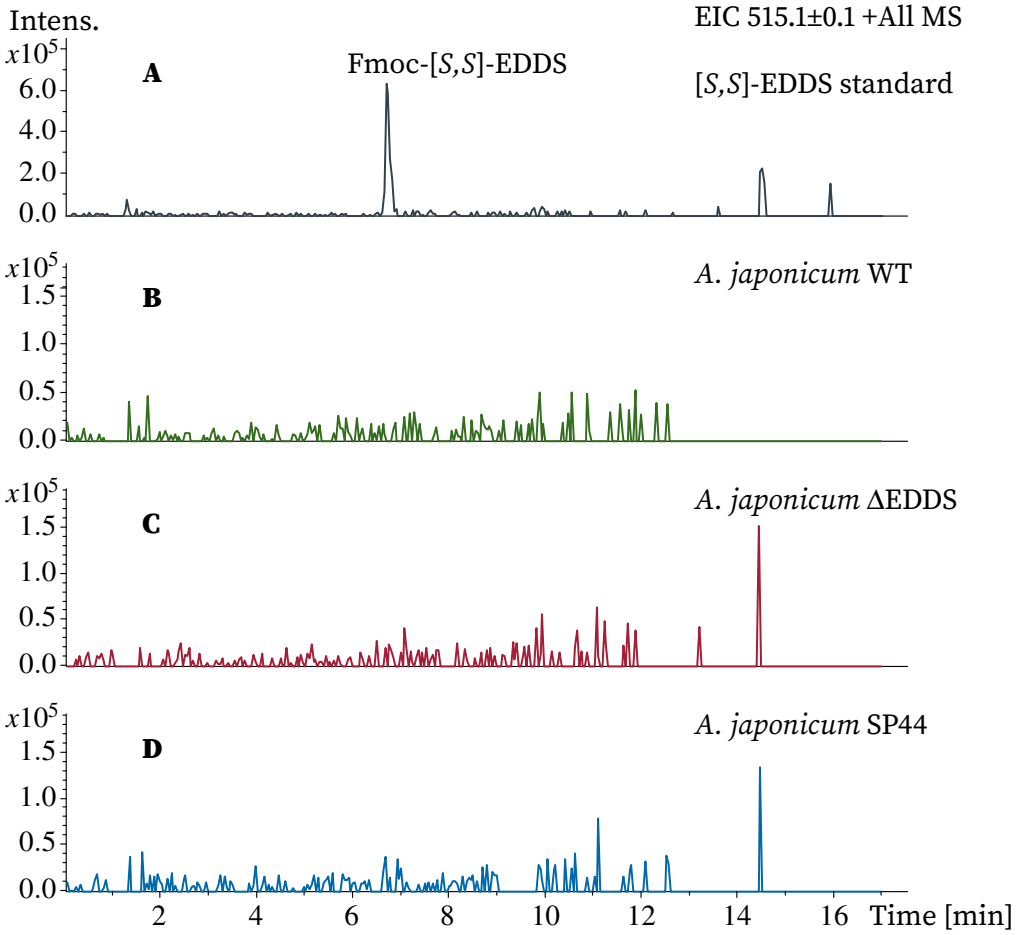

Figure 3.5. **HPLC-MS analysis of soil samples inoculated with *A. japonicum* strains.** Extracted ion chromatogram (EIC) for Fmoc-[*S,S*]-EDDS, *m/z* 515.1 $[M+H]^+$. (A) [*S,S*]-EDDS standard. (B) *A. japonicum* WT. (C) *A. japonicum* ΔEDDS. (D) *A. japonicum* SP44.

3.1.3 Evaluation of the ability of *A. japonicum* SP44 to enhance micronutrient uptake in plants

Zinc deficiency is a prevalent issue in a wide range of soil types, such as high-pH calcareous soils, sandy soils, and soils with an excess of phosphorus-containing fertilizers. The primary factor contributing to the limited availability of zinc in calcareous soils with high pH levels is the adsorption of zinc to clay or calcium carbonate (Trehan and Sekhon, 1977). Zinc deficiency is a common problem for *Phaseolus vulgaris* plants grown on calcareous soils (Marschner, 2012).

Chelating agents have been successfully used for iron, manganese, copper and zinc fertilization under conditions simulating calcaroeus soil (López-Rayo *et al.*, 2012, 2015). In particular, fertilization with Zn^{2+}-[*S,S*]-EDDS has been shown to provide sufficient Zn^{2+} to plants at a similar rate to EDTA (López-Rayo *et al.*, 2015) and is therefore suitable to replace EDTA. However, due to the biodegradability of [*S,S*]-EDDS in the soil, regular applications of Zn^{2+} -[*S,S*]-EDDS have been proposed (López-Rayo *et al.*, 2015).

The aim of this study was to investigate the potential of *A. japonicum* SP44 as a biofertilizer for *Phaseolus vulgaris* plants. These experiments were carried out despite the fact the that it was not possible to identify [*S,S*]-EDDS produced by *A. japonicum* in the soil (Section 3.1.2.3) . Detection of complexing agents in soil by HPLC is very difficult; they may be produced in very small amounts (Rai *et al.*, 2020) and form complexes with the ions present in the soil. Therefore, the possibility that [*S,S*]-EDDS is produced by *A. japonicum* in soil is not necessarily excluded. Further experiments were carried out to evaluate the potential of the bacterium as a biofertilizer. By including the [*S,S*]-EDDS null mutant in these experiments, it was possible to distinguish whether an improvement in zinc uptake by plants was due to the [*S,S*]-EDDS produced by *A. japonicum* or whether the strain itself had a positive effect on plant growth.

This study was carried out under controlled conditions, from the initial stages of seed germination, followed by hydroponic growth where Zn^{2+}-deficiency was induced. Plants were transplanted into pots and one day later the different treatments (conditions 1-5) were applied. Five replicate pots per treatment were considered. Each pot was inoculated with 10^8 *A. japonicum* spores (*A. japonicum* WT, *A. japonicum* SP44 and *A. japonicum* ΔEDDS).

Plants treated with the [*S,S*]-EDDS standard were used as a positive control and untreated plants as a negative control. Plants were grown under these conditions for 24 days. Sampling was performed at 7 days post treatment (DPT), 21 DPT and 24 DPT. To evaluate the efficacy of the treatment, three analyses were performed: 1) chlorophyll development using the soil plant analysis development (SPAD) chlorophyll meter, 2) plant growth, measuring the dry weight (g/plant) of the different plant organs and 3) analysis of micronutrient content (Zn^{2+}, Fe^{2+}, Cu^{2+}, and Mn^{2+}) in the leaves, stems, and roots by atomic absorption spectrometry (AAS).

Plant analysis

Zn^{2+} deficiency in plants is characterized by stunted plants, smaller leaves, and chlorosis (Figure 3.6). The evolution of the chlorophyll content was evaluated using the chlorophyll meter SPAD in all leaf stages, as described by (López-Rayo *et al.*, 2015).

The chlorophyll content of a plant gives an indication of its health status and is used to determine the best time to apply the optimized amount of fertilizer to achieve higher yields, better quality crops and reduce environmental impact.

The chlorophyll content of the leaves was measured (only the values measured on the youngest fully expanded leaf (third leaf stage) are shown in (Figure 3.7). An ANOVA analysis revealed that no significant differences were found for the treatments, compared to the negative control, from the beginning of the experiment until the last day (24 DPT).

Figure 3.6. **Zn^{2+} deficiency in *Phaseolus vulgaris* cv. Black pole (common bean)**. Stunted plants, smaller leaves and chlorosis are visible.

To determine the impact of the treatments on plant growth and development, the dry weight of leaves stems and roots were measured. Hence, it is possible to determine the actual amount of plant material produced. This amount which can then be compared to the dry weight of the non-treated plants to determine the effectiveness of the treatment. The results did not show significant differences between the dry weight of treated and untreated plant organs (Figure 3.8).

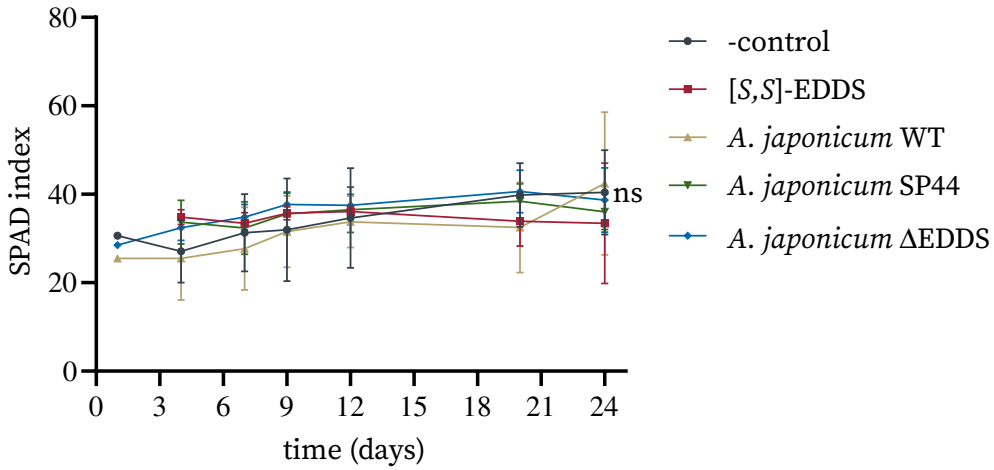

Figure 3.7. **Chlorophyll content of the plants grown in the presence of *A. japonicum* strains**. Stage 3 leaves average and standard error of the soil and plant analyzer development (SPAD) index over a 24-day period post following treatments (DPT). Error bars indicate the mean of standard deviation of 3 replicates of SPAD readings. Statistical significance was determined by ANOVA. ns., not significant $p > 0.05$.

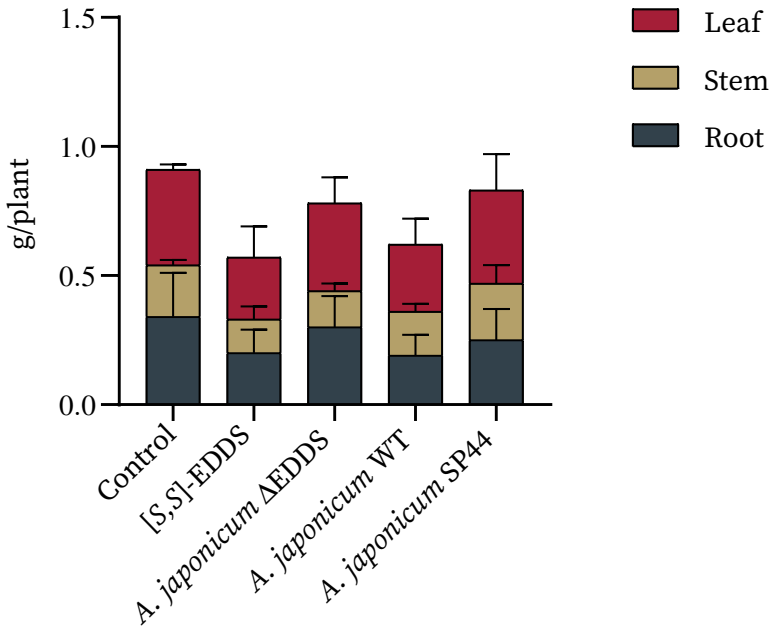

Figure 3.8. **Dry weight of leaves, stems, and roots of plants undergoing the different treatments.** Samples were taken after 7 days of treatment. Error bars indicate the mean and SD of 5 replicates. Statistical significance was determined by two-way ANOVA using Dunnett's multiple comparisons test.

The effectiveness of the treatments concerning the improvement of micronutrient concentration was also assessed by atomic absorption spectrophotometry (AAS). After 7, 21 and 24 DPT, leaves, stems and roots samples were taken to analyze the content of Zn^{2+}, Fe^{2+}, Cu^{2+} and Mn^{2+}. The use of *A. japonicum* SP44 strain as a biofertilizer did not lead to an increase in Zn^{2+} in the plant organs after 7 (Figure 3.9), 21 (Figure S2) or 24 days (Figure S3).

The application of *A. japonicum* SP44 did not result in any improvement in the uptake of microelements such as iron, copper, and manganese in the plant at 7, 21 or 24 DPT (Figure S4-S9). On the other hand, the concentration of Zn^{2+} was significantly increased in the three plant organs at 7 DAT DPT with [*S,S*]-EDDS, compared to the untreated plants. This indicates that [*S,S*]-EDDS successfully solubilizes Zn^{2+} and makes it available for the plant. However, the effectiveness of *A. japonicum* SP44 as a biofertilizer has not been demonstrated.

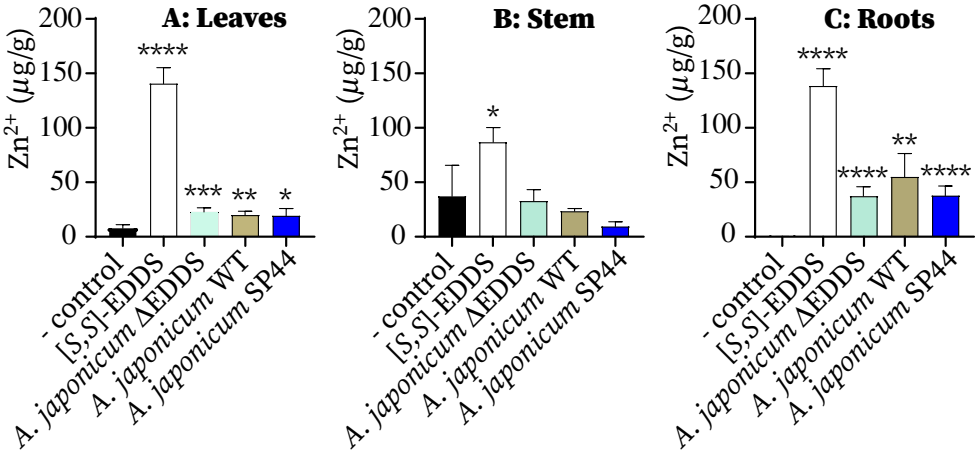

Figure 3.9. **Zn^{2+} content in *Phaseolus vulgaris***. Measurements were performed with samples obtained from the leaves, stems and roots 7 days post treatments. Error bars indicate the mean and standard deviation of 5 replicates. Statistical significance (*p<0.05, **p<0.01, ***p<0.001, ****p<0.0001) was determined by unpaired Student´s test.

Discussion

For micronutrient fertilization recalcitrant chelating agents such as ethylenediamine tetraacetic acid (EDTA) are traditionally used. EDTA forms very stable complexes with metals, making it recalcitrant in soil. It can persist in the environment for long periods and can lead to the accumulation of heavy metals in the soil (Saifullah *et al.*, 2009; Satroutdinov *et al.*, 2000). The use of EDTA is currently not considered sustainable or environmentally friendly in agriculture (López-Rayo *et al.*, 2016). Simulation data of the EDTA biodegradation shows that once EDTA forms a complex with Fe^{2+}, it cannot be biodegraded (Willett and Rittmann, 2003). The degradation of EDTA was also studied in soil experiments, showing only 14 % of EDTA degraded after 20 days (Wen *et al.*, 2009). Therefore, there is an increasing interest in using biodegradable chelating agents as fertilizers in agriculture, which can serve the same function as EDTA without causing harm to the environment

An alternative approach is the use of [*S,S*]-EDDS, a biodegradable chelating agent and structural isomer of EDTA (Schowanek, 1997). Zn^{2+}-[*S,S*]-EDDS application has been shown to increase zinc nutrition in plants (López-Rayo *et al.*, 2016). [*S,S*]-EDDS has been shown to be degraded after a lag phase of 7-11 days with a half-life of 4.18-5.60 days (Tandy *et al.*, 2006). However, the good biodegradability of [S,S]-EDDS in this case has the disadvantage that [*S,S*]-EDDS needs to be applied to soil on a regular basis (López-Rayo *et al.*, 2015)

A possible solution could be the use of *A. japonicum*, a soil bacterium that naturally produces [*S,S*]-EDDS. The continuous growth of the bacterium in the soil could ensure a constant supply of [*S,S*]-EDDS. To evaluate the suitability of *A. japonicum* as a biofertilizer, the zinc deregulatory overproducer strain *A. japonicum* SP44 was used, to counteract the inhibition of [*S,S*]-EDDS by the zinc concentration present in the soil. *A. japonicum* WT, in which [*S,S*]-EDDS production is zinc-regulated (inhibited at Zn^{2+} concentrations ≥ 2), and *A. japonicum* ΔEDDS, in which the [*S,S*]-EDDS genes have been deleted, were included in the experiment as negative controls. Although typical bacterial growth of all *A. japonicum* strains could be detected in the soil selected for our experiments, [*S,S*]-EDDS could not be detected in any of the soil samples.

The growth curve of *A. japonicum* strains grown in soil was compared with the growth curve of strains grown in synthetic medium (SM) M7 (Zwicker *et al.*, 1997)

optimized for [S,S]-EDDS production. The exponential phase was less prolonged in soil culture. This difference is probably due to sub-optimal nutrient availability in the soil after three days of growth, whereas sufficient glycerol (25 g/l) is provided in SM-medium to sustain an extended prolonged exponential growth phase. A prerequisite for these experiments was the use of sterile soil. A three-step sterilization treatment was required to render the soil sterile. Such a procedure has also been described by (Shuab *et al.*, 2014).

Transcriptional analysis showed that the [*S,S*]-EDDS biosynthesis genes of *A. japonicum* SP44 were expressed when this strain was grown in soil. As expected, the transcription of [*S,S*]-EDDS biosynthesis genes was inhibited in *A. japonicum* WT, because although the experiments were carried out in calcareous soil with a low zinc concentration, it was still higher than 2 μM Zn^{2+}. This result confirmed the role of [*S,S*]-EDDS as a zincophore and was consistent with the observation that no [S,S]-EDDS production was detected in media with zinc concentrations of 2 μM (Zwicker *et al.*, 1997; Spohn *et al.*, 2016). In addition to *A. japonicum* WT, *A. japonicum* SP44 did not appear to produce [*S,S*]-EDDS in soil.

For the extraction and detection of [*S,S*]-EDDS from soil, a method described by (Tandy *et al.*, 2005) was used. The soil sample was first treated with EDTA buffer prior to Fmoc-Cl the derivatization and HPLC-MS analysis. The EDTA buffer was used to achieve maximal conversion of [*S,S*]-EDDS to the Fmoc derivative, since EDTA compplexes the metals present in the soil sample, [S,S]-EDDS remains "free" an derivatization can occur. Furthermore, although both compounds have the same mass and can be detected by HPLC-MS at 293.1 *m/z* $[M+H]^+$, the two structures differ in terms of the amino groups. EDTA contains tertiary instead of secondary amines like [*S,S*]-EDDS These results demonstrated that EDTA was not derivatized by Fmoc-Cl (Figure S1), since Fmoc-Cl is suitable for the derivatization of primary and secondary amines (Ho, 2005). The [S,S]-EDDS detection limit of the method based on UV-detection, was found to be 0.097 μM , which is less sensitive than the detection limit reported by (Tandy *et al.*, 2005). However, in Tandy's approach (Tandy *et al.*, 2005), the Fmoc-[*S,S*]-EDDS derivative was detected using a fluorescence detector. Fluorescence detection has advantages over UV detection of low detection limits and high sensitivity due to low interferences (Tandy *et al.*, 2005). However, such a device was not available during the experimental phase of the project.

Another factor which should be taken into account, is the fact that calcareous soil was used. This type of soil is known to contain high levels of $CaCO_3$, which can make the extraction of [*S,S*]-EDDS difficult, as [*S,S*]-EDDS forms complexes with Ca^{2+} (Vandevivere *et al.*, 2001; Whitburn *et al.*, 1999). Therefore, the presence of $CaCO_3$ in the sample could interfere with derivatization and detection of Fmoc-[S,S]-EDDS by HPLC-MS.

Finally, it remains uncertain whether *A. japonicum* produces [*S,S*]-EDDS in soil. Although transcription analysis indicated expression of *aes* genes, the product could not be detected. Further research needs to be done to determine whether [*S,S*]-EDDS production occurs in this environment.

In the experiments investigating the effect of *A. japonicum* and [*S,S*]-EDDS on plant growth, the micronutrient concentrations in leaves, stems or roots, were not improved after the application of *A. japonicum* SP44, compared to the negative controls (plants without treatment, and treatment with *A. japonicum* WT. Since no [*S,S*]-EDDS could be detected in the soil after the inoculation with *A. japonicum*, this could be the reason why no improvement in the uptake of Zn^{2+} and other trace elements by the plants was observed. As a positive control, a single dose of [*S,S*]-EDDS (24 μmol/pot) was applied, which resulted in increased Zn^{2+} uptake by plants after at 7 DPT. However, this effect dissipated by day 21 DPT. These findings are consistent with those of (López-Rayo *et al.*, 2015), who reported increased Zn^{2+} concentrations in plants treated with formulations containing Zn^{2+}-[*S,S*]-EDDS (2.36 μmol/kg) after at 7 DPT, but showed no effect at 21 DPT. There was an increase in the uptake of Fe^{2+}, Mn^{2+} and Cu^{2+} in the leaves at 7 DPT. In the case of Zn^{2+} the application of the three strains *A. japonicum* WT, *A. japonicum* ΔEDDS and *A. japonicum* SP44, resulted in a remarkable increase of Zn^{2+} concentration in the roots at 7 days DPT. However, this increase is not caused by [*S,S*]-EDDS. Since *A. japonicum* has the genetic potential for the synthesis of other complexing agents, such as albachelin, mirubactin (predicted by antiSMASH v7.0), and amycolachrom (Cebulla, 1995), this effect could also be the consequence of the appearance of these complex agents.

In addition to [*S,S*]-EDDS, the production of these complexing agents could be responsible for the uptake of the ions into the plant. However, they were not detected in the soil samples. Further research is needed to fully evaluate the potential of *A. japonicum* as a biofertilizer and to determine the optimal bacterial concen-

tration required for application to maximize efficacy.

3.2 Studies on the import of Zn-EDDS

Various bacteria, including *Brevundimonas sp.* TN-3 (Mizunashi, 2001), the bacterial strain DSM 9103 (Witschel and Egli, 1997) and *Chelativorans sp.* isolated from industrial wastewater (Poddar *et al.*, 2018), have been shown to be capable of degrading [*S,S*]-EDDS. The degradation involves a step that cleaves [*S,S*]-EDDS to fumarate and ethylenediamine, which is catalysed by the key enzyme EDDS lyase. As this enzyme also catalyses the reverse reaction, it has been used in semi-synthetic approaches to synthesise [*S,S*]-EDDS from fumarate and ethylenediamine (Poddar *et al.*, 2018). The aim of this project was to investigate whether an [*S,S*]-EDDS lyase might be involved in the degradation of the [*S,S*]-EDDS-zinc complexes in *A. japonicum*.

3.2.1 Identification of a putative EDDS lyase in *A. japonicum*

A sequence similarity search was performed in the NCBI microbial database using BLASTP with the EDDS lyase amino acid sequence of *Chelativorans sp.*BNC1 as the query. This search yielded an *A. japonicum* protein with 33 % sequence identity, annotated as a putative argininosuccinate lyase (Asl) (NCBI reference sequence WP_038511517.1) (Figure S13). The corresponding gene encoding a putative argininosuccinate lyase (Asl) (EC 4.3.2.1) in *A. japonicum* was amplified using the primers AslAj-BglII-F and AslAj-HindIII-R (Table 2.6) and cloned into the expression vector pGM1192. Using this expression plasmid, Asl_{Aj} was produced in *E. coli* Rosetta (DE3) as an N-terminal Strep-tagII fusion protein. Strep-tagII-Asl_{Aj} was purified by a Strep-Tactin XT affinity chromatography protocol following the instructions described by providers (Figure 3.10).

3.2.2 Characterization of the Asl of *A. japonicum* (Asl_{Aj})

Asl is responsible for catalyzing the cleavage of argininosuccinate (ASA) into fumarate and arginine (Mishra A, 2017) (Figure 3.11 A). To first evaluate the biological activity of the *A. japonicum* Asl (Asl_{Aj}) produced in *E. coli*, the enzyme was

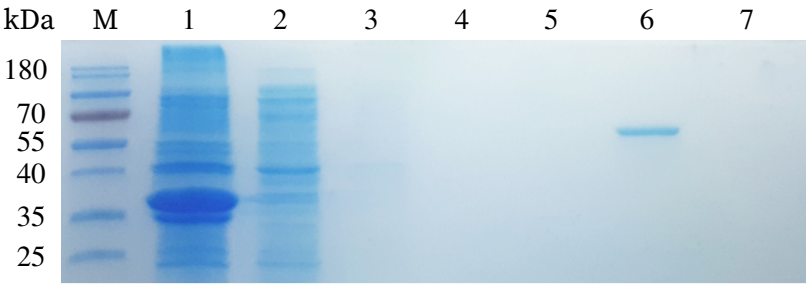

Figure 3.10. **SDS-PAGE of purified argininosuccinate lyase (Strep-Asl$_{Aj}$)** (12% gel). (M) protein ladder (PageRuler Prestained, Thermo Fisher scienific # 26616). (1) cell crude extract from *E. coli* Rosetta (DE3). (2-4) washing fractions. (5-7) elution fractions. (6) elution fraction 2 containing the purified Strep-Asl$_{Aj}$, MW of Strep-Asl$_{Aj}$: $\sim$ 52 kDa.

incubated with ASA and the formation of fumarate was measured using both, spectrophotometric techniques at 240 nm and HPLC-MS. Activity assays were performed using 0.5 mM or 1 mM ASA with Asl$_{Aj}$ and the appearance of fumarate over time at 240 nm was monitored. The absorbance at 240 nm increased progressively over time, indicating fumarate synthesis (Figure 3.11 B). The presence of fumarate was further confirmed by analyzing a sample (taken after 1 hour of reaction) via HPLC-MS, using a fumarate standard (3 mM). The chromatogram revealed a peak with a *m/z* value of 114.9 in the extracted ion chromatogram (EIC) in negative ionization mode, with the same mass and retention time as the fumarate standard (Figure 3.11, C). These findings indicated that Asl$_{Aj}$ was biologically active.

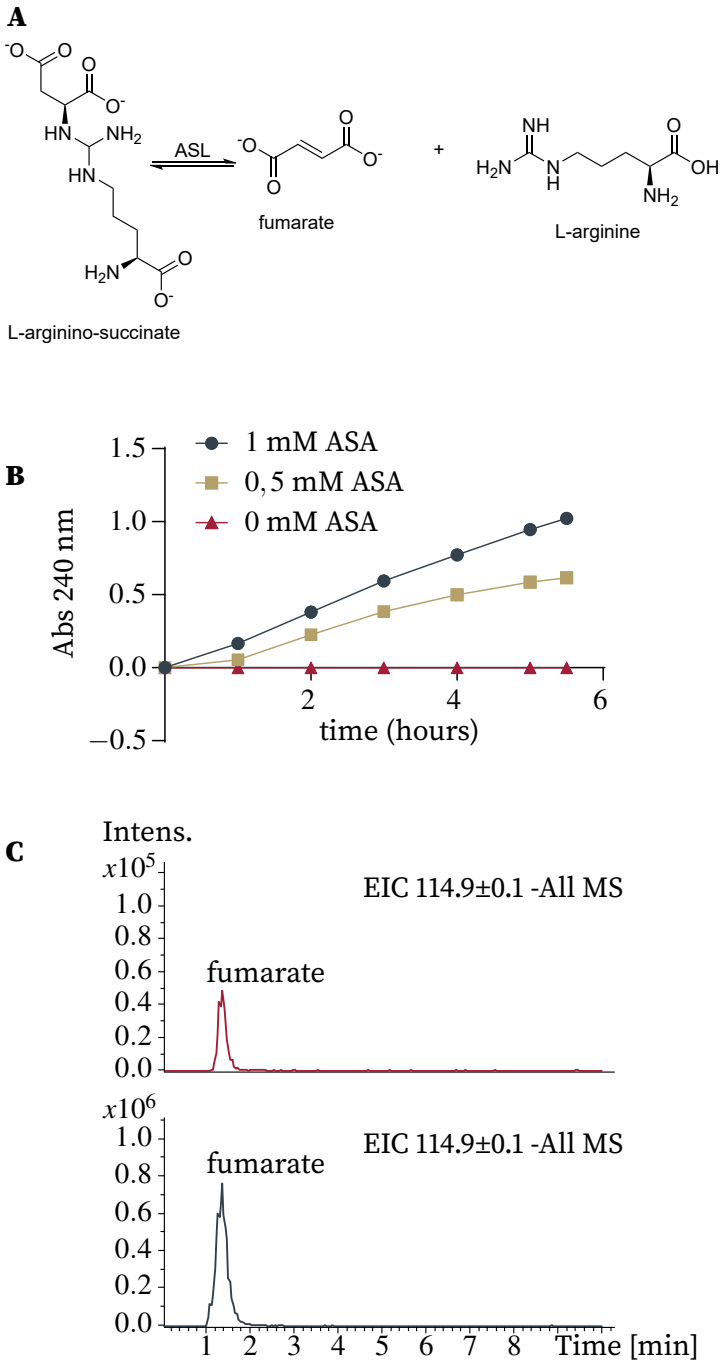

Figure 3.11. **Argininosuccinate lyase activity assay**. (A) Reversible reaction catalyzed by Asl_{Aj}. (B) Spectrophotometric detection (240 nm) of fumarate production over time using 0 mM, 0.5 mM or 1 mM ASA. (C) HPLC-MS detection of fumarate (m/z 114.9) in negative mode. Fumarate produced after 1 hour of reaction (in red). Fumarate standard, 3 mM (in black).

3.2.3 Investigating the Asl_{Aj} activity using [S,S]-EDDS

The investigate the potential of Asl_{Aj} to catalyze the reaction of an EDDS lyase, an enzymatic assay was performed using 10 μM ASL incubated with 0.2 mM [S,S]-EDDS. The formation of fumarate was monitored by recording the absorbance at 240 nm. Additionally, the reaction was assessed over time using HPLC-DAD, with samples taken at 1 and 3 hours to determine any changes in the concentration of [S,S]-EDDS. In addition, Zn^{2+}-[S,S]-EDDS was used as a substrate. The absorbance of a mixture of 10 µM Asl_{Aj} and 0.2 mM Zn^{2+}-[S,S]-EDDS was monitored at 240 nm over a period of three hours. As the absorbance at 240 nm remained at the same level over the time period (Figure 3.12, B), it can be assumed that there was no detectable hydrolysis of the [*S,S*]-EDDS. Quantification of [*S,S*]-EDDS by HPLC-DAD confirmed that its concentration remained constant. The data showed that Asl_{Aj} is incapable of catalyzing the degradation of free [*S,S*]-EDDS or the Zn^{2+}-[*S,S*]-EDDS complex and is therefore not an EDDS lyase (Figure S16).

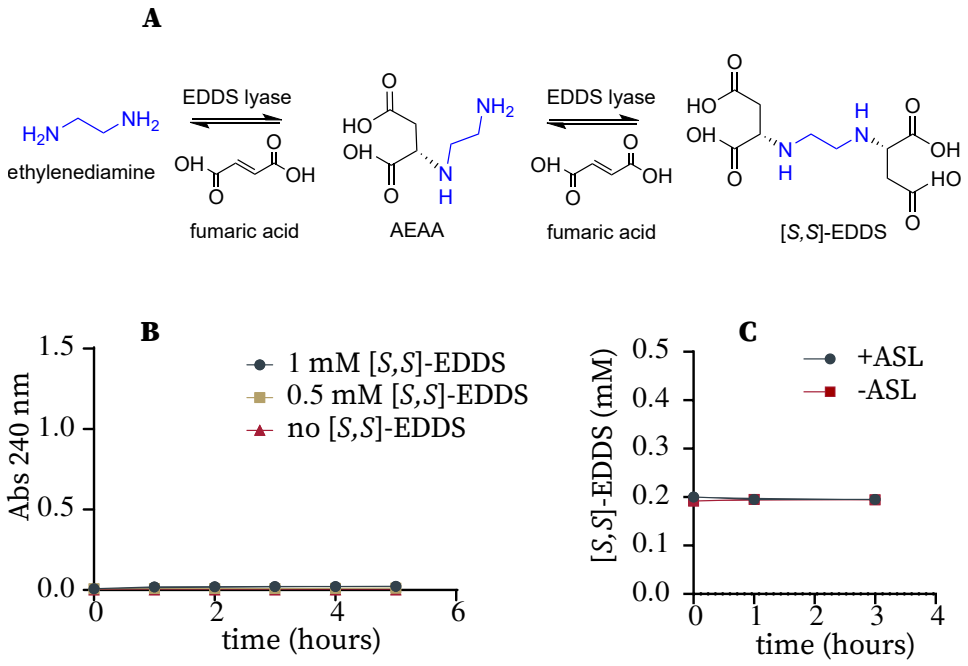

Figure 3.12. **Enzymatic reaction of the argininosuccinate lyase of *A. japonicum* (Asl_{Aj}) using [*S,S*]-EDDS as substrate.** (A) Reversible two-step deamination of [*S,S*]-EDDS catalyzed by the EDDS lyase from *Chelativorans sp.*BNC1 (Poddar *et al.*, 2018). (B) Spectrophotometric measurement at 240 nm to detect the formation of fumarate during a reaction catalyzed by 10 μM (Asl_{Aj}) and [*S,S*]-EDDS (0.5 mM or 1 mM) in Tris-HCL buffer (pH 8.0). As negative control, a reaction containing 10 μM Asl_{Aj} in Tris-HCL buffer (pH 8.0). (C) HPLC-DAD analysis of Asl_{Aj} reaction with [S,S]-EDDS after 1, 2 and 3 hours.

Discussion

The regulation of zinc homeostasis is essential for all organisms. In bacteria, a large number of proteins involved in diverse cellular processes require Zn^{2+} in their structure or as a catalytic cofactor. 5-6 % of bacterial proteins use Zn^{2+} as cofactor (Blindauer, 2015).

Under conditions of limited availability, several key enzymes involved in bacterial metabolism are inactive, compromising cell survival. Conversely, an excess of zinc can be toxic to cells due to mis-metallation of metalloproteins (Foster *et al.*, 2014). Therefore, proper control of zinc uptake and release determines the ability to survive in zinc-deficient or sufficient environments.

In many environments zinc availability is limited, which can lead to zinc deficiency. To acquire sufficient Zn^{2+}, bacteria possess homologous of Znu/Adc, an ATP binding cassette (ABC) permease (Patzer and Hantke, 1998; Blindauer, 2015). Some bacterial species also possess ZupT, an additional zinc import system member of the ZIP family (Grass *et al.*, 2002), which is becoming increasingly importance in pathogenic bacteria under zinc-limiting conditions, such as during infection (Cerasi *et al.*, 2014).

A third type of zinc import system is known as the Cnt (also called Zrm) system, which is involved in the import of the zincophore-Zn^{2+} complex and has been described in *Staphylococcus aureus* and *Pseudomonas aeruginosa* (Grim *et al.*, 2017; Mastropasqua *et al.*, 2017; Lhospice *et al.*, 2017).

Zincophores are small molecules produced by bacteria under zinc-deficient conditions. Their wide distribution among different bacterial species highlights their importance under these conditions (Morey *et al.*, 2020). Zincophores such as staphylopine, pseudopaline and yersinopine have been identified in several human pathogens, where they play a crucial role in zinc acquisition during infection (Grim *et al.*, 2017; Lhospice *et al.*, 2017; Morey *et al.*, 2020). Soil-associated bacteria produce zincophores such as bacillopaline (Morey *et al.*, 2020), coelibactin (Zhao *et al.*, 2012) and [*S,S*]-EDDS (Nishikiori *et al.*, 1984). [*S,S*]-EDDS is the first zincophore described in the literature Patzer and Hantke (1998).

[*S,S*]-EDDS is produced by the soil bacterium *A. japonicum* (Nishikiori *et al.*, 1984). Its production occurs exclusively under zinc-limiting conditions, while other metal ions have no effect on [*S,S*]-EDDS biosynthesis, suggesting that it is used by *A. ja-*

ponicum as a zincophore, to obtain Zn^{2+} under zinc-limiting conditions (Zwicker *et al.*, 1997; Cebulla, 1995; Hantke, 2001).

After synthesis, [*S,S*]-EDDS is probably exported from the cell by the EDDS-specific exporter AesD. In analogy to siderophores trafficking, it is proposed that once [*S,S*]-EDDS is outside the cell and binds Zn^{2+}, it should be reimported as a zincophore-Zn^{2+} complex (Morey *et al.*, 2020). In general, the BGC encodes efflux and import systems (Morey *et al.*, 2020). However, no gene encoding an ABC transporter homologous to zincophore-Zn^{2+}, such as Cnt, was identified in or near the [S,S]-EDDS operon. This suggests that *A. japonicum* uses a different zinc-uptake system to reimport [S,S]-EDDS-Zn^{2+}. The fate of internalized [S,S]-EDDS-Zn^{2+} in *A. japonicum* is not fully understood. It is possible that, similar to siderophore-iron complexes, [*S,S*]-EDDS may be degraded intracellularly or exported for re-use by bacteria (Andrews *et al.*, 2003). [*S,S*]-EDDS degrading enzymes cleaving the C-N-bond between a succinyl residue and the central Dae moetie have already been isolated in several bacteria including *Brevundimonas* sp. TN-3 (Mizunashi, 2001), DSM 9103 (Witschel and Egli, 1997), and *Chelativorans sp.* (Poddar *et al.*, 2018). One such enzyme was identified as an EDDS lyase, a member of the aspartase/fumarase superfamily, which also includes argininosuccinate lyase enzymes (Poddar *et al.*, 2018). Genome analysis allowed the identification of an argininosuccinate lyase in *A. japonicum* (Asl_{Aj}) that shares 33 % sequence identity with the EDDS lyase of *Chelativorans sp*. This suggested that the putative (Asl_{Aj}) may play a role in the degradation of [*S,S*]-EDDS after the import of the [*S,S*]-Zn^{2+} complex.

Enzymatic assays showed that (Asl_{Aj}) catalyzed the reaction of an Asl, but showed no activity when [*S,S*]-EDDS or [*S,S*]-EDDS-Zn^{2+} complex was used as substrate. These results are consistent with previous studies where no lyase activity capable of degrading [*S,S*]-EDDS was observed in *A. japonicum* cell-free extracts (Stegmann, 1999). The function of Asl is associated with primary metabolism, catalyzing the final step of arginine biosynthesis (Hani and Chan, 1994) The *A. japonicum* genome contains only one gene enconding an Asl_{Aj}, the genetic location strongly suggests its function in arginine biosynthesis rather than [S,S]-EDDS hydrolysis (Spohn *et al.*, 2016). Overall, it has been demonstrated *in vitro* that Asl_{Aj} does not catalyze the degradation of [*S,S*]-EDDS or the [*S,S*]-EDDS-Zn^{2+} complex. It may be that, analogous to the siderophore pyoverdin (PVD) mechanism, dissociation of [*S,S*]-EDDS-Zn^{2+} complex occurs in the cytoplasm, and instead of being degraded

and used as a carbon and nitrogen source, [*S,S*]-EDDS is exported to the extracellular space and recycled. Further studies are required to elucidate the fate of the [*S,S*]-EDDS-Zn^{2+} complex in *A. japonicum*.

3.3 Study of [*S,S*]-EDDS biosynthesis in *A. japonicum*

In previous work, the [*S,S*]-EDDS biosynthetic gene cluster (BGC) was identified (Figure 3.13). The binding sites for the transcriptional the zinc uptake regulator (Zur) could be identified (Spohn *et al.*, 2016) and the zinc dependent repression could be confirmed. Feeding experiments demonstrated that L-aspartic acid was incorporated in [*S,S*] EDDS (Cebulla, 1995). Inactivating the genes involved in the synthesis of *O*-phosphoserine resulted in the loss of [*S,S*]-EDDS production, thus demonstrating that *O*-phosphoserine also acts as a precursor for [*S,S*]-EDDS synthesis (Edenhart *et al.*, 2020). However, these two amino acids are not linked via the typical non-ribosomal peptide synthetase (NRPS) or NRPS-independent siderophore (NIS) pathways typically used to synthesize other ionophores such as staphyloferrin B from *Staphylococcus aureus* (Kobylarz *et al.*, 2016) (Figure S21). The corresponding genes are missing in the [S,S]-EDDS BGC. Three possible pathways have been proposed for the biosynthesis of [*S,S*]-EDDS, (Cebulla, 1995) (Spohn *et al.*, 2016) and (Wang *et al.*, 2022) (Figure 1.1, 1.2 1.3) providing a starting point for further investigation into the biogenesis of [*S,S*]-EDDS.

The objective of this study was to investigate the biosynthesis of [*S,S*]-EDDS and explore methods for increasing its production using metabolic engineering approaches. Through biochemical, genetic, and feeding techniques, the underlying molecular mechanisms of [*S,S*]-EDDS biosynthesis were investigated.

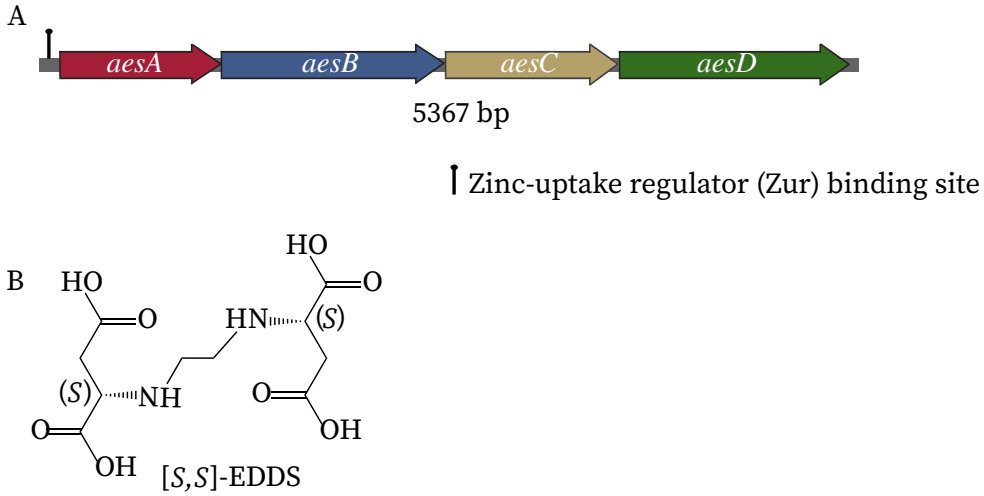

Figure 3.13. **[*S,S*]-EDDS biosynthetic gene cluster and structure.** (A) [*S,S*]-EDDS biosynthetic gene cluster, the operon *aesA-D* (AJAP_RS08340-55). The zinc-uptake regulator Zur binding site is shown. (B) [*S,S*]-EDDS structure.

Table 3.1. [*S,S*]-EDDS biosynthetic genes and predicted protein function

Gene	Annotation	Predicted encoded function
aesA	AJAP_RS08340	ornithine cyclodeaminase
aesB	AJAP_RS08345	PLP-dependent decarboxylase
aesC	AJAP_RS08350	PLP-dependent cysteine synthase
aesD	AJAP_RS08355	MATE family efflux transporter

3.3.1 Investigation of the function of AesA-C encoded in the biosynthetic gene cluster

3.3.1.1 Evaluation of the [*S,S*]-EDDS production in *A. japonicum aesA-C* mutant strains

In order to study the function of the enzymes encoded by *aesA*, *aesB* and *aesC* in the biosynthesis of [*S,S*]-EDDS, *A. japonicum* mutants that were deficient in one or two of the *aes* genes, were used. Metabolomic analyses of each strain were car-

ried out to identify the [*S,S*]-EDDS intermediates that accumulate in the respective mutants, since the biosynthesis of [*S,S*]-EDDS was interrupted at different sites in each of the mutants.

Different mutants, previously constructed (Edenhart, unplublished) were used in this study. For the generation of these mutants, *A. japonicum* ΔEDDS (in which the three genes *aesA-C* were deleted) (Spohn *et al.*, 2016), was used. The genes *aesA*; ornithine cyclodeaminase, *aesB*; amino acid decarboxylase and *aesC*; cysteine synthase were cloned individually and in combination (*aesA* + *aesB*) (*A. japonicum* ΔEDDS (*aesAB*), *aesA* + *aesC* (*A. japonicum* ΔEDDS (*aesAC*) or *aesB* + *aesC* (*A. japonicum* ΔEDDS (*aesBC*) into the integrative vector pIJ10257 under the control of the SP44* promoter. The plasmids were transferred by conjugation to *A. japonicum* ΔEDDS. The integration into the chromosome occurred via the ΦBT1 attachment site. This approach allowed six recombinant strains to be generated (Edenhart, unpublished) (Table 2.5).

To evaluate the [*S,S*]-EDDS production in the mutants, a production test was conducted in SM-medium for 7 days. The supernatants were derivatized with Fmoc-Cl and analyzed by HPLC-MS. As expected, the [*S,S*]-EDDS production was completely abolished in *A. japonicum* mutants. The *m/z* value of 515, corresponding to Fmoc-[*S,S*]-EDDS, was only observed in *A. japonicum* WT (Figure 3.14).

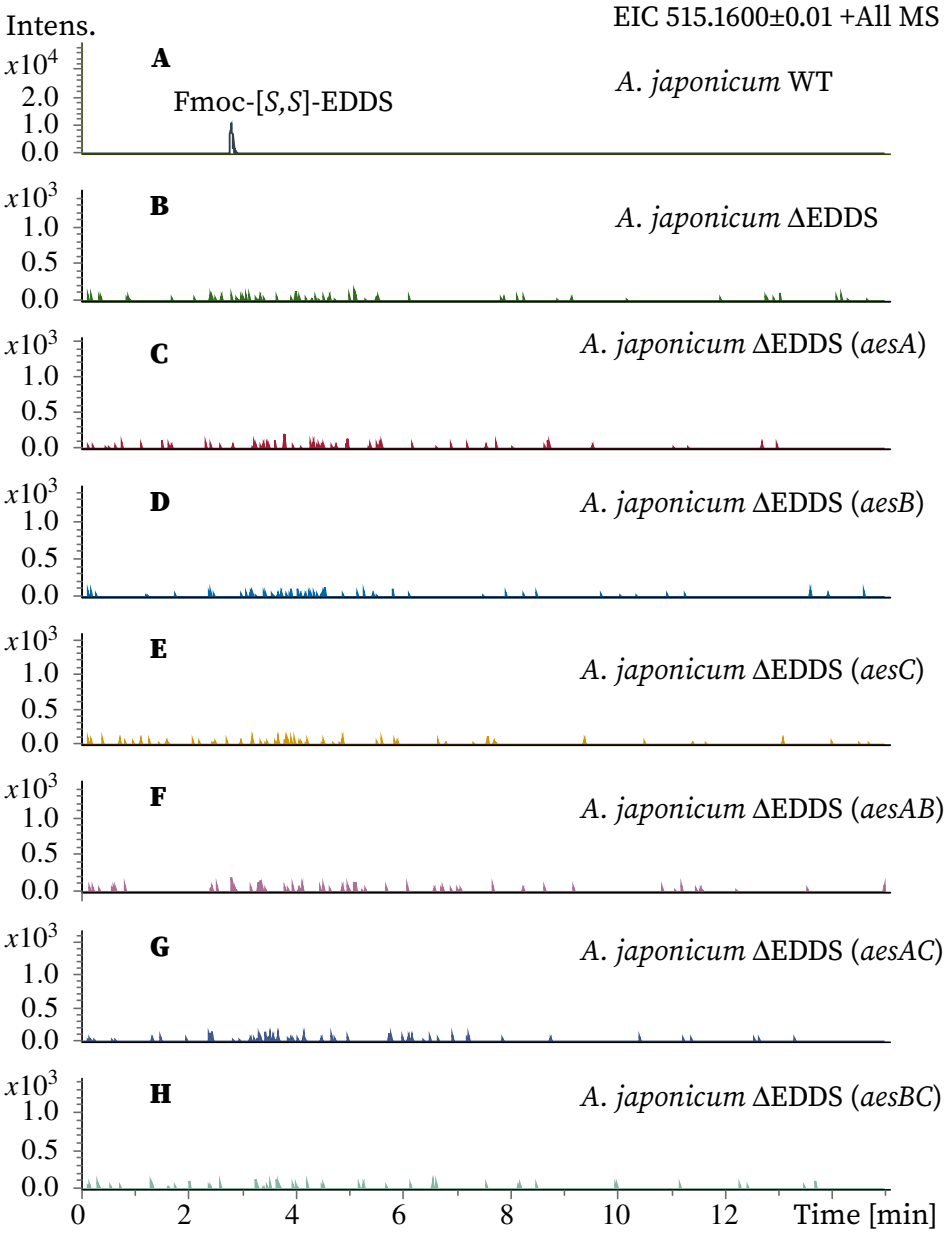

Figure 3.14. **HPLC-MS analysis of *A. japonicum* WT and mutants culture supernatants grown on M7 medium for 7 days**. The samples were treated with Fmoc in order to derivatize [*S,S*]-EDDS before the HPLC-MS analysis. Extracted Ion Chromatogram (EIC) of Fmoc-[*S,S*]-EDDS *m/z* value of 515.1 $[M+H]^+$.

3.3.1.2 [*S,S*]-EDDS pathway intermediates elucidation through gene deletion studies

For the detection of potential intermediates in the biosynthesis pathway, a metabolome analysis was conducted by HPLC-MS. *A. japonicum* WT and the *A. japonicum* mutants were cultured under [*S,S*]-EDDS production conditions, and supernatants and pellets were collected for analysis after 7 days. The pellets were treated using methanol 1:1 (v/v) for 1 hour in agitation and the resulting extracts were derivatized with Fmoc-Cl before analysis. Similarly, Fmoc-Cl was added to the supernatants prior HPLC-MS analysis.

The chromatograms of all the pellet extracts showed the same pattern. There was no unique peak in any of the samples that would indicate that a substance or intermediate was accumulating in a mutant (Figure 3.15). After HPLC-MS analysis of the supernatants, a peak at a retention time of 3 minutes with a *m/z* of 443.14 $[M+H]^+$ was identified in the chromatogram in positive mode, which occurred only in *A. japonicum* ΔEDDS (*aesAC*) (Figure 3.16, G, peak 1). The mutant contained *aesA* and *aesC*, but not *aesB*. The *m/z* value of 443.14 is consistent with the calculated mass for Fmoc-(S)-2-amino-2carboxyethyl)-L-aspartic acid (ACEAA) (Figure 3.17), a putative intermediate in the biosynthesis of [S,S]-EDDS. In the first step of the two postulated biosynthetic pathways (Figure 1.2), (Figure 1.3), ACEAA is synthesized from L-aspartic acid and *O*-phospho-serine via AesC. In the absence of AesB, the ACEAA was not further metabolized and accumulated in the supernatant. No unique peak was identified in the supernatants of the other mutant extracts.

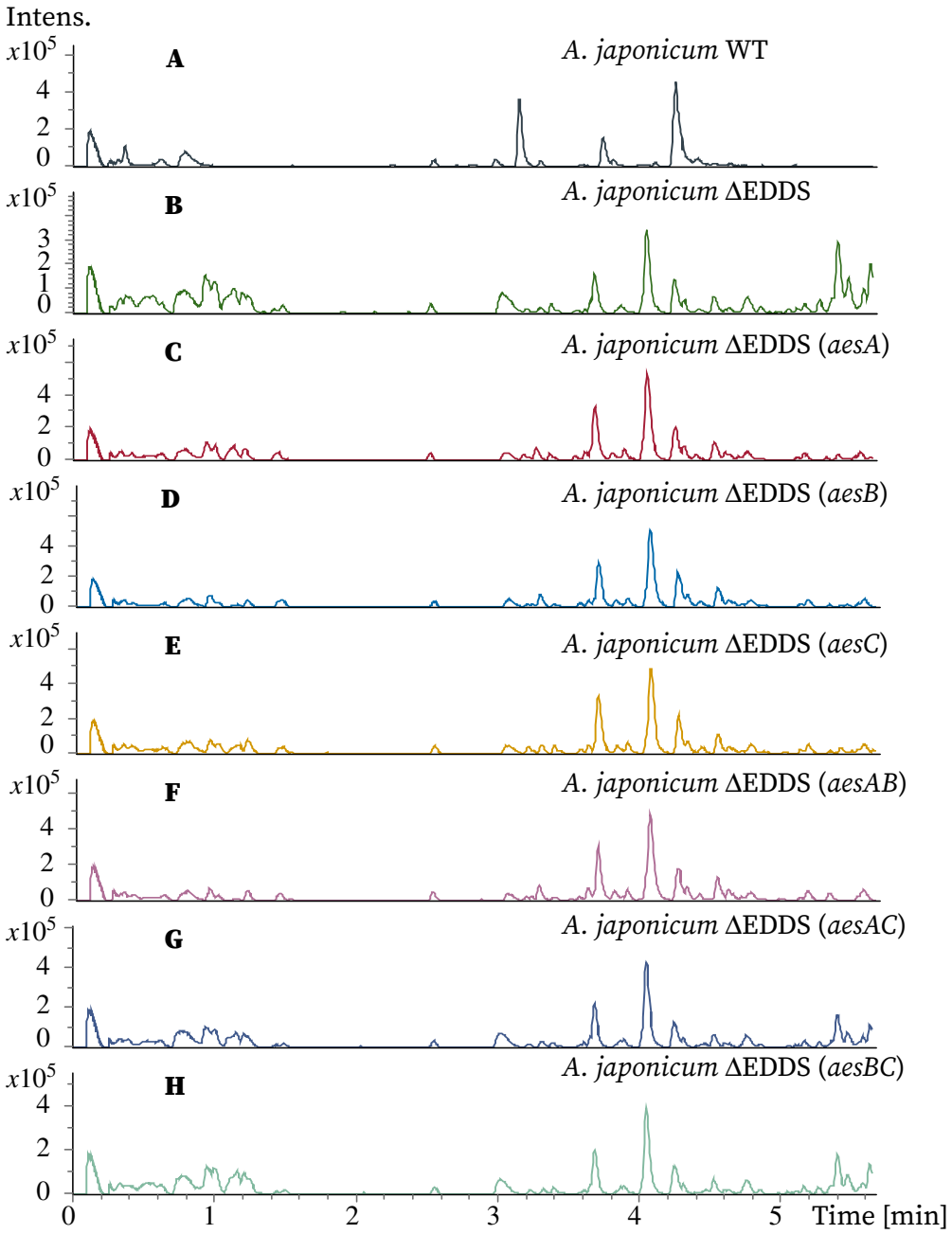

Figure 3.15. **HPLC-MS analysis of *A. japonicum* WT and *A. japonicum* mutants pellet extracts.** The samples were derivatized with Fmoc-Cl. Base Peak Chromatograms (BPC) are shown. The cultures were analyzed after 7 days of growth in SM-medium.

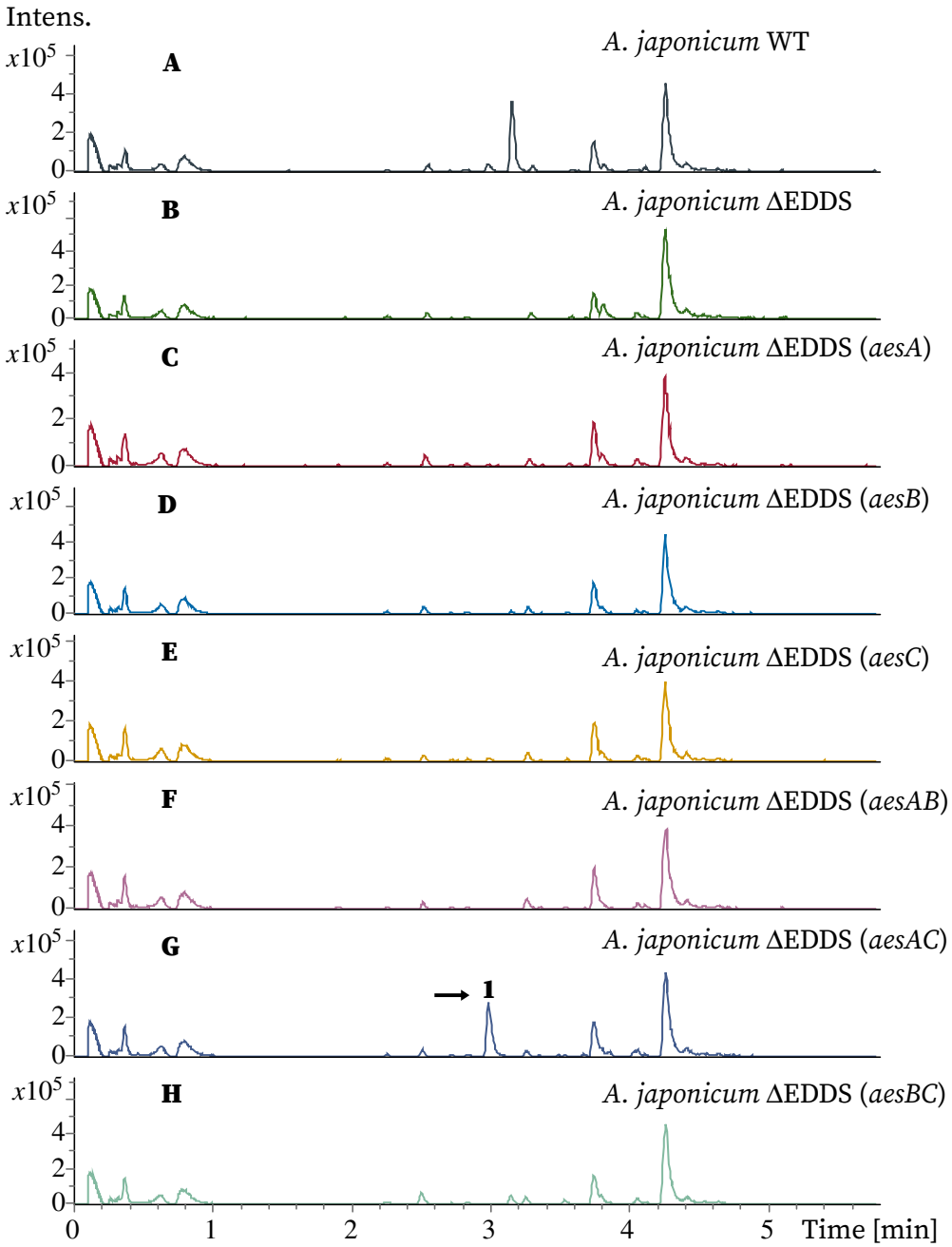

Figure 3.16. **HPLC-MS analysis of *A. japonicum* WT and *A. japonicum* mutants culture supernatants**. The samples were derivatized with Fmoc-Cl. Based peak chromatograms (BPC) are shown. The cultures were analyzed after 7 days of growth in SM-medium. The peak indicated by the number **1** possesses a mass of *m/z* 443.14 $[M+H]^+$, consistent with the calculated mass for Fmoc-ACEAA), a postulated intermediate.

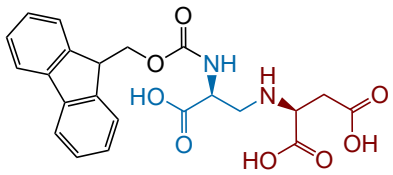

Fmoc-(*S*)-2-amino-2-carboxyethyl)-L-aspartic acid
(Fmoc-ACEAA)
Exact Mass: 442.14

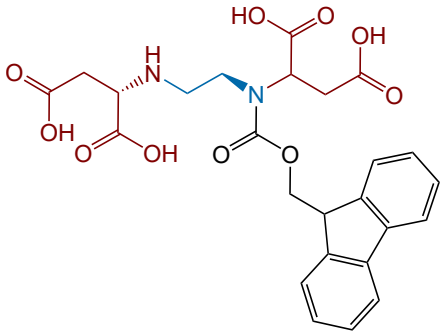

Fmoc-[*S,S*]-EDDS
Exact Mass: 514.16

Figure 3.17. **Structures of (S)-2-amino-2carboxyethyl)-L-aspartic acid (ACEAA) and [*S,S*]-EDDS derivatized with Fmoc-Cl (Fmoc-ACEAA and Fmoc-[*S,S*]-EDDS)**. ACEAA is a putative intermediate of [*S,S*]-EDDS biosynthetic pathway. The exact mass of both structures were predicted using Chemdraw.

3.3.1.3 Study of the biosynthesis by biochemical approach

The [*S,S*]-BGC encodes four proteins responsible for the biosynthesis (AesA, AesB and AesC) and the export of [*S,S*]-EDDS (AesD) (Spohn *et al.*, 2016). The putative functions for AesA-D (Table 3.1), predicted previously (Spohn *et al.*, 2016), were confirmed using the EggNOG mapper. To gain insight into their configuration, their sequences were applied to Alphafold v2.3.1 (Jumper *et al.*, 2021). It was predicted that AesA, AesB and AesC exist as dimers (Figure3.18). The estimated sizes

for the dimers were 68 kDa, 96 kDa and 74 kDa respectively (Figure 3.18).

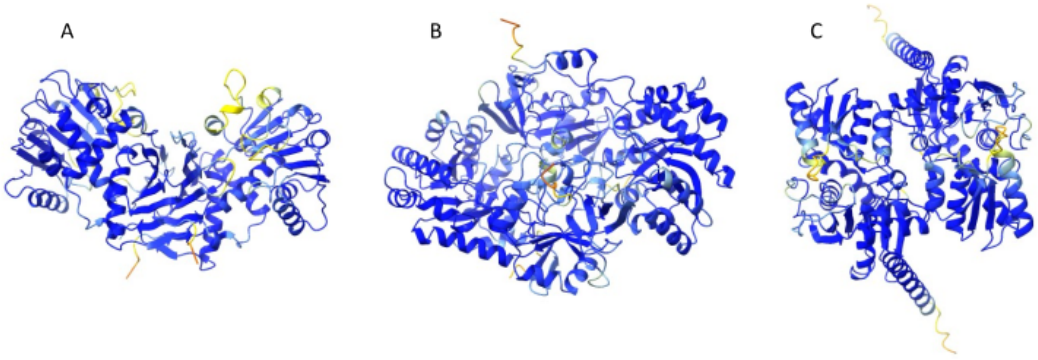

Figure 3.18. **Structure prediction by AlphaFold (ColabFold v1.5.2) Cartoon representation of the dimers (A) AesA. (B) AesB. (C) AesC.** The structures are colored based on the confidence metric (pLDDT) provided by Alphafold analysis; from blue (high confidence) to red (low confidence).

A) Studying the function of AesA, AesB, and AesC in [*S,S*]-EDDS Biosynthesis

In order to biochemically analyze the role of AesA, AesB and AesC in the biosynthesis of [*S,S*]-EDDS, the strains *A. japonicum*::pIJSP44-Strep-aesA, *A. japonicum*::pIJSP44-Strep-aesB and *A. japonicum*::pIJSP44-Strep-aesC (Edenhart, unpublished) were used. The strains were grown under EDDS-production conditions. After 7 days of cultivation is SM-medium, the cultures were harvested and the pellets were frozen at -80°C for protein isolation (Section 2.2.21 from Materials and methods) The Strep-Tactin® XT system was used for the purification of the proteins. After concentrating the samples on Amicon ultra centrifugation filters, the protein content was determined by BCA assay. A yield of 1 mg/ml was obtained for AesA and 2 mg/ml for AesB. The resulting fractions showed a monomer size of approximately 35 kDa for StrepII-AesA and 49 kDa for StrepII-AesB when analyzed on a 12% SDS-PAGE (Figure 3.19). However, this procedure failed to yield AesC as a soluble protein. Since AesC could not be isolated from *A. japonicum* either, an *in vitro* system was used.

The NEB Express® Cell-free *E. coli* Protein Synthesis System is based on an extract-based transcription/translation system derived from *E. coli* cells that have been engineered for high *in vitro* synthesis performance. All the components required for

protein synthesis are provided, except for the target template DNA. In the process, the sequence encoding for AesC is cloned in the PURExpress DHFR Control (see Section 2.2.16) and the protein synthesis is achieved after a short incubation of the plasmid with the kit components. The synthesized protein was analyzed on a 12 % SDS PAGE. Following Commassie staining, a protein band of approximately 38 kD was observed, which corresponds to the size of an AesC monomer. This method made it possible to produce AesC for the first time. However, the amount of the purified protein (less than 10 µg) were so low (measured by BCA) that it could not be used for biochemical assays.

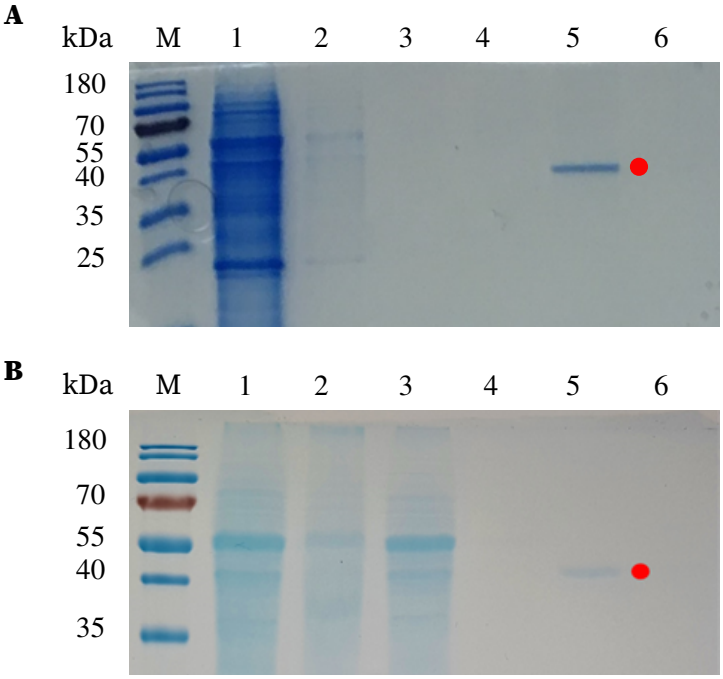

Figure 3.19. **SDS-PAGE analysis (12% gel) of purified Strep-tagII proteins produced in *A. japonicum*.** (A) (M) protein ladder (PageRuler Prestained, Thermo Fisher scienific # 26616), lane 1: cell crude extract, lane 2-4: washing fractions, lane 5: elution fraction 1, lane 6: elution fraction 2 containing the purified Strep-tagII-AesA, lane 7: elution fraction 3, MW of Strep-tagII-AesA: 35 kDa. (B) (M) protein ladder (PageRuler Prestained, Thermo Fisher scientific # 26616), lane 1: cell crude extract, lane 2-4: washing fractions, lane 5: elution fraction 1, lane 6: elution fraction 2 containing the purified Strep-tagII-AesB, lane 7: elution fraction 3, MW of Strep-tagII-AesB: 49 kDa.

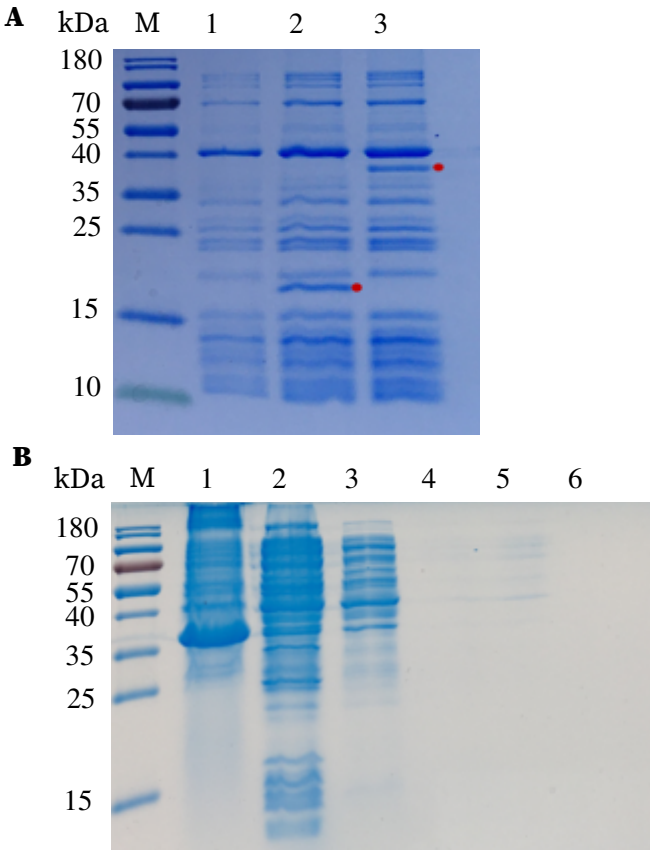

Figure 3.20. **SDS-PAGE analysis (12% gel) of purified Strep-tagII-AesC**. (A) Protein synthesis using the PURE cell-free system, molecular weight of 37 kDa (monomeric state). M: protein ladder (PageRuler Prestained, Thermo Fisher scientific # 26616). 1: Reaction without template DNA. 2: Reaction containing empty PURExpress DHFR control plasmid. 3: Reaction containing the PURExpress plasmid where the sequence encoding for Strep-AesC was introduced. (B) Recombinant Strep-AesC produced in *E. coli* (codon-optimized *aesC* sequence for its expression in *E. coli*). M: protein ladder (PageRuler Prestained, Thermo Fisher scientific # 26616). 1: pellet extract presumably containing Strep-AesC in inclusion bodies, the molecular weight is 37 kDa (monomeric state). 2-4: Washing fractions. 5-7: Elution fractions.

B) Biochemical characterization of AesA

AesA is homologous to proteins annotated as ornithine cyclodeaminase (OCD) involved in the biosynthesis of some antibiotics and the siderophore Stahyloferrin B (Figure S17). Since the functional annotation predicted by EggNOG-mapper (Cantalapiedra *et al.*, 2021) suggested that AesA is a putative ornithine cyclodeaminase, a standard reaction for ornithine cyclodeaminase was carried out to confirm that AesA was purified in an active form. In this reaction a NAD^+ dependent ornithine cyclodeaminase converts L-ornithine into L-proline and NH_4 (Figure 3.21). To elucidate the role of AesA, 10 µM of AesA, 1mg/ml of L-ornithine and 50 µM of NAD+ were used pipetted in 1ml of 25mM Tris/HCL buffer pH 7.5 and the reaction was incubated for one hour at 29°C. After the treatment of the reaction mixture with Fmoc-Cl, HPLC-MS analysis was performed. As a negative control, AesA was omitted from the reaction. The results showed that no proline was detected (Figure 3.22), suggesting that AesA catalyzes a different reaction.

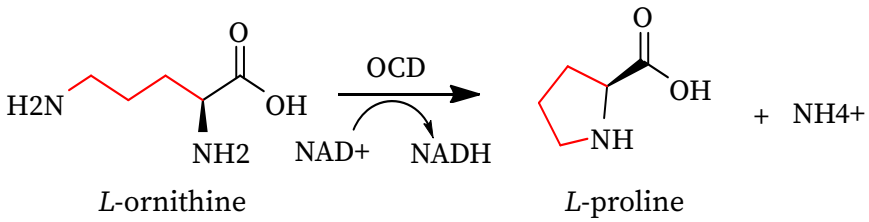

Figure 3.21. **Standard reaction catalyzed by an ornithine cyclodeaminase (OCD)**. This enzyme catalyzes the conversion of L-ornithine to L-proline by a NAD^+-dependent reaction, releasing ammonia.

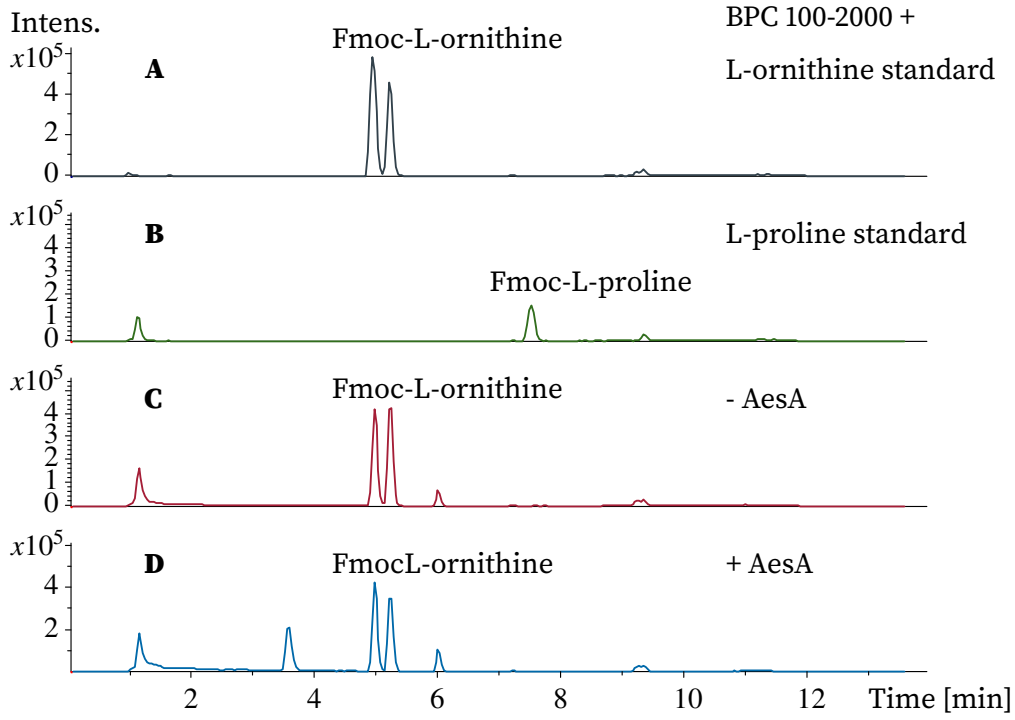

Figure 3.22. **HPLC-MS of the reaction mixture containing AesA, a putative ornithine cyclodeaminase**. A: L-ornithine standard derivatized with Fmoc-Cl, *m/z*-value of 355.1, $[M+H]^+$, B: L-proline standard derivatized with Fmoc-Cl, mass peak with *m/z* value of 338.1 of [M+H]+, C: negative control of the reaction without AesA, the mass of the Fmoc-L-ornithine is observed (*m/z*-value of 355.1), D: reaction containing AesA, the mass of Fmoc- L-ornithine is observed with *m/z*-value of 355.1.

Evaluation of the enzymatic activity of AesA based on the postulated pathway from Spohn *et al.*, 2016.

In the hypothetical [*S,S*]-EDDS biosynthetic pathway postulated by (Spohn *et al.*, 2016), AesC catalyzes the formation of (S)-2-amino-2-carboxyethyl)-L-aspartic acid (ACEAA) from L-aspartic acid and *O*-phosphoserine in a PLP-dependent manner. Subsequently, ACEAA and oxaloacetate (OAA) serve as substrates for AesA to generate L-diaminopropionic acid (L-DAPP) and OAA in a NAD^+-dependent reaction (Figure 1.2).

As ACEAA is not commercially available, the direct reaction catalyzed by AesA using NAD^+ and ACEAA as a substrate could not be measured directly. Therefore,

to test the hypothetical pathway, a reaction was initiated from L-aspartic acid and *O*-phosphoserine. Since no soluble AesC could be isolated, whole cell lysate from the mutant *A. japonicum aesC* was used instead. This mutant contains only the *aesC* gene under the control of the Sp44 promoter, while the other genes are deleted.

To conduct the first reaction from the putative pathway described by (Spohn *et al.*, 2016) (Figure 1.2), *A. japonicum* ΔEDDS (*aesC*) was grown under EDDS production conditions for 7 days, and the mycelium was harvested and lysed to obtain total proteins. The protein extract was then incubated with 20 μg AesA, 200 mM L-aspartic acid, 200 mM O-phospho-L-serine, 100 mM PLP, and 20 mM NAD^+. The reaction was carried out at 29°C for three hours, using 25 mM Tris/HCL buffer pH 7.5 and 50 mM HEPES buffer pH 8.0. The two different buffers were selected to evaluate which one was suitable for the reaction. To detect L-DAPP, the samples were treated with Dansyl chloride (DNS-Cl), which has been previously used for the detection of L-DAPP (Wang *et al.*, 2020). The chromatogram showed no peak with *m/z* values of 338.1, which is the expected value for DNS-L-DAPP. Therefore, the synthesis of L-DAPP could not be confirmed in this experiment (Figure 3.23).

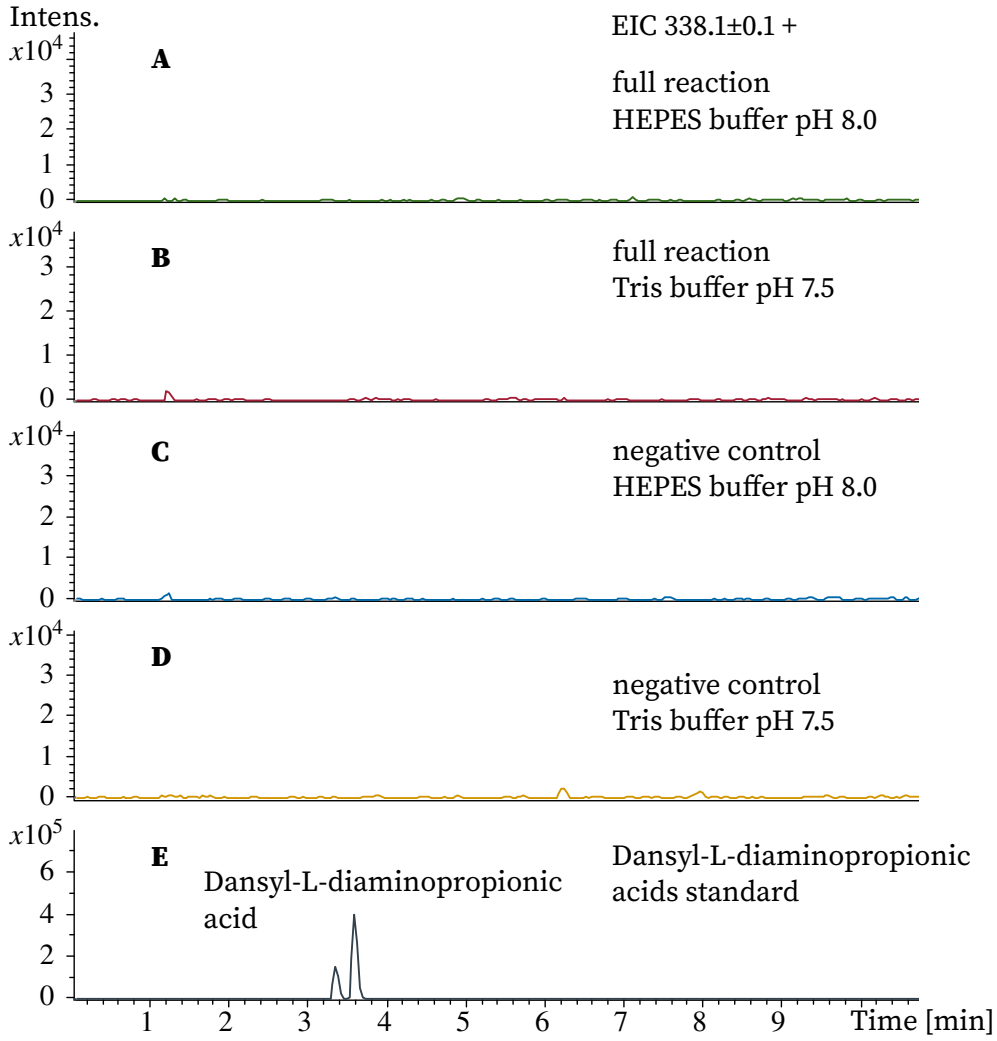

Figure 3.23. **HPLC-MS analysis of the reaction containing AesA and AesC, the putative L-Diaminopropionic acid (L-DAPP) biosynthetic enzymes**. Enzymatic reaction containing L-aspartic acid (2 mM), O-phospho-L-serine (2 mM), PLP (0.5 mM), NAD^+ (2 mM), AesA (10 μg) AesC lysate in two different reaction buffer (50mM HEPES, pH 8.0) or (100mM Tris buffer pH 7.5). (A) Measurement after 1h reaction in HEPES buffer (B) measurement after 1h reaction in buffer Tris buffer (C) negative control, reaction containing all the components, without AesA and AesC in buffer phosphate (D) negative control, reaction containing all the components, without AesA and AesC in buffer Tris-HCL. (E) 2mM L-DAPP standard derivatized with Dansyl chloride (*m/z* value of 338.1) $[M+H]^+$.

Many enzymes catalyze both, the forward and reverse reactions. Since ACEAA is not commercially available, it was investigated whether AesA could use L-DAPP and OAA as substrates and NADH as a cofactor (Figure 3.24 A). AesA was incubated with OAA, L-DAPP and NADH in Tris-HCL buffer pH 8 at 29°C°C and the NADH consumption was measured at 340 nm for 60 minutes. When AesA was tested with NADH as a cofactor and L-DAPP and OAA as substrates, a decrease in absorbance at 340 nm was observed (Figure 3.24 B, highlighted in gold). However, the same trend was observed when only OAA but not L-DAPP was present (Figure 3.24 B, highlighted in red). These results indicate that only OAA is accepted as a substrate by AesA, and that AesA requires NADH as a cofactor, whereas NAD^+ is not accepted (Figure 3.24 B, highlighted in dark green).

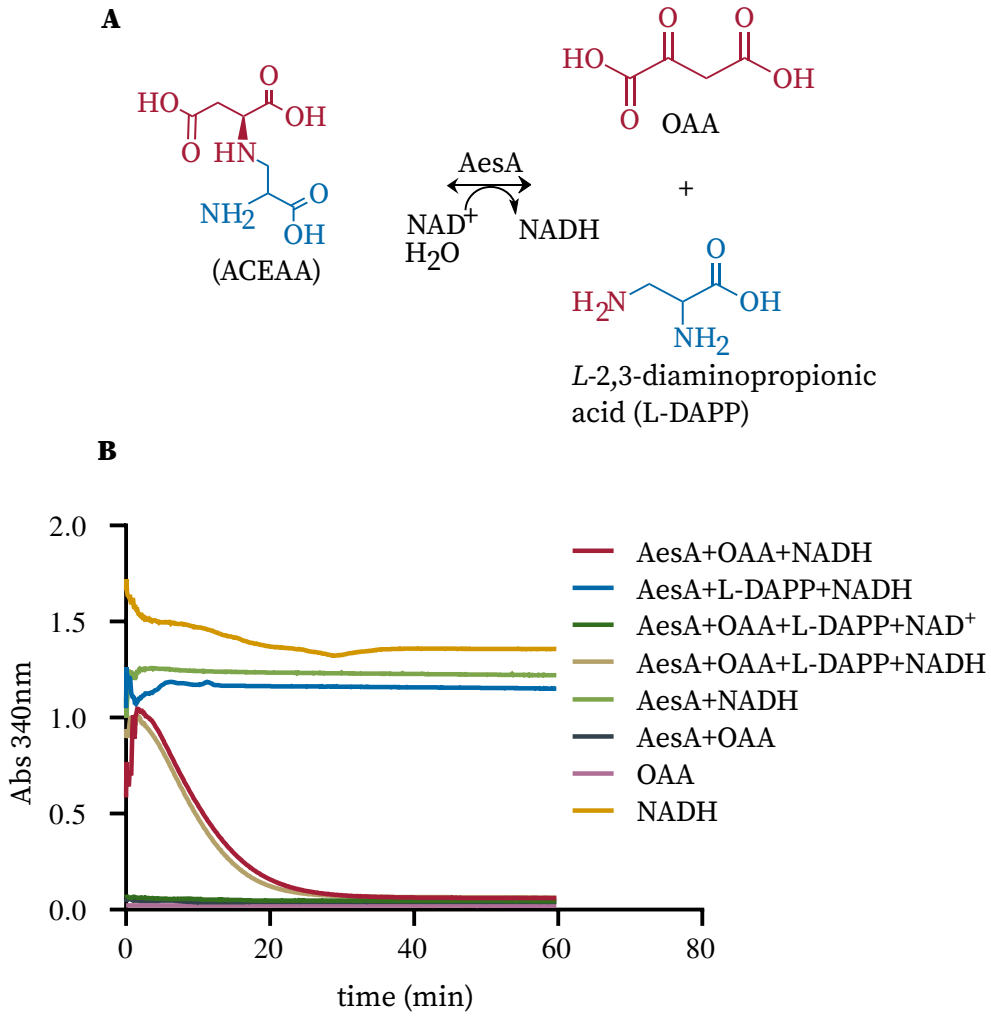

Figure 3.24. **Biochemical analysis of AesA according to (Spohn *et al.*, 2016).** (A) proposed enzymatic reaction for AesA in the [*S,S*]-EDDS biosynthetic pathway postulated by (Spohn *et al.*, 2016). (B) AesA activity monitored via the consumption of NADH. The direct reaction (the deamination of L-aspartic acid via NAD^+-dependent reaction) and inverse reaction (the NADH-dependent amination of OAA) were assessed.

Evaluation of the enzymatic activity of AesA based on the postulated pathway from Wang *et al.*, 2022

In a recent publication by (Wang *et al.*, 2022), an alternative hypothetical biosynthetic pathway for [*S,S*]-EDDS has been proposed. In this pathway, L-Dapp is not described as a precursor and the formation of the second C-N bond is catalyzed by AesA. Specifically, the formation of [S,S]-EDDS is postulated to occur in three steps (Figure 1.3). AesA catalyzes the formation of OAA in a NAD^+-dependent manner using L-aspartic acid as substrate. This leads to the release of NH_3 (Figure S19, A). In a subsequent reaction, OAA reacts with 2-aminoethyl-L-aspartic acid to form the second C-N bond, and finally [*S,S*]-EDDS is synthesized.

To evaluate the hypothetical reaction catalyzed by AesA (Figure S19, A), two different reactions were carried out. First, the reductive amination was repeated with OAA as substrate and NADH as a cofactor. Again, a gradual decrease in absorbance at 340 nm was observed over time (Figure S19 B, highlighted in red). Furthermore, it was investigated whether AesA catalyses the postulated NAD^+-dependent deamination of L-aspartic acid. However, there was no increase in absorbance at 340 nm, indicating that no NADH was formed (Figure 3.22 B, highlighted in grey) (Figure S19 B, highlighted in grey).

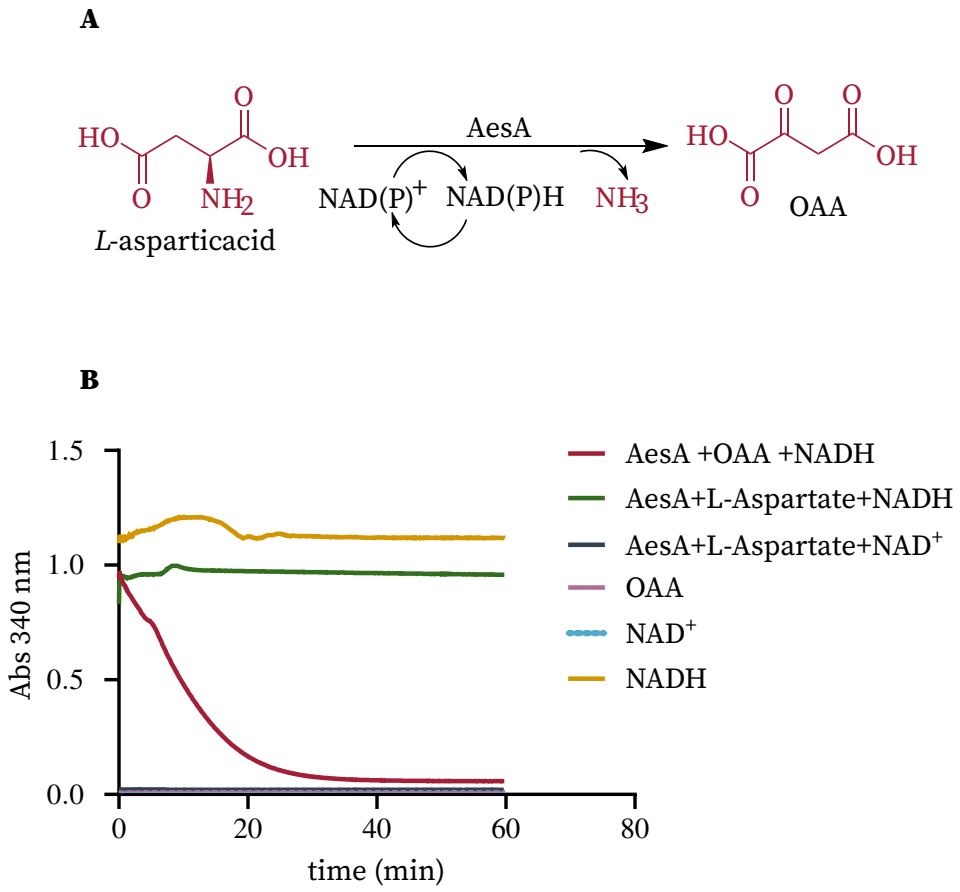

Figure 3.25. **Biochemical analysis of AesA according to (Wang *et al.*, 2022).** (A) Proposed enzymatic reaction for AesA in the [*S,S*]-EDDS biosynthetic pathway postulated by (Wang *et al.*, 2022). (B) Spectrophotometric measurement (340nm) of AesA reverse reaction over time. The decrease in absorbance at 340 nm indicates the consumption of NADH in the reaction

3.3.2 Determination of [*S,S*]-EDDS biosynthesis precursors

3.3.2.1 Investigation of L-diaminopropionic acid as a precursor for [*S,S*]-EDDS biosynthesis

L-DAPP is an essential building block for the synthesis of several antibiotics and natural compounds, e.g staphyloferrin B (Beasley *et al.*, 2011), viomycin (Thomas *et al.*, 2003) and capreomycin (Felnagle *et al.*, 2007). The [*S,S*]-EDDS BGC contains two genes encoding AesA and AesC proteins, which are homologous to the enzymes responsible for L-DAPP formation in various organisms (Table 3.2). Of these homologous proteins, SbnB and SbnA are of particular interest because these enzymes use *O*-phosphoserine and L-glutamic acid as substrates to synthesise L-DAPP. Since previous experiments have shown that *O*-phosphoserine and L-aspartic acid are precursors of [S,S]-EDDS, we wanted to investigate whether L-DAPP is synthesized from these precursors via AesA and AesC in *A. japonicum*.

Table 3.2. List of AesA and AesB homologues

Organism	Homologous protein AesA/AesC	Similarity % (AesA/AesC)	Related product	References
Staphylococcus aureus	SbnB/SbnA	22/31	staphyloferrin B	(Beasley *et al.*, 2011)
Saccharothrix mutabilis subsp. capreolus	CmnK/CmnB	24/33	capreomycin	(Felnagle *et al.*, 2007)
Bacillus thuringiensis	zwa5B/zwa5A	-	zwittermicin A	(Zhao *et al.*, 2008)
Streptomyces sp. strain ATCC 11861	VioK/VioB	25/32	viomycin	(Thomas *et al.*, 2003)
Streptomyces alanosinicus DSM 4060S	AlnE/AlnD	26/33	L-alanosine	(Wang *et al.*, 2020)
Streptomyces albulus PD-1	NjxB/NjxA	31/34	PDAP	(Xu *et al.*, 2015)
A. japonicum (BGC1)	AJAP_RS19050/ AJAP_RS19040	26/36	-	this work
A. japonicum (BGC2)	AJAP_RS22275/ AJAP_RS22260	25 / 33	-	this work

Evaluation of the recovery of [*S,S*]-EDDS synthesis after feeding *A. japonicum* ΔEDDS(*aesB*) with L-diaminopropionic acid

In order to verify that the genes *aesA* and *aesC* are involved in the synthesis of L-DAPP and that L-DAPP is an intermediate in the synthesis of [*S,S*]-EDDS, the strain *A. japonicum* ΔEDDS(*aesB*) (Table 2.5) was used. The mutant was inoculated in SM-medium, supplemented with 5 mM L-DAPP and cultured for five days. As a negative control, the mutant was cultured without the addition of L-DAPP. If AesA and AesC are involved in the production of L-DAPP, the synthesis of [*S,S*]-EDDS should be restored when L-DAPP is added to the *A. japonicum* Δ (*aesB*) culture (as shown in Figure 1.2). To investigate whether [*S,S*]-EDDS was synthesized, the culture supernatants were measured by HPLC-MS. However, [*S,S*]-EDDS could not be detected in any of the samples, indicating that L-DAPP is not an intermediate in the synthesis of [*S,S*]-EDDS and, consequently, that AesA and AesC are not involved in the synthesis of L-DAPP (Figure 3.26).

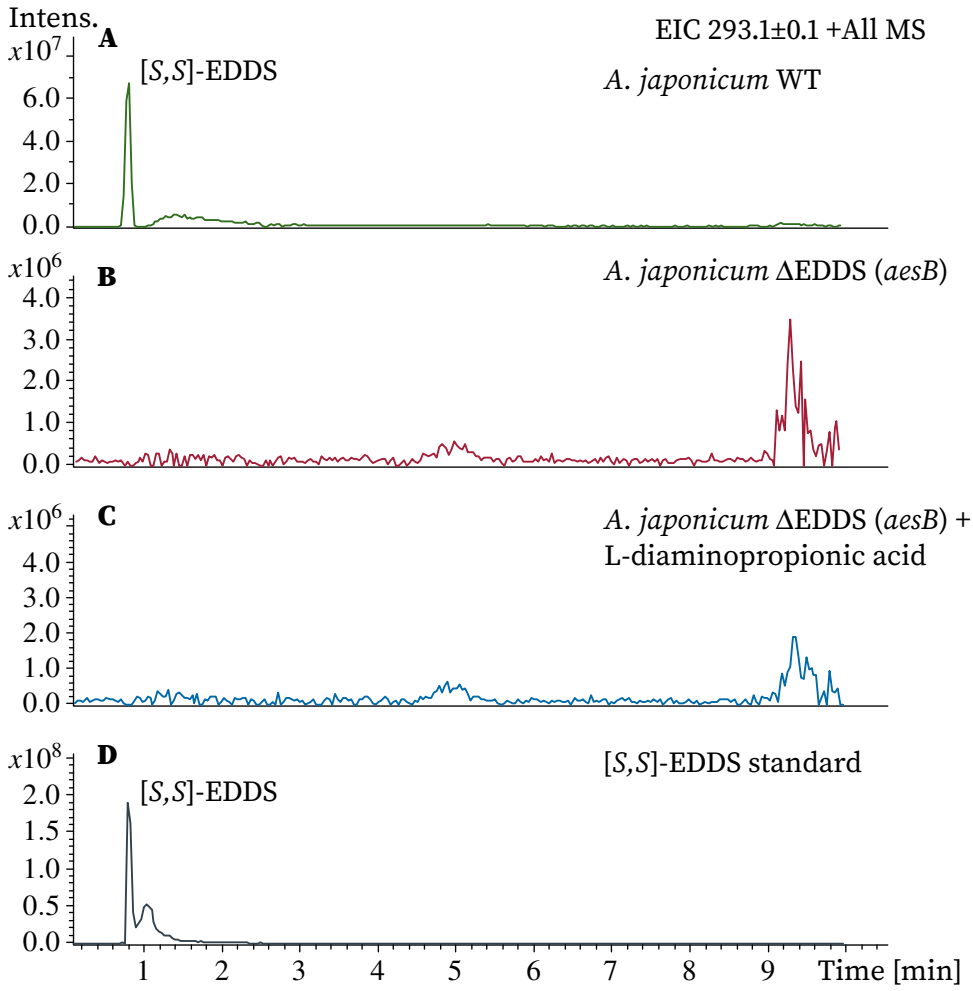

Figure 3.26. **HPLC-MS analysis of *A. japonicum* ΔEDDS (*aesB*) culture supernatants after feeding with L-DAPP.** (A) *A. japonicum* WT (positive control for the [*S,S*]-EDDS production) (B) *A. japonicum* ΔEDDS (*aesB*)(C) *A. japonicum* ΔEDDS (*aesB*) fed with 5mM L-diaminopropionic acid (L-DAPP at the beginning of the growth (D) [*S,S*]-EDDS standard. The strains were cultivated for 5 days in SM-medium.

Investigation of the role of *aesA* and *aesC* homologous genes in *A. japonicum*

In order to explore the potential presence of enzymes capable of synthesizing L-DAPP, which serves as a precursor for the biosynthesis of [*S,S*]-EDDS, a protein Blast analysis was conducted using the SbnA and SbnB proteins as queries. L-DAPP synthesis occurs in Staphylococcus aureus during the biosynthesis of staphyloferrin B, facilitated by the enzymes SbnA and SbnB.

The objective of this analysis was to investigate whether *A. japonicum* possesses enzymes encoded within its genome that exhibit similarity to SbnA and SbnB, thus potentially enabling L-DAPP synthesis. By identifying such enzymes, it would be possible to infer the capacity of *A. japonicum* to produce L-DAPP and potentially utilize it as a precursor for the biosynthesis of [*S,S*]-EDDS. Blast analysis revealed not only the presence of AesA and AesC proteins, known to participate in the biosynthesis of [*S,S*]-EDDS, but also homologous proteins in *A. japonicum*, which encoding genes were located as part of other BGC in the genome.

The proteins encoded by the genes AJAP_RS19050 (named *dappA1*) and AJAP_RS19040 (named *dappC1*), DappA1 and DappC1 shared 30/47 and 41/59 identity/similarity (%) with SbnB and SbnA, respectively. Functional annotation predicted by eggNOG-mapper suggested that these proteins are likely ornithine cyclodeaminase and cysteine synthase. The genes are located as part of a BGC, which product is predicted to be synthesized via NRPS (region 14, defined by antiSMASH) (Blin *et al.*, 2021).

AJAP_RS22275 (named *dappA2*) and AJAP_RS22260 (named *dappC2*), encoded the proteins DappA2 and DappC2, respectively. Protein blast analysis showed that these proteins shared 26/47 and 35/54 identity/similarity (%) with SbnB and SbnA, respectively.

These proteins are annotated as ornithine cyclodeaminase and PLP-dependent enzymes. The genes are located as part of a region (presumably a BGC) not identified by antiSMASH. Within the putative BGC, apart of dappA2 and dappC2, several genes are located, including genes encoding for putative asparagine synthase (AJAP_RS22280), putative iron-containing redox enzyme family protein (AJAP_RS22270) and putative ornithine carbamoyltransferase (AJAP_22255). Interestingly, these proteins DappA1 / DappC1 and DappA2 / DappC2 also showed homology to AesA/AesC ([*S,S*]-EDDS biosynthetic proteins).

To investigate whether the homologous proteins DappA1 and DappC1 or DappA2 and DappC2 could replace AesA and AesC in biosynthesizing [S,S]-EDDS, the corresponding genes were introduced together with *aesB* under the control of the constitutive promoter *ermEp** into the genome of *A. japonicum* ΔEDDS. Therefore, dappA1/dappC1 and dappC2/dappA2 the genes were amplified via Gibson assembly, using the primers listed in Table 2.6 and cloned into the pRM4 vector under the control of *ermEp**, which integrated into the genome via the ϕC31 attachment site. The resulting plasmids pLDAPP1 and pLDAPP2 were separately introduced into *A. japonicum* ΔEDDS via conjugation. As a result, the strains *A. japonicum* LDAPP1 and *A. japonicum* LDAPP2 were constructed (Table 2.5). After five days of cultivation of *A. japonicum* LDAPP1 and *A. japonicum* LDAPP2 in SM-medium, the culture filtrates were analyzed via HPLC-DAD to evaluate [*S,S*]-EDDS production. The chromatograms of both samples did not show a peak corresponding to [*S,S*]-EDDS, indicating that the homologous genes were not able to complement *aesA* and *aesC* genes in *A. japonicum* ΔEDDS (Figure 3.28, lines gold and gray).

Additionally, pellet cultures were treated with methanol for compound extraction. The resulting soluble fraction was derivatized with Dansyl chloride for the detection of L-DAPP. An L-DAPP standard was used as positive control. The expected mass for Dandyl-L-DAPP corresponds to *m/z* value of 338.1 $[M+1]^+$. The chromatograms of pellet cultures of *A. japonicum* LDAPP1 and LDAPP2 did not show a signal with the expected *m/z* value of 338.1 at the same retention time as the L-DAPP standard. The synthesis of L-DAPP could not be confirmed in *A. japonicum* mutants containing AesA and AesC homologous genes.

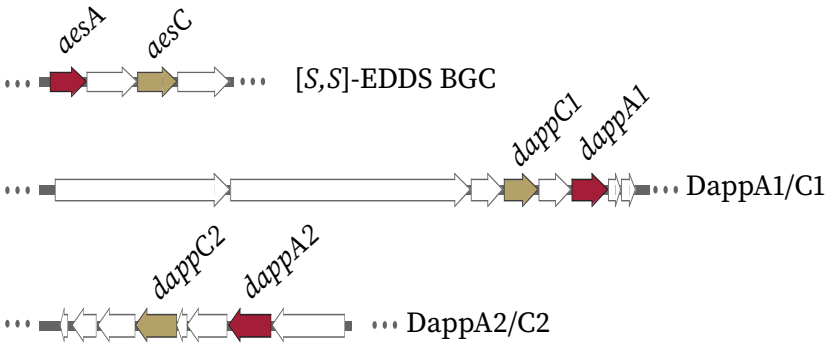

Figure 3.27. **Schematic representation of *A. japonicum* showing *aesA* and *aesC* homologous genes**. [*S,S*]-EDDS BGC, DappA1/C1, and DappA2/C2. Within the [*S,S*]-EDDS BGC, two proteins, AesA and AesC, are encoded. AesA is a putative ornithine cyclodeaminase (highlighted in red), while AesC is a putative PLP-dependent cysteine synthase (highlighted in gold). DappA1/C1 (AJAP_RS19050 and AJAP_RS19040) encode proteins sharing 41% and 49% similarities to AesA and AesC, respectively. Similarly, DappA1/C1 (AJAP_RS22275 and AJAP_RS22260) encode proteins sharing 37% and 49% similarities to AesA and AesC, respectively.

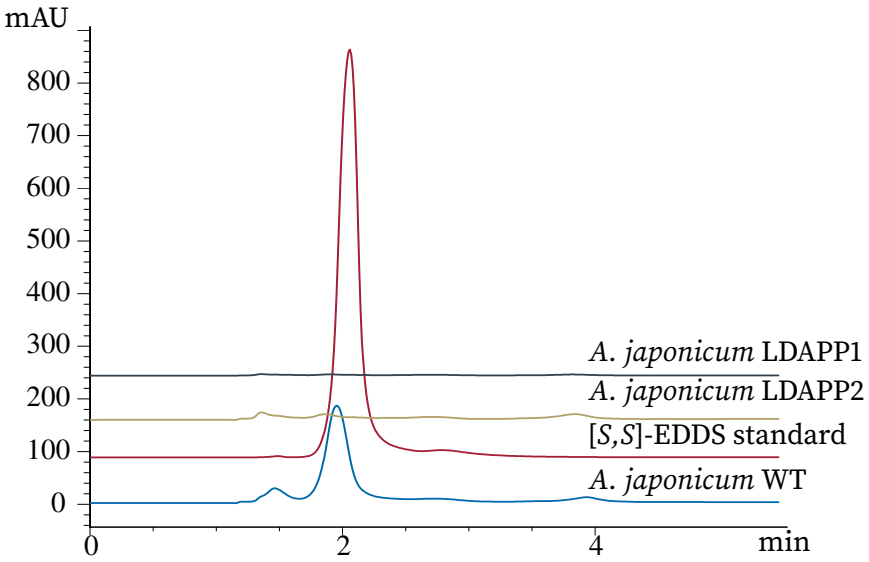

Figure 3.28. **HPLC-DAD chromatogram of culture supernatant of *A. japonicum* LDAPP1 and *A. japonicum* LDAPP2.** The strains were grown in deionized flasks in SM-medium in the absence of zinc. Commercial [*S,S*]-EDDS was used as a standard.

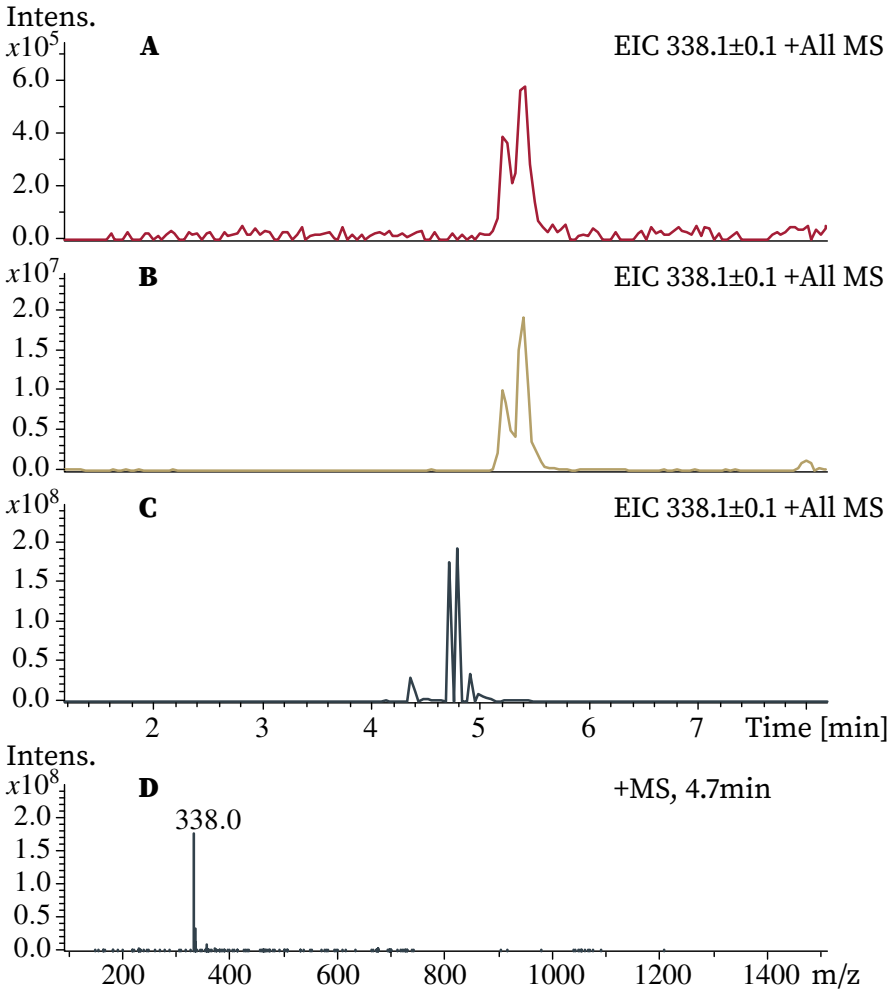

Figure 3.29. **HPLC-MS chromatogram of culture pellet of *A. japonicum* LDAPP1 and *A. japonicum* LDAPP2.** The strains were grown in deionized flasks in SM-medium in the absence of zinc. Commercial L-DAPP was used as a standard.

3.3.2.2 Determination of precursors involved in [*S,S*]-EDDS biosynthesis by feeding with naturally occurring potential precursors

To evaluate further potential precursors for the [*S,S*]-EDDS biosynthesis, feeding experiments using naturally occurring amino acids were conducted. Since L-aspartic acid was previously confirmed as a precursor for [*S,S*]-EDDS (Cebulla, 1995), this amino acid was used as a positive control. In addition, OAA, L-ornithine, and L-

glutamate were also used in the experiment. *A. japonicum* WT was inoculated in SM-medium and the potential precursors were added to each culture in final concentrations of 5 mg/ml. After five days, the culture supernatants were analyzed by HPLC-DAD. The production of [S,S]-EDDS was analyzed by HPLC-DAD using an [*S,S*]-EDDS standard curve (0.08 mg/ml to 0.3 mg/ml).

Evaluation of the results revealed that feeding with L-aspartic acid, L-ornithine, and L-glutamic acid led to increased [*S,S*]-EDDS production compared to the negative control without feeding. Of these, L-glutamic acid had the most statistically significant effect. However, the feeding with OAA resulted in a significant decrease in [*S,S*]-EDDS production (Figure 3.30)

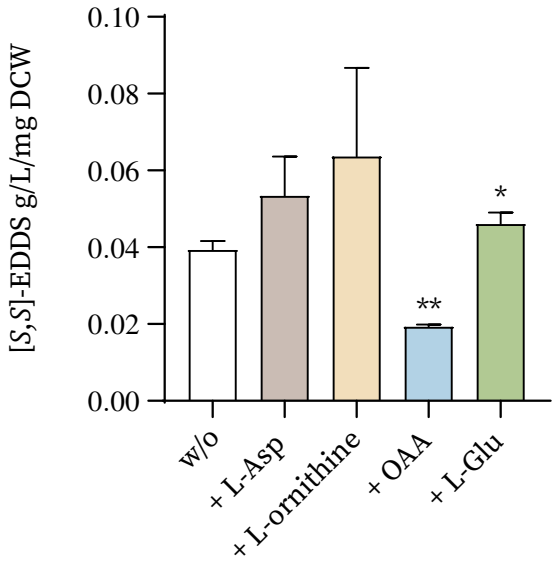

Figure 3.30. **Feeding *A. japonicum* WT with putative precursors of [*S,S*]-EDDS biosynthesis.** Cells were fed with L-aspartic acid (L-asp), L-ornithine, oxaloacetate (OAA) and L-glutamic acid (L-Glu)(5 mg/ml final concentration) and grown in zinc-depleted SM-medium for five days. Production has been normalized to the dry weight of the cells (DCW). Statistical significance (*p<0.05, **p<0.001) was determined by unpaired Student´s test.

3.3.3 Determination of precursors involved in [*S,S*]-EDDS biosynthesis by feeding with stable isotope labeled amino acids

3.3.3.1 Feeding with 1,4-^{13}C2;^{15}N- L-aspartic acid and ^{15}N-L-aspartic acid

Previous studies have shown that 4-^{13}C aspartic was incorporated into [*S,S*]-EDDS (Cebulla, 1995). However, due to the symmetric nature of the [*S,S*]-EDDS structure, it was not possible to determine whether one or two L-aspartic acid molecules were required for synthesizing [*S,S*]-EDDS. Furthermore, the origin of the nitrogen in [*S,S*]-EDDS remained unclear. To address this, feeding experiments using C and N-labeled (1,4-^{13}C2;^{15}N) and only N-labeled (^{15}N) L-aspartic acid were performed in *A. japonicum* OP2 grown in SM-medium in 6-well culture plates. *A. japonicum* strain OP2 was chosen for these experiments because this is a zinc-deregulated overproducer strain, in which the [*S,S*]-EDDS production has been optimized (Edenhart *et al.*, 2020). This allows feeding experiments in SM-medium (without the need for pre-culture in complex medium) and the production of sufficient amounts of [*S,S*]-EDDS for HPLC-MS analysis. Isotope-labeled L-aspartic acid (1,4-^{13}C2;^{15}N) or N-labeled (^{15}N), were added to each culture to a final concentrations of 5 mM. Feeding was performed for six hours, and 1 ml of labeled precursor was added to the culture every hour. After 24 hours, the cultures were harvested and culture supernatants were analyzed by HPLC-MS.

HPLC-MS analysis showed that the major signal with *m/z* value of 296.0 $[M+H+3]^+$ for [*S,S*]-EDDS, increased by 37 % after the feeding with 1,4-^{13}C2;^{15}N. (Figure 3.31B, 3.31A). The increasing signal intensity indicated the incorporation of three labeled isotopes, ^{13}C or ^{15}N into [S,S]-EDDS. The incorporation of ^{13}C and ^{15}N from L-aspartic acid (1,4-^{13}C2;^{15}N) was further confirmed by ^{13}C NMR and ^{15}N NMR, performed in cooperation with Dr. Chambers Hughes (Figure S14, S15). However, as shown by (Cebulla, 1995), due to the symmetrical nature of the [*S,S*]-EDDS molecule (Figure 3.13B), it was not possible to determine whether stable isotope incorporation occurs only once or twice (on both sides of the molecule). Feeding with ^{15}N showed increasing signal intensity of *m/z* value of 294$[M+H+1]^+$ from 12 % (naturally abundance of ^{13}C) to 46 % (Figure 3.32C). The presence of a signal with *m/z* value of 294 $[M+H+1]^+$ strongly suggested the incorporation of the ^{15}N from L-aspartic acid into [S,S]-EDDS.

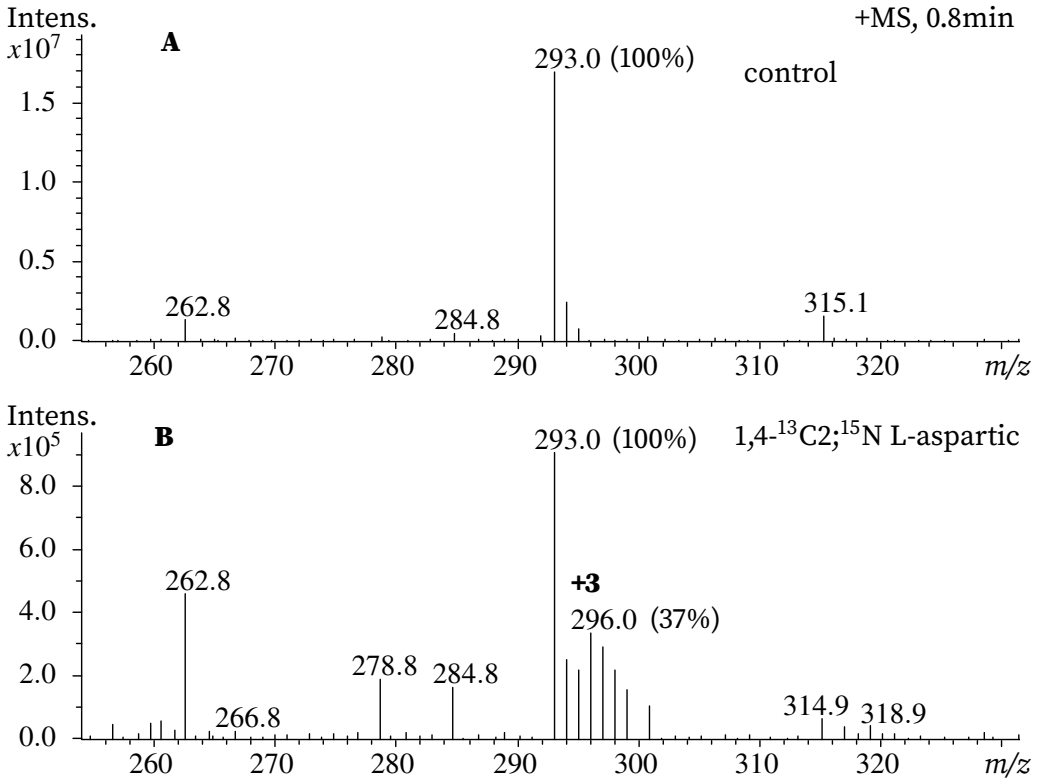

Figure 3.31. **HPLC-MS chromatogram of [S,S]-EDDS from culture supernatant of *A. japonicum* OP2 after feeding with 1,4-^{13}C2;^{15}N-L-aspartic acid**. (A) control, [*S,S*]-EDDS *m/z* value of 293.0 $[M+H]^+$ in culture supernatant of *A. japonicum* OP2 without feeding. (B) [*S,S*]-EDDS *m/z* value of 296.0 $[M+H+3]^+$ after feeding with 5 mM 1,4-^{13}C2;^{15}N-L-aspartic acid.

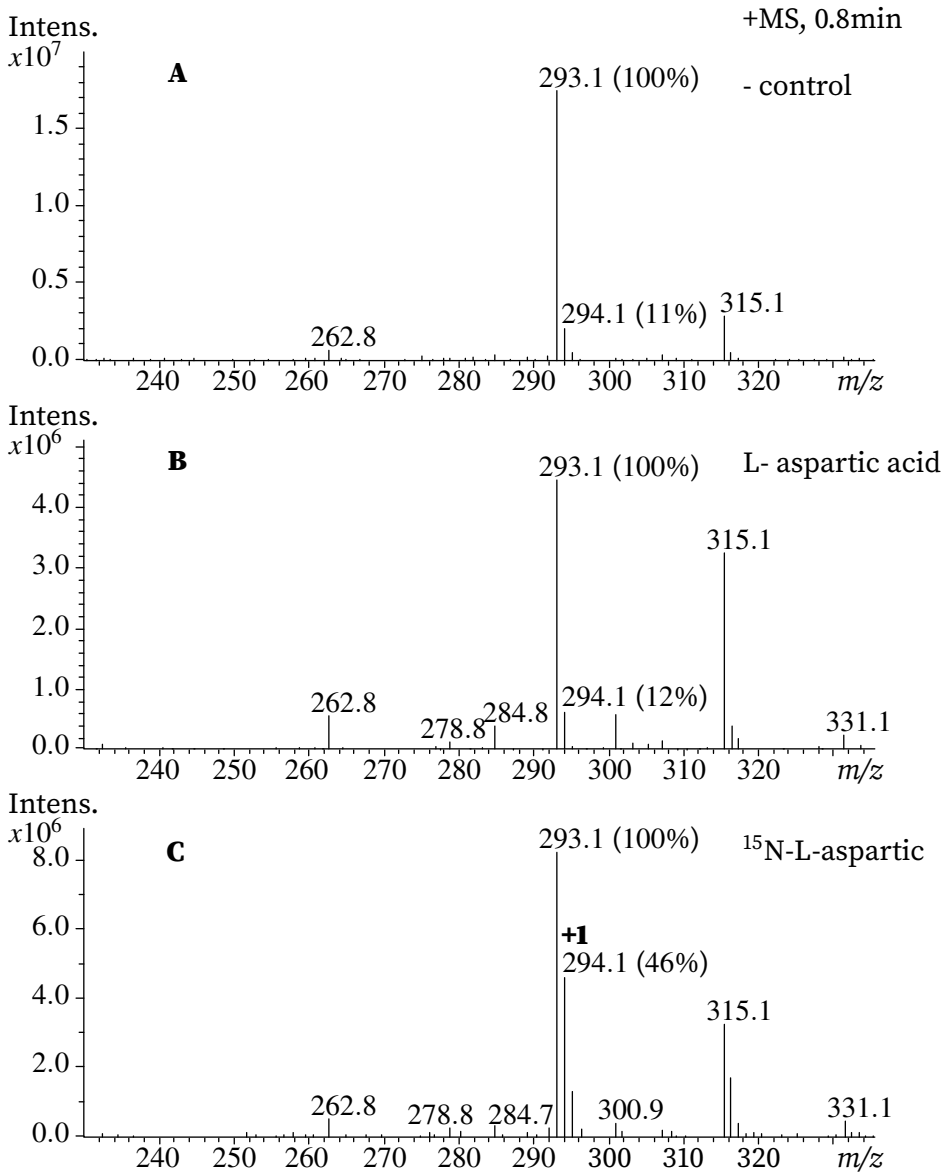

Figure 3.32. **HPLC-MS chromatogram of [*S,S*]-EDDS from the supernatant of *A. japonicum* OP2 after feeding with ^{15}N-L-aspartic.** (A) control, [*S,S*]-EDDS *m/z* value of 293.1 $[M+H]^+$ in culture supernatant (B) [S,S]-EDDS *m/z* 293.1 after feeding with 10 mM naturally occurring L-aspartic acid. (C) [*S,S*]-EDDS *m/z* 294.1 $[M+H+1]^+$ after feeding with 10 mM ^{15}N-L-aspartic.

3.3.3.2 Feeding with L-ornithine (^{13}C5,^{15}N2), L-ornithine (Alpha-^{15}N) and L-ornithine (5-^{15}N)

AesA and AesC exhibit similarities to L-DAPP forming enzymes involved in the biosynthesis of natural products such as viomycin (Thomas *et al.*, 2003) and capreomycin (Felnagle *et al.*, 2007) (Table3.2). Their synthetic pathway differs from that of staphyloferrin B (Figure S21), which uses *O*-phosphoserine and L-glutamic acid as precursors. In viomycin and capreomycin, L-DAPP synthesis occurs with L-ornithine and L-serine/O-acetyl-L-serine as precursors. Given the similarity between AesA and AesC and the enzymes responsible for L-DAPP synthesis in viomycin and capreomycin (Table 3.2), we hypothesize that L-ornithine together with *O*-phosphoserine may act as precursor, for the synthesis of L-DAPP in [S,S]-EDDS biosynthesis, as proposed in (Figure 3.33).

To test our hypothesis, feeding experiments with L-ornithine:HCL (^{13}C5,^{15}N2) were performed. HPLC-MS analysis revealed dominant peaks, with mass signals of *m/z* value of 297.9 $[M+H+4]^+$ and *m/z* value of 300.7 $[M+H+7]^+$, indicating possible incorporation of part (**+4**) or the entire (**+7**) L-ornithine:HCL (^{13}C5,^{15}N2) molecule into [*S,S*]-EDDS (Figure 3.34 B).

In order to analyze whether one of the N-atom moieties of the [S,S]-EDDS is derived from L-ornithine, additional feeding experiments were carried out with L-ornithine:HCL (alpha-^{15}N) and L-ornithine:HCL (5-^{15}N). *A. japonicum* OP2 strain was grown SM-13C medium, fed with L-ornithine:HCL (alpha-^{15}N) or L-ornithine:HCL (5-^{15}N) at time 0 of cultivation. The cultures were incubated for four days and culture supernatants were analyzed by HPLC-MS. In the supernatants of the cultures fed with L-ornithine (alpha-^{15}N), an isotopic mass peak with *m/z* value of 294.1 $[M+1+H]^+$ showed an increase from 14% to 46%, compared to the peak of the supernatant of the untreated culture (Figure 3.35 D). This result indicate the incorporation of the alpha-N from L-ornithine into [*S,S*]-EDDS. No incorporation of ^{15}N from L-ornithine (5-^{15}N) into [*S,S*]-EDDS was detected. (Figure 3.35 C).

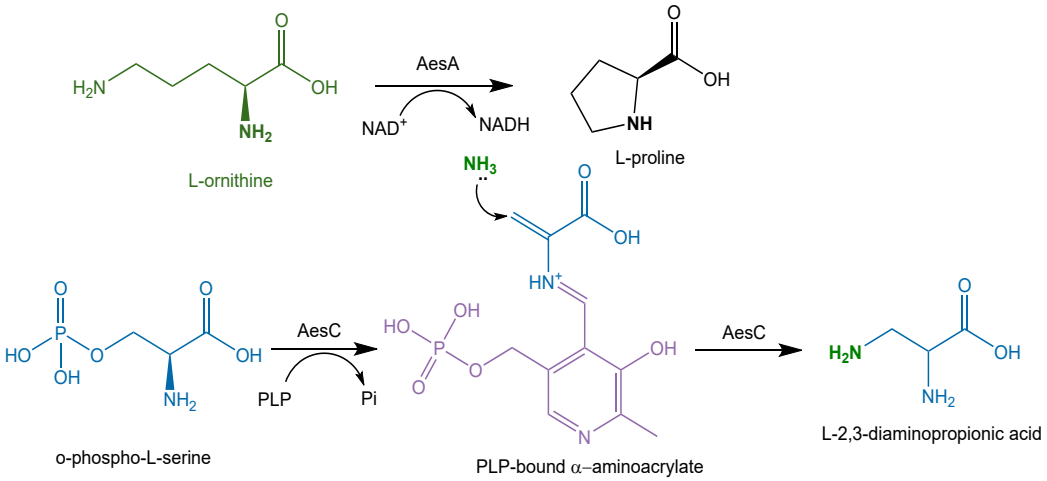

Figure 3.33. **Proposed scheme for AesA- and AesC-dependent synthesis of L-2,3-diaminopropionic acid (L-DAPP).** The scheme is based on the formation of L-DAPP during the synthesis of viomycin (Thomas *et al.*, 2003).

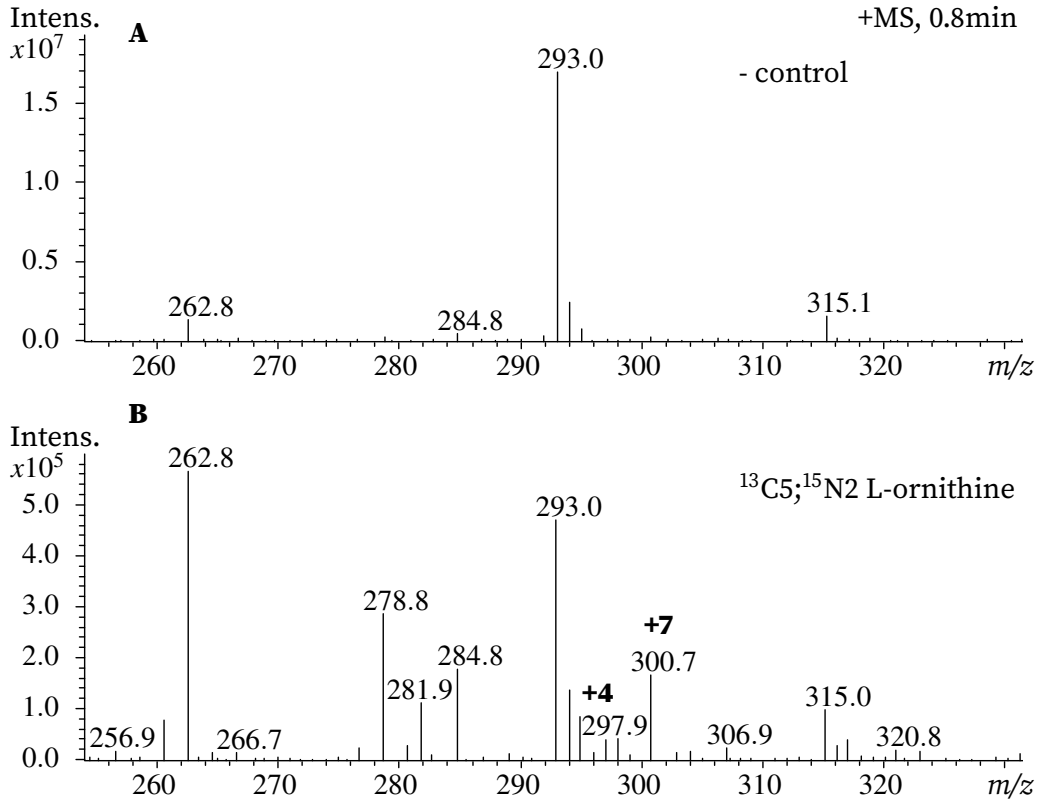

Figure 3.34. **HPLC-MS chromatogram of [S,S]-EDDS from the supernatant of *A. japonicum* OP2 fed with L-ornithine (^{13}C5,^{15}N2)**. (A) control, [*S,S*]-EDDS *m/z* value of 293.1 $[M+H]^+$ in culture supernatant of OP2 without feeding (B) [*S,S*]-EDDS *m/z* value of 297.9 or 300.7 after feeding with 5 mM L-ornithine (^{13}C5,^{15}N2).

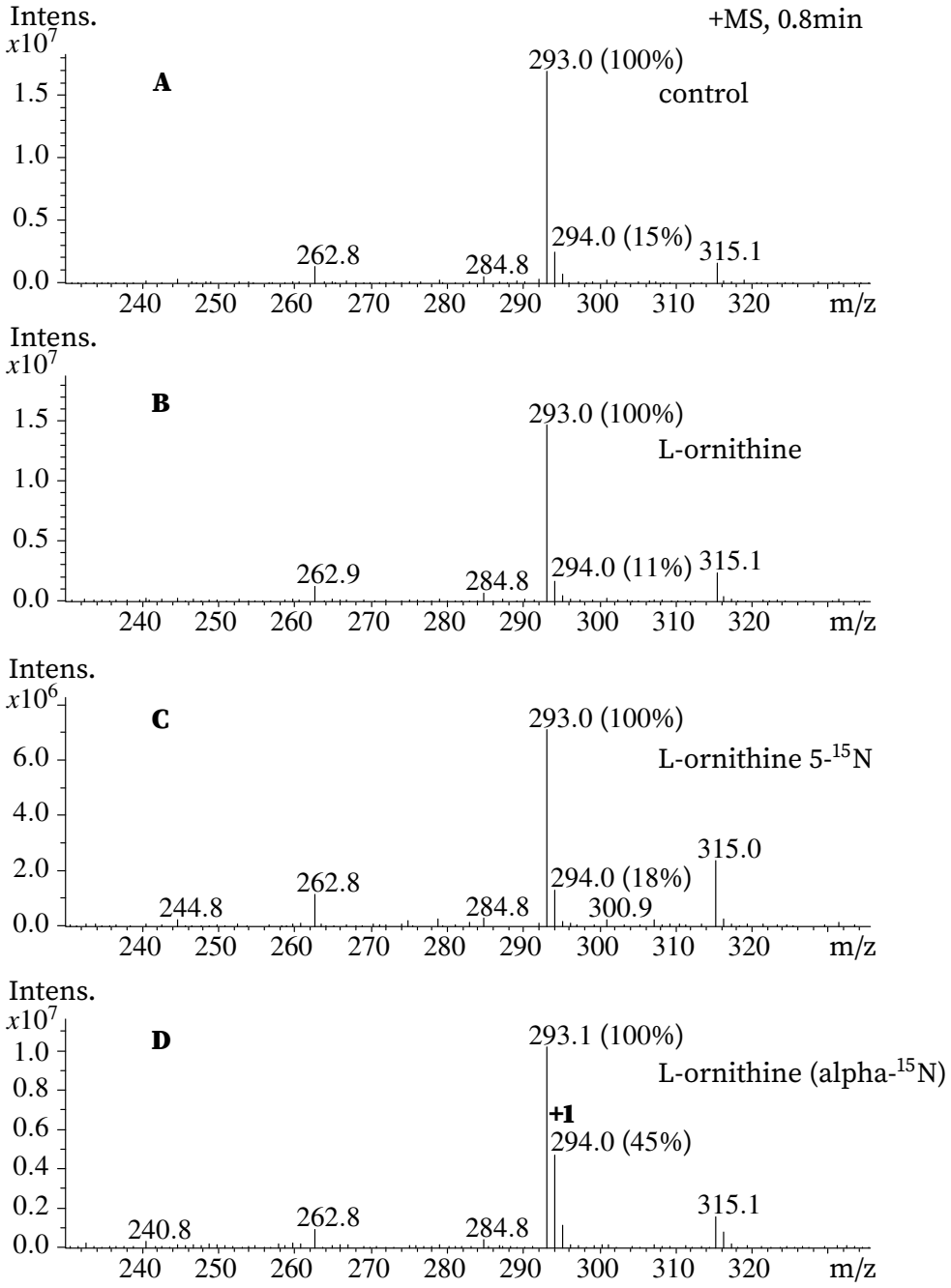

Figure 3.35. **Chromatogram of [*S,S*]-EDDS from culture supernatant from *A. japonicum* OP2 fed with isotope-labeled L-ornithine**. (A) Unlabeled culture. (B) Culture fed with 5mM naturally occuring L-ornithine. (C) Culture fed with L-ornithine 5-^{15}N. (D) Culture fed with L-ornithine (alpha-^{15}N).

3.3.4 Determination of precursors involved in [*S,S*]-EDDS biosynthesis using inverse labeling approach

Isotope labeling is limited by the availability of isotopically labeled precursors. This problem can be avoided by using the inverse labelling approach. Inverse labeling involves growing bacteria on a ^{13}C carbon or ^{15}N nitrogen source, thereby labelling all the carbon or nitrogen atoms of the natural product under investigation.

A negative shift in the *m/z* value of the LC-MS analysis after feeding with unlabelled precursors indicates partial or complete incorporation of the precursors. The inverse labeling approach has been successfully used to identify precursors for the biosynthesis of the cofactor pyrroloquinolone quinone (PQQ) biosynthesis (van Kleef and Duine, 1988) and to identify natural products from methylotrophs (Cummings *et al.*, 2021). To apply this methodology for the elucidation of precursors for the [*S,S*]-EDDS biosynthesis in *A. japonicum*, it was necessary to optimize the production medium.

Inverse labeling with ^{13}C-glycerol optimized medium

[*S,S*]-EDDS production is currently typically performed in SM-medium (Cebulla, 1995; Spohn *et al.*, 2016), containing not only glycerol as a main C-source, but also sodium glutamate monohydrate and ferric citrate are present. To perform the inverse labeling approach, a medium containing glycerol as sole carbon source, was required. Therefore, sodium glutamate monohydrate was substituted by ammonium chloride and ferric citrate was replaced by ferric chloride, while mantaining the same final concentrations.

The optimized medium for the inverse labeling approach with ^{13}C-glycerol was named SM-13C. *A. japonicum* OP2 was inoculated in SM-13C medium for four days and the supernatant was analyzed by HPLC-MS. *A. japonicum* OP2 was used for these experiments since it grows in SM-13C medium and produces [*S,S*]-EDDS in sufficient ammounts to be analyzed by HPLC-MS.

The chromatograms from of the culture supernatant of *A. japonicum* OP2 grown in ^{12}C-glycerol, showed a main signal for [*S,S*]-EDDS with *m/z* value of 293.1[M+H]$^+$. On the other hand, when the culture was grown in ^{13}C-glycerol, the chromatograms revealed a main signal for [*S,S*]-EDDS with an *m/z* value of 303.1 [M+H+10]$^+$. This

result indicates the incorporation of ten ^{13}C atoms into [*S,S*]-EDDS (Figure 3.36).

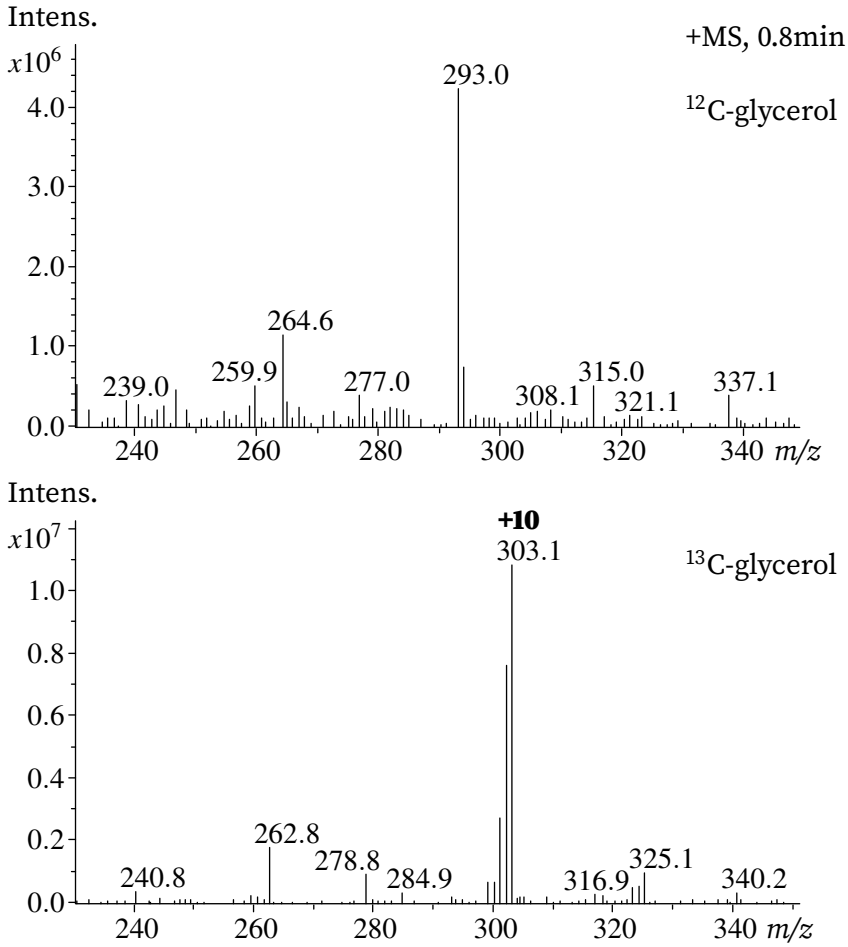

Figure 3.36. **HPLC-MS analysis of [*S,S*]-EDDS produced by *A. japonicum* OP2 grown on ^{12}C-glycerol and ^{13}C-glycerol**. (A) Growth in SM-medium (standard ^{12}C-glycerol containing medium) main signal for [*S,S*]-EDDS *m/z* 293.1. (B) Growth in SM-13C (^{13}C-glycerol containing medium), main peak for [*S,S*]-EDDS with *m/z* value 303.1, in positive mode.

Inverse labeling with $^{15}NH_4Cl$ optimized medium

A similar procedure was applied to optimize SM-medium for the inverse labeling approach using $^{15}NH_4Cl$. In this case, the sole N-source of SM-medium, sodium

glutamate monohydrate, was replaced by $^{15}NH_4Cl$. This optimized medium was named SM-15N. *A. japonicum* OP2 was inoculated in SM-15N and cultured for four days. As negative control, *A. japonicum* OP2 was grown in $^{14}NH_4Cl$. The culture supernatants were analyzed by LC-MS. The negative control, *A. japonicum* OP2 grown in $^{14}NH_4Cl$, showed a main major signal with a *m/z* value of 293.1$[M+H]^+$ for [*S,S*]-EDDS, whereas *A. japonicum* OP2 grown in $^{15}NH_4Cl$, showed a major signal for with a *m/z* value of 295.0 $[M+H+2]^+$, indicating the incorporation of two ^{15}N isotopes (Figure 3.37).

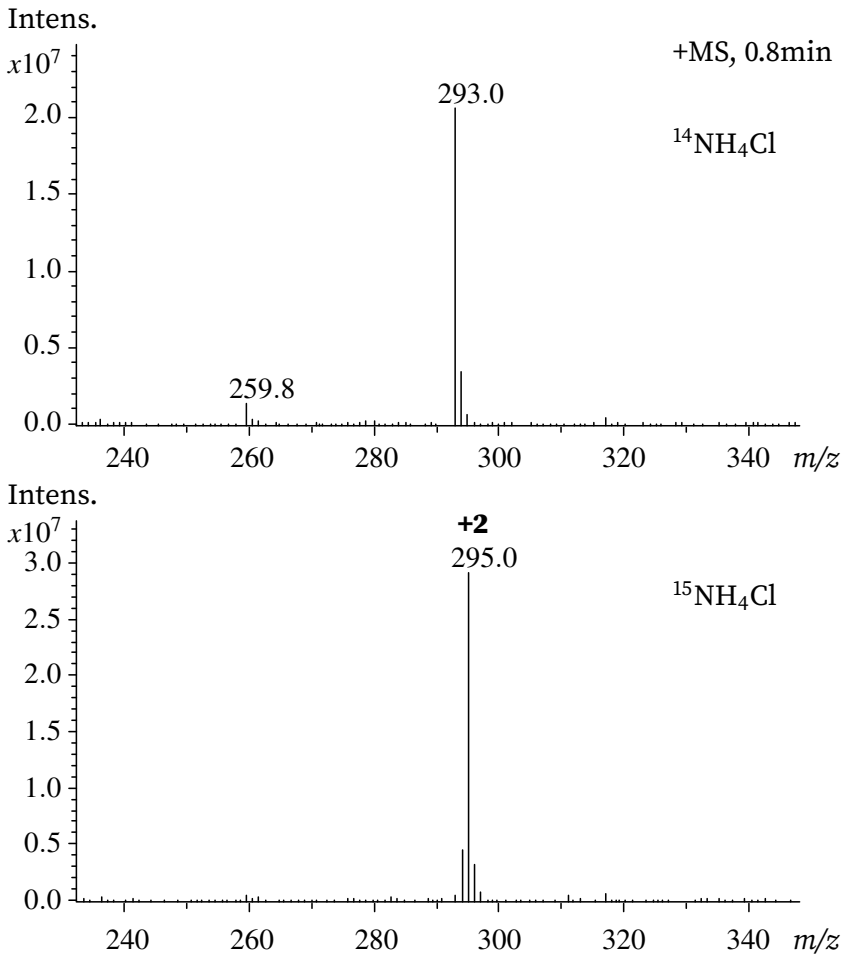

Figure 3.37. **HPLC-MS analysis of [*S,S*]-EDDS produced by *A. japonicum* OP2 grown on $^{14}NH_4Cl$ and $^{15}NH_4Cl$**. (A) Growth in SM-medium ($^{14}NH_4Cl$ containing medium) main signal for [*S,S*]-EDDS *m/z* value of 293.1. (B) Growth in SM-15N ($^{15}NH_4Cl$ containing medium) major peak for [*S,S*]-EDDS *m/z* value of 295.1, in positive mode

.

3.3.4.1 Inverse ^{13}C labeling for determination of carbon contribution to [*S,S*]-EDDS

In order to elucidate the origin of the C-atoms from [*S,S*]-EDDS, feeding with potential ^{12}C-precursors was performed. For this purpose, *A. japonicum* OP2 was grown in the medium SM-13C and was fed with different ^{12}C precursors at a final concentration of 5 mM directly at the beginning of the growth (t = 0).

To determine the partial or complete incorporation of ^{12}C precursors, the culture supernatants were analysed by HPLC-MS after four days of cultivation. As a negative control, *A. japonicum* OP2 was cultured in a medium supplemented with ^{12}C-glycerol.

[*S,S*]-EDDS produced in *A. japonicum* OP2 grown in ^{12}C-glycerol containing medium showed a major signal at retention time 0.8 min, with *m/z* value of 293.1 $[M+H+1]^+$. By growing *A. japonicum* OP2 in SM-13C, a peak with *m/z* value of 303.1 at the same retention time was observed in the supernatant, which corresponds to fully-^{13}C-labeled [*S,S*]-EDDS. Analysis of the chromatogram supernantant from *A. japonicum* OP2 grown SM-13C in the presence of ^{12}C-precursors, showed a signal after the feeding with ^{12}C-L-aspartate as the same retention time of 0.8 minutes. The corresponding mass was reduced by eight *m/z* units, suggesting the incorporation of two ^{12}C-L-aspartic acid. No shift to lower masses was observed in after the addition of ^{12}C-L-ornithine or ^{12}C-L-diaminopropionic acid (L-DAPP). These results confirmed L-aspartic acid as a precursor for the biosynthesis and demonstrated experimentally that two molecules of L-aspartic acid (or OAA) are directly incorporated into the [*S,S*]-EDDS (Figure 3.38), 3.39).

Growth medium	^{12}C-glycerol	^{13}C-glycerol	^{13}C-glycerol+ 12C- L-aspartic acid
[*S*,*S*]-EDDS labeling pattern	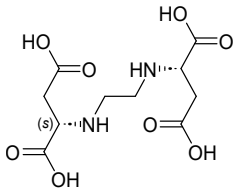	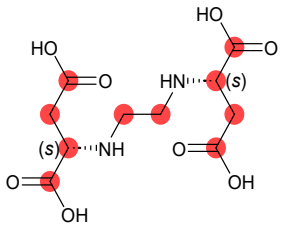	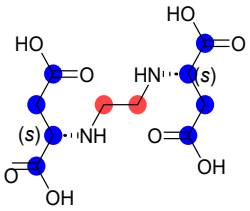
	[*S*,*S*]-EDDS	[*S*,*S*]-EDDS	[*S*,*S*]-EDDS
Mass	293.1	303.1	295.1
	M	M+10	(M+10) -8

Figure 3.38. **Principle of inverse labeling approach for [*S*,*S*]-EDDS**

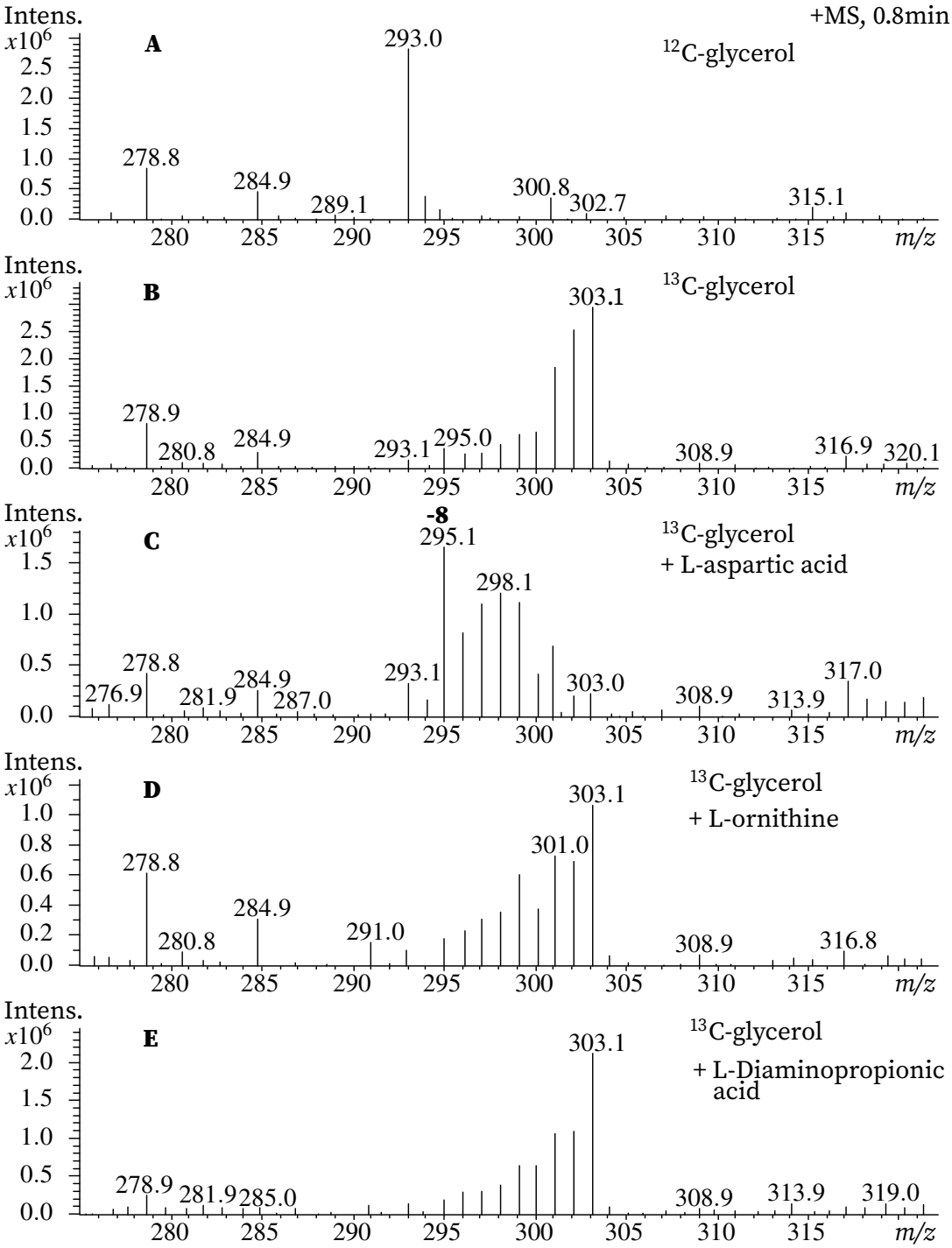

Figure 3.39. **HPLC-MS analysis of the inverse labeling experiments after feeding with potential ^{12}C-precursors**. *A. japonicum* OP2 was grown in ^{13}C-glycerol containing medium and fed with 5 mM ^{12}C-precursors.

3.3.4.2 Inverse labeling using $^{15}NH_4Cl$

In order to elucidate the origin of the N-atoms from [*S,S*]-EDDS, feeding with potential ^{14}N-precursors was performed.

A. japonicum OP2 cultures were grown in SM-15N and fed separately with 5 mM of each 14N precursor at time 0 of cultivation. After four days, the culture supernatants were analyzed by HPLC-MS to evaluate the incorporation of ^{14}N-precursors. The inverse labeling experiment of ^{14}N-L-ornithine in a full-labeled ^{15}N medium confirmed the incorporation of a ^{14}N into [*S,S*]-EDDS (Figure 3.40 D). The incorporation of one or two ^{14}N from ^{14}N-L-aspartic acid was indicated by the appearance of the signals with *m/z* values of 294.0 and 293.0 (Figure 3.40 C). Similar results were obtained after feeding with ^{14}N-L-diaminopropionic acid, where a signal with *m/z* value of 294.0 was detected (Figure 3.40). These results confirmed the incorporation of one ^{14}N from L-aspartic acid, confirming that the complete structure of L-aspartic acid is incorporated into the [*S,S*]-EDDS structure during the biosynthesis (Figure 3.40 C). Furthermore, based on the obtained results, it was observed that one nitrogen atom from L-ornithine is incorporated into the structure of [*S,S*]-EDDS (Figure 3.40 D). However, it is imperative to comprehensively analyze all the feeding experiments conducted with L-ornithine to ascertain whether this incorporation is genuinely observed or if it may be attributed to a scrambling effect. Incorporation of N-atom from L-DAPP into [*S,S*]-EDDS was not confirmed (Figure 3.40 E).

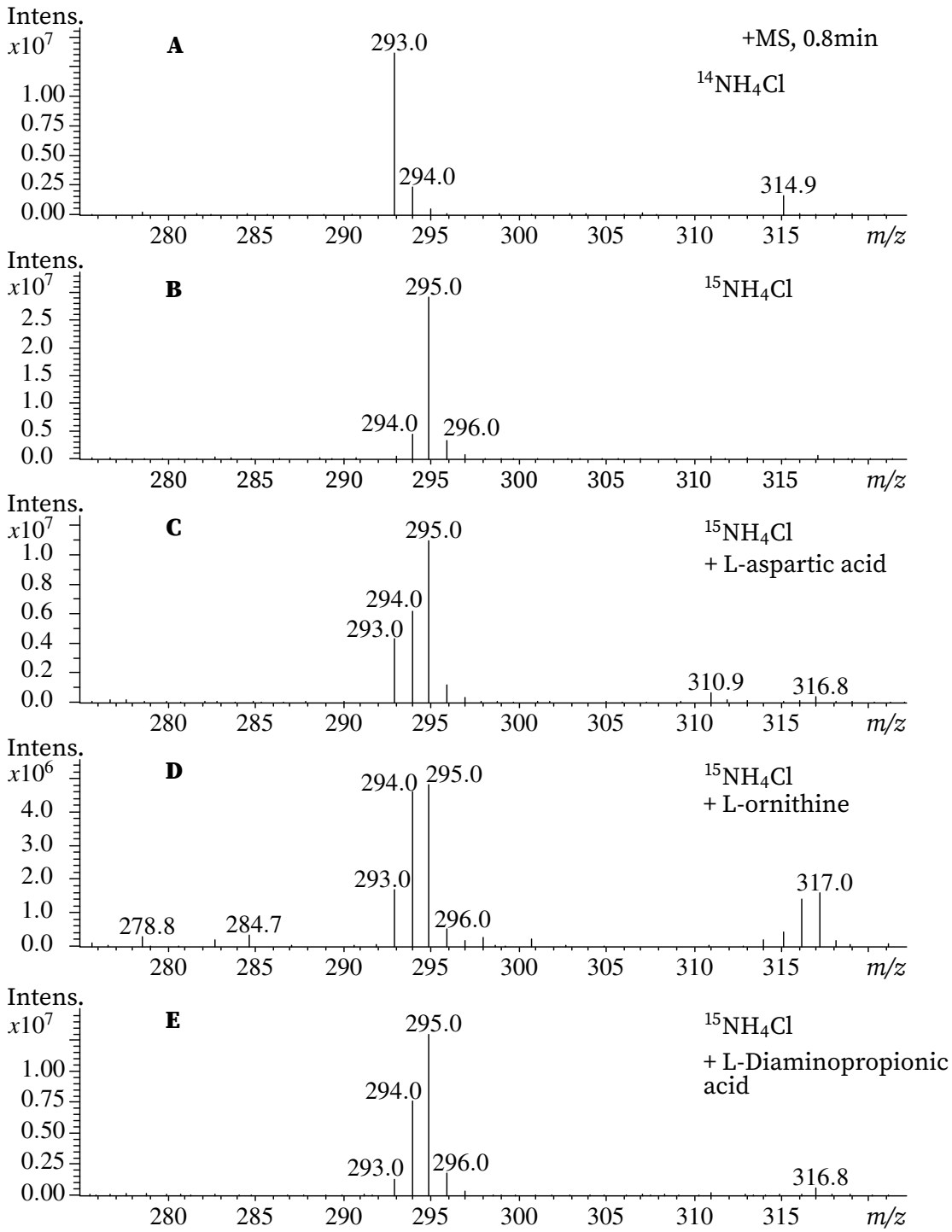

Figure 3.40. **Identification of ^{14}N-precursors from [*S,S*]-EDDS biosynthesis by inverse stable isotopic labeling approach**. *A. japonicum* OP2 was grown in $^{15}NH_4Cl$-containing medium and fed with 5mM ^{14}N-precursors.

Discussion

The production of [*S,S*]-EDDS in *A. japonicum* is likely a survival strategy used by the bacterium to scavenge zinc from the environment under conditions of zinc deficiency, thus acting as a zincophore (Cebulla, 1995; Patzer and Hantke, 1998). In addition to the natural function of [S,S]-EDDS, it has been shown that [*S,S*]-EDDS can replace EDTA in many industrial applications. However, the overproducer *A. japonicum* OP2 (Edenhart *et al.*, 2020) is not suitable for the establishment of an industrial biotechnological process as the quantities produced are still too low. The elucidation of the biosynthetic pathway for [*S,S*]-EDDS is a prerequisite for further optimization of yields, e.g. by improving the precursor supply or increasing the transcription of the biosynthetic genes.

The enzymes involved in [S,S]-EDDS biosynthesis; AesA, AesB and AesC, a putative ornithine cyclodeaminase, a putative amino acid decarboxylase and a putative cysteine synthetase, are distinct from those involved in the biosynthesis of other characterized zincophores, such as histidine racemase (CntK), nicotianamine synthase (CntL) and staphylopin dehydrogenase (StaphDH; CntM)
(Morey *et al.*, 2020). Furthermore, despite the analysis conducted using antiSMASH 7.0, the [*S,S*]-EDDS assembly mechanism could not be identified. Notably, neither the non-ribosomal peptide synthetase (NRPS) nor the NRPS-independent siderophore (NIS) pathways, which are commonly associated with ionophore biosynthesis (Pollack *et al.*, 1970; Gibson and Magrath, 1969), were observed in the analysis.

In the present study, different approaches like genetic manipulation of the producer, biochemical analysis, and feeding studies were used to investigate the assembly of [*S,S*]-EDDS. The results obtained provided a wide range of perspectives to elucidate the biosynthetic pathway. In a genetic manipulation approach, different *A. japonicum* strains have been genetically engineered to be deficient for one or more *aes* genes (Edenhart, unpublished). Intermediates of the pathway, which may accumulate in the individual mutants, were analyzed in culture supernatant and pellets. As the intermediates are expected to be polar, the samples were derivatized with Fmoc-Cl to facilitate the HPLC-MS analysis.

Analysis of culture supernatants and pellets of the mutants did not reveal accumulation of biosynthesis intermediate, except for the culture supernatant of the strain *A. japonicum* ΔEDDS (*aesAC*). The HPLC-MS chromatogram showed a signal

peak with a *m/z* value of 443.14 $[M+H]^+$, accumulated exclusively in this strain, in which the genes *aesA* and *aesC* were present, while *aesB* was deleted. This mass was consistent with the predicted mass for the putative pathway intermediate (S)-2-amino-2carboxyethyl)-L-aspartic acid (ACEAA) derivatized with Fmoc (*m/z* 442.14). ACEAA was predicted as a putative intermediate in the two proposed pathways for [*S,S*]-EDDS biosynthesis (Figure 1.2, 1.3). However, to confirm that the signal peak with a *m/z* value of 443.14 $[M+H]^+$ corresponds to Fmoc-ACEAA, compound purification and NMR analysis are required.

Furthermore, biochemical experiments were performed to elucidate the substrate specificity of the [*S,S*]-EDDS biosynthetic enzymes. L-aspartic acid and OAA were used as substrates to characterize the enzyme AesA. A reaction using purified AesA, OAA as substrate and NADH as cofactor, resulted in a noticeable decrease in absorbance at 340 nm over time, strongly indicating the consumption of NADH in the reaction. These results strongly suggested that OAA serves as a precursor for the biosynthesis of [*S,S*]-EDDS. However, in the reaction with NAD^+ and L-aspartic acid, no changes in NADH absorbance over time were observed, indicating no NADH formation.

These results suggest that AesA may catalyze the reaction with OAA and that either the reaction is not reversible, or another substrate is used required for the reverse reaction. Therefore, its activity was investigated with two additional substrates: malate and alanine. The malate dehydrogenase activity of AesA was evaluated using NAD^+, which involves a reversible reaction between malate and OAA (Takahashi-Íñiguez *et al.*, 2016). Additionally, the alanine dehydrogenase activity of AesA was assessed with the reversible reaction between alanine and OAA (Schröder *et al.*, 2004). In both cases, however, no AesA activity was detected, as indicated by the constant absorbance values at 340 nm, which means the absence of NADH formation. Based on these results, it is hypothesized that AesA catalyzes a NAD^+-dependent reaction, where OAA is accepted as a substrate.

Enzymatic reactions involving AesB and AesC could not be performed. In case of AesB, the two putative substrates based on the pathways postulated by (Spohn *et al.*, 2016; Wang *et al.*, 2022) (Figure 1.2, 1.3) were OAA-Dap imine or ACEAA, respectively, which are not commercially available. In the case of AesC, it was not possible to obtain soluble protein despite many efforts using different purification strategies. The Strep-tag system for protein purification resulted in insoluble pro-

teins, which were found as inclusion bodies in the cell pellet. *In vitro* protein synthesis allowed the production of AesC, but the low protein yield was insufficient for further enzymatic assays. Additionally, the *aesC* sequence was codon-optimized for expression in *E. coli*. However, no soluble AesC was obtained. To gain more insights, the AesC structure was predicted using Alphafold and compared with the structure of the homologous protein SbnA from *Staphylococcus aureus*. SbnA is an enzyme involved in the biosynthesis of Staphylofferin B, that shares 33 % similarities with AesC and has previously been successfully purified. The alignment of the two structures revealed that AesC contains an extra C-terminal alpha-helix not present in SbnA, which may be responsible for protein misfolding and for precipitation. Further experiments are needed to study this hypothesis.

Previous feeding experiments with DL-4-^{13}C-L-aspartic acid showed incorporation of aspartic acid into [*S,S*]-EDDS (Cebulla, 1995). In this study, feeding experiments with 1,4^{13}C2;^{15}N-L-aspartic acid and ^{15}N-L-aspartic acid showed incorporation of one ^{15}N and two ^{13}C atoms from L-aspartic acid. As L-aspartic acid was labeled on the C-atoms at positions 1 and 4, it can be assumed that the whole molecule was incorporated into the structure of [*S,S*]-EDDS. This was concluded from the HPLC-MS, and NMR analysis. The inverse stable isotope labeling method showed that two L-aspartic acids (or one L-aspartic acid and one OAA) were indeed incorporated into [*S,S*]-EDDS. OAA is formed by deamination of L-aspartic acid. Incorporation was detected by a negative shift in the mass-to-charge ratio (*m/z*), consistent with the incorporation of 8-^{12}C precursors.

However, presumably because of isotopic dilution after feeding with 1,4-^{13}C2;^{15}N-L-aspartic acid, it was difficult to determine the exact number of ^{13}C atoms incorporated into [*S,S*]-EDDS (Muchmore *et al.*, 1989). Although NMR analysis confirmed the incorporation of 2-^{13}C and 1-^{15}N, the symmetry of the [*S,S*]-EDDS molecule prevented the determination of whether the same incorporation occurred on the other side.

To circumvent this problem, the inverse stable isotope labeling method was used. In this approach, *A. japonicum* OP2 was grown on ^{13}C-glycerol or $^{15}NH_4Cl$ and fed with ^{12}C or ^{14}N precursors to assess incorporation. Incorporation can be detected by a negative shift in the mass-to-charge ratio (*m/z*), depending on whether all or only part of the ^{12}C or ^{14}N precursor is incorporated. A prerequisite for the application of this approach was the optimization of a minimal medium

containing only ^{13}C-glycerol as a carbon source (to determine the incorporation of C-atoms) or $^{15}NH_4Cl$ as only nitrogen source (to determine the incorporation of N-atoms). The SM-medium used for [*S,S*]-EDDS production contains glycerol, ferric citrate and sodium glutamate monohydrate as carbon sources. Ferric citrate and sodium glutamate monohydrate were replaced by $FeCl_3$ and NH_4Cl, respectively. It was shown that [*S,S*]-EDDS production occurred in the modified SM-13C medium, as HPLC-MS analysis identified signal with *m/z* value of 293.1 $[M+H]^+$, corresponding to the [*S,S*]-EDDS structure. After culturing *A. japonicum* in ^{13}C-glycerol, a signal with a *m/z* value of 303.1 $[M+10+H]^+$ was identified in the supernatant for [*S,S*]-EDDS. This indicates an [*S,S*]-EDDS structure in which all 10 carbon atoms are labeled. However, additional peaks were observed indicating the incorporation of external ^{12}C atoms. A possible explanation is that *A. japonicum* can incorporate ^{12}C atoms from ambient CO_2 into its metabolism, as described for *Streptomyces thermoautotrophicus* UBT1 (Gadkari *et al.*, 1992) (Gadkari et al., 1992). This is a hypothesis that requires further experimental verification.

All the results so far clearly indicate that OAA and L-aspartic acid are precursors of [*S,S*]-EDDS biosynthesis. Furthermore, genetic engineering studies have demonstrated that *O*-phospho-serine is required as a precursor for the biosynthesis of [*S,S*]-EDDS (Edenhart *et al.*, 2020). However, feeding experiments with this amino acid could not be carried out, because *A. japonicum* cannot take up this amino acid. As the exact biosynthetic mechanism has not yet been elucidated, other precursors and intermediates, such as ornithine and L-diaminopropionic acid (L-DAPP), have been investigated for their involvement in the biosynthesis using various methods. L-DAPP has been proposed to be involved in the postulated biosynthetic pathways of [*S,S*]-EDDS (Spohn *et al.*, 2016), and L-ornithine has been described as a precursor for L-DAPP formation in the biosynthesis of viomycin and capreomycin (Thomas *et al.*, 2003; Wang and Gould, 1993).

In order to investigate the possibility of L-DAPP biosynthesis from L-ornithine and *O*-phosphoserine in analogy to the biosynthesis of viomycin and capreomycin (Thomas *et al.*, 2003; Wang and Gould, 1993), feeding experiments with L-ornithine were carried out. However, the chromatogram from direct feeding with isotopically labeled ^{13}C5;^{15}N2-L-ornithine indicated that ornithine is not incorporated directly, but after its conversion to other metabolites by the central metabolism of *A. japonicum* (so-called scrambling). The results pointed to the incorporation of

the alpha-amino group of L-ornithine into the [*S,S*]-EDDS. In addition, feeding the bacteria with naturally occurring L-ornithine led to an increase in [*S,S*]-EDDS production. Both results suggested an (indirect) involvement of L-ornithine in [*S,S*]-EDDS biosynthesis.

A possible explanation for the incorporation of a N-atom from L-ornithine into [*S,S*]-EDDS is its linkage to *O*-phosphoserine. L-ornithine is converted to glutamate via L-glutamate-5-semialdehyde. Glutamate acts as an amino group donor in the synthesis of *O*-phosphoserine from 3-phosphooxypyruvate (Figure 3.41).

In the biosynthetic pathway postulated by (Spohn *et al.*, 2016), L-DAPP is produced in two stages from L-aspartic acid and *O*-phosphoserine using AesA and AesC. In order to perform biochemical assays, the enzymes had to be purified. The AesA protein could be purified, but AesC could not. To overcome this problem, L-aspartic acid and *O*-phosphoserine were added together with AesA to a cell lysate of *A. japonicum* ΔEDDS (*aesC*). In this strain, *aesA* and *aesB* have been deleted and only *aesC* is present in the genome. No L-DAPP was detected by HPLC-MS. In the postulated biosynthetic pathway, L-DAPP is the substrate of AesB. Thus, L-DAPP feeding of the *A. japonicum* mutant containing *aesA* and *aesC*, but not *aesB* should allow [*S,S*]-EDDS synthesis (Figure 1.2). However, no [*S,S*]-EDDS could be detected in this experiment. Inverse labeling experiments with ^{13}C-glycerol or ^{15}N-NH4Cl cultures fed with L-DAPP showed no incorporation of L-DAPP C/N atoms into [*S,S*]-EDDS.

A further genetic experiment was carried out to investigate the role of L-DAPP in [*S,S*]-EDDS biosynthesis. Two gene pairs, *dappA1* and *dappC1*, and *dappA2* and *dappC2*, were identified at different positions in the *A. japonicum* genome. Protein blast analyses showed that the encoded proteins were homologous to proteins that catalyze the synthesis of L-DAPP. To test this hypothesis, the *dappA1/C1* or *dappA2/C2* genes were cloned into the pRM4 plasmid together with *aesB* and transferred into *A. japonicum* ΔEDDS. The genes were cloned under the control of the constitutive promoter *ermEp** in pRM4, which integrates into the *A. japonicum* chromosome via the ϕ31 att site. The mutants were grown under EDDS production conditions. However, neither L-DAPP synthesis (Figure 3.29) nor [*S,S*]-EDDS was detected when HPLC-MS was performed (Figure 3.28).

All these results indicate that L-DAPP is not an intermediate in [*S,S*]-EDDS biosynthesis.

Various experiments have been carried out to analyze the stepwise biosynthesis of [*S,S*]-EDDS. However, none of the methods used could provide a complete picture. Therefore, in order to postulate a biosynthetic pathway, it was important to combine the results of the individual experiments. Different experimental approaches confirmed that L-aspartic acid and OAA are the primary precursors for [*S,S*]-EDDS production. Specifically, the experiments showed that one molecule of L-aspartic acid and one molecule of OAA are incorporated into the [*S,S*]-EDDS structure. In addition, this study identified a putative intermediate, ACEAA, which was found exclusively in the *A. japonicum* ΔEDDS (*aesAC*) strain, in which both the *aesA* and *aesC* genes are present. This suggests that AesA may catalyse the conversion of OAA to L-aspartic acid prior to the synthesis of ACEAA from L-aspartic acid and *O*-phosphoserine. Notably, no evidence was found for the contribution of L-DAPP to [*S,S*]-EDDS biosynthesis. The ^{14}N-labeled form of L-ornithine found in [*S,S*]-EDDS during inverse labeling experiments was thought to result from the direct incorporation of L-ornithine into [*S,S*]-EDDS. However, the metabolic link between L-ornithine and *O*-phosphoserine, a direct precursor of [*S,S*]-EDDS, may explain why the labelling of the alpha-amino group of L-ornithine was incorporated into [*S,S*]-EDDS (Figure 3.41). Based on these findings, a novel biosynthetic pathway for [*S,S*]-EDDS has been proposed (Figure3.42). However, further experiments will be required to confirm this pathway.

Overall, this work sheds light on the [*S,S*]-EDDS biosynthetic pathway in *A. japonicum* and the findings have significant implications for the development of new pathway elucidation strategies.

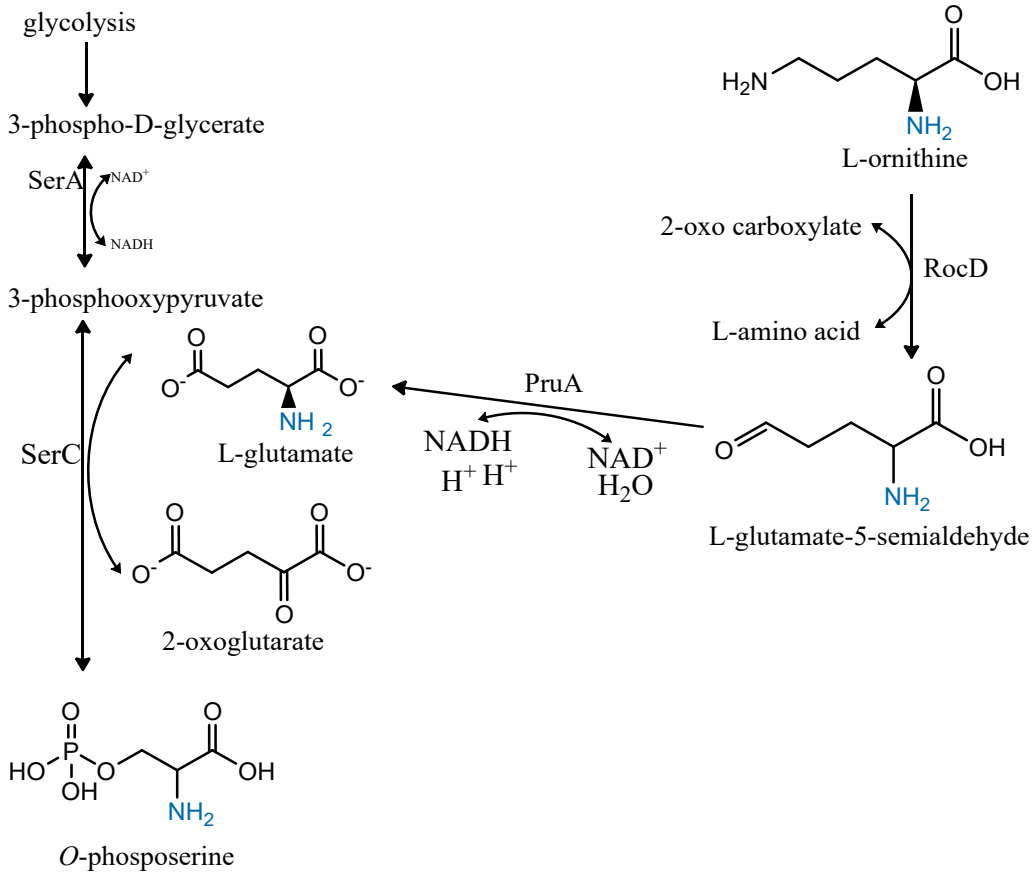

Figure 3.41. **Metabolic connection between L-ornithine and *O*-phosphoserine**. Isotope-labeled alpha-NH_2 from L-ornithine is shown in blue.

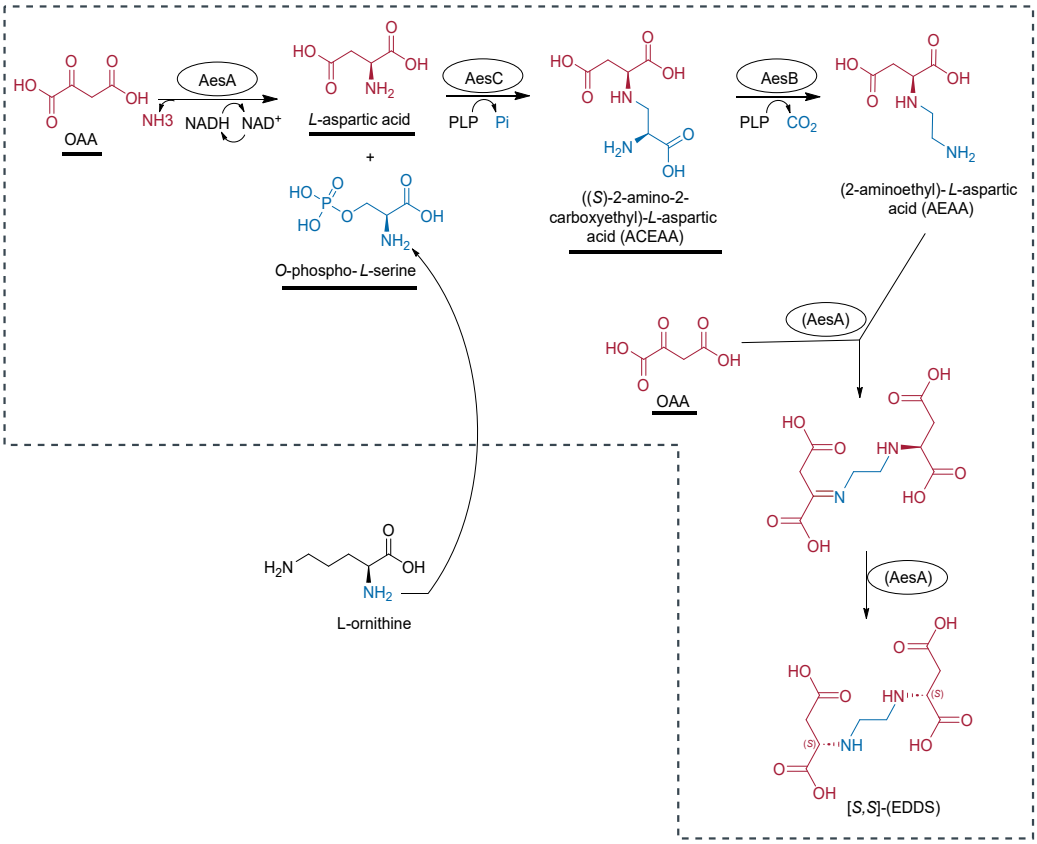

Figure 3.42. **[*S,S*]-EDDS proposed biosynthetic pathway in *A. japonicum*.** Inside the box, a proposed pathway including the intermediate ACEAA and precursors for [S,S]-EDDS biosynthesis from Cebulla, 1995, Spohn *et al.,* 2016 and this study, underlined with a black line. In circles [*S,S*]-EDDS biosynthetic enzymes.

Chapter 4

Publications

4.1 Declaration of author contribution

Publication: Research article

"Secondary Metabolite Transcriptomic Pipeline (SeMa-Trap), an expression-based exploration tool for increased secondary metabolite production in bacteria"

Under the supervision of PD. Dr. Evi Stegmann, I developed the *A. japonicum* mutants used in this manuscript and conducted the [*S,S*]-EDDS production test. I wrote the section "Proof of principle" with input from PD. Dr. Evi Stegmann and prepared the graphical abstract for the manuscript.

4.2 Improvement of [*S,S*]-EDDS production in *A. japonicum*

[*S,S*]-EDDS is a functional equivalent to ethylene-diamine-tertraacetate (EDTA), a widely used chelating agent in industrial, domestic, and agricultural applications due to its ability to complex metals. EDTA finds use in a range of applications, including pulp, paper, and textile production, cleaning and laundry operations, soil remediation, food products, tanning processes, photography, wastes and effluents treatment, pharmaceuticals, and cosmetics (Knepper, 2003; Nowack and VanBriesen, 2005). EDTA is not removable by conventional wastewater treatment and can remain in high concentrations in aquatic environments, posing constant environmental threats by undesirably mobilizing metal ions (Thomas P. Knepper ,Johannes Driemler, Anke Maes, Jutta Müller,Darius Soßdorf, 2001).

[S,S]-EDDS, with similar metal coordination chemistry to EDTA and comparable chelating properties (Whitburn *et al.*, 1999), stands out for its readily biodegradable nature until complete mineralization (Schowanek, 1997; Takahashi *et al.*, 1997). The [S,S] configuration is readily biodegradable (Schowanek, 1997), (Takahashi *et al.*, 1997). [S,S]-EDDS, a structural isomer of EDTA with similar chelating properties (Chen *et al.*, 2010), is exclusively produced by *A. japonicum*. By optimizing the synthetic medium with suitable phosphate, nitrogen, and carbon sources, a yield of about 20g/L of [S,S]-EDDS has been achieved (Zwicker *et al.*, 1997). However, biotechnological production of [*S,S*]-EDDS has been prevented by low-μM zinc concentrations that are ubiquitous. An *A. japonicum* mutant Δzur, which bypasses the zinc regulation, was sucessfully constructed by (Spohn *et al.*, 2016). This mutant's availability has created the opportunity to develop a biotechnological process. Recently, a zinc-deregulated overproducer strain was constructed using metabolic engineering approaches, improving the availability of the precursor *O*-phosphoserine. This *A. japonicum* strain OP2 produced 9.8 g/l within 135 hours of fermentation time (Edenhart *et al.*, 2020).

Despite the impressive chemical properties of [*S,S*]-EDDS, a cost-effective biotechnological production process for [*S,S*]-EDDS has not yet been established. To make a biotechnological production process economically viable for industrial applications, it is necessary to increase the yield of [*S,S*]-EDDS.

As our understanding of metabolic pathways continues to evolve and genetic tools become more sophisticated, rational strain improvement by means of me-

tabolic engineering is proving to be an effective way to increase natural product yields. Redirecting metabolic flux towards the production of desired metabolites can be achieved through various genetic strategies, such as enhancing precursor supply, optimizing enzyme efficiency, modifying gene regulation, reducing unwanted byproducts, competing pathways, or even reconstituting entire pathways within a heterologous host. However, many genes not involved in regulation, precursor biosynthesis, or product-related processes are often overlooked. Therefore, having a tool that provides valuable information for prioritizing target genes using metabolic engineering is crucial (Lee *et al.*, 2009). The Secondary Metabolite Transcriptomic Pipeline (Sema-Trap) is a powerful tool for RNA-Seq-based transcriptome analysis. By analyzing the co-expression patterns between the gene clusters of interest and specific genes, Sema-Trap enables the identification of potential targets for genetic engineering to overexpress a desired biosynthetic gene cluster (BGC). This approach provides a valuable strategy for enhancing the production of secondary metabolites of interest.

4.3 Results and discussion

4.3.1 Identification of target genes to increase [*S,S*]-EDDS production using SeMa-Trap

[*S,S*]-EDDS production is inhibited by zinc at concentrations $\geq$2 mM in *A. japonicum* WT strain and the zinc-responsive [*S,S*]-EDDS biosynthesis is known to be regulated by the zinc uptake regulator Zur. To overcome this limitation, a *zur* deletion mutant was developed by (Spohn *et al.*, 2016), which was found to be capable of producing [*S,S*]-EDDS in zinc-containing media. *A. japonicum* Δ*zur* provided an opportunity to develop a biotechnological process for the production of [*S,S*]-EDDS without being limited by zinc-mediated repression. SeMa-Trap was used as proof of concept to examine the transcriptomic data from *A. japonicum*. RNA-Seq analyses of *A. japonicum* wild type WT and *A. japonicum* Δ*zur* cultured in the presence and absence of zinc for 24 h were performed. Thereby, a direct correlation between *zur* gene expression and the [*S,S*]-EDDS biosynthetic genes (BGs) could be observed. Using SeMa-Trap, genes that exhibited high co-expression with the [*S,S*]-EDDS BG (concordantly regulated genes) and genes regulated in the oppo-

site manner (discordantly regulated genes) were identified. As expected, SeMa-Trap showed a correlation between the expression of *zur* (annotated as Fur) and the production of [*S,S*]-EDDS. Zur showed the highest score from the "discordantly regulated genes", which means that the expression of *zur* decreases (suppress, in this case) the expression of [*S,S*]-EDDS biosynthetic genes. The entire analysis is available online [1].

Several concordantly regulated genes predicted to be involved in regulation and metabolism were shown in SeMa-Trap analysis (Figure4.1, 4.2). The proof of concept was performed with concordantly regulated genes, since overexpression of the target gene is a straightforward approach, while the deletion is a multi-step and time-consuming process. Genes with regulatory functions and genes connected to metabolism were the main focus. Based on literature search, the second and fifth most co-regulated genes with regulatory functions, AJAP_RS36645 (*bldC*) and AJAP_RS11995 (*lacI*) were selected for overproduction experiments, since genes having the best co-expression score were unlikely to play a role in [*S,S*]-EDDS production. Similarly, the gene AJAP_RS11230, glutamate synthase, having the second-best co-expression score, was selected.

[1] `https://sema-trap.ziemertlab.com/results/4985a8de-4c61-426f-8011-51b6aaa51350`

Other Significant Genes

Show only genes with attributes: Regulation

Filter tables

281 genes

Concordantly regulated genes

Gene	Score	Combination	Relative position to cluster	Product	Annotation
AJAP_RS15075	78.93	(2)	1503045	NAD(P)H-binding protein	None
AJAP_RS36645	37.78	(2)	6235770	BldC family transcriptional regulator	None
AJAP_RS13380	36.94	(2)	1111660	sugar isomerase	None
AJAP_RS21735	36.92	(2)	2994223	Gfo/Idh/MocA family oxidoreductase	None
AJAP_RS11995	30.92	(2)	757671	LacI family transcriptional regulator	K02529-LacI family transcriptional regulator (1 other annotation) +
AJAP_RS21740	28.5	(2)	2995608	TetR family transcriptional regulator	None
AJAP_RS06655	28.4	(2)	-356706	nitrate- and nitrite sensing domain-containing protein	None

Figure 4.1. **SeMa-Trap predicted targeted genes with "regulation attributes"**. The first five targeted genes with the highest score in the category "regulation" are shown. Genes selected for overexpression in *A. japonicum* (*bldC* and *lacI*) are highlighted.

Secondary Metabolism Specific KEGG terms

Metabolism (128/547) x Choose...

Other KEGG terms

Choose...

Concordantly regulated genes

Gene	Score	Combination	Relative position to cluster	Product	Annotation
AJAP_RS15070	77.51	(2)	1501244	glycerol-3-phosphate dehydrogenase	K00111-glycerol-3-phosphate dehydrogenase +
AJAP_RS11230	48.42	(2)	604162	glutamate synthase subunit beta	K00266-glutamate synthase (NADPH) small chain (1 other annotation) +
AJAP_RS11225	46.35	(2)	599601	glutamate synthase large subunit	K00265-glutamate synthase (NADPH) large chain (3 other annotations) +
AJAP_RS21600	43.23	(2)	2966272	enoyl-CoA hydratase/isomerase family protein	K01692-enoyl-CoA hydratase (12 other annotations) +
AJAP_RS24210	41.91	(2)	3571397	5-methyltetrahydropteroyltriglutamate--homocysteine S-methyltransferase	K00549-5-methyltetrahydropteroyltriglutamate--homocysteine methyltransferase (1 other annotation) +
AJAP_RS13390	38.69	(2)	1113449	class II fructose-bisphosphate aldolase	K01624-fructose-bisphosphate aldolase, class II (5 other annotations) +
AJAP_RS35215	36.18	(2)	5945743	ADP-forming succinate--CoA ligase subunit beta	K01903-succinyl-CoA synthetase beta subunit (3 other annotations) +
				succinate dehydrogenase hydrophobic	K00242-succinate dehydrogenase / fumarate reductase, membrane anchor subunit (3

Figure 4.2. **SeMa-Trap predicted targeted genes with metabolic functions**. The targeted gene with metabolic functions and the second highest score, glutamate synthease (glts) is highlighted. This gene was selected for over-expression in *A. japonicum*.

4.3.2 Overexpression of targeted genes predicted by SeMa-Trap in *A. japonicum*

The genes annotated as *bldC*, *lacI* and *glts* were cloned individually, or the tree genes together into pRM4 plasmid under the control of the constitutive promoter *ermEp**. The plasmids were introduced into *A. japonicum* WT via conjugation and [*S,S*]-EDDS production test was performed. The results showed a significant increase in the [*S,S*]-EDDS production after the overexpression of *bldC* or *glts*. Notably, simultaneous overexpression of these genes resulted in an increased [*S,S*]-EDDS production by 3-fold compared to *A. japonicum* WT (Figure 4.3). These results are in agreement with the analysis performed by Sema-Trap and confirmed the usefulness of Sema-Trap for the identification of target genes for secondary metabolite overproduction.

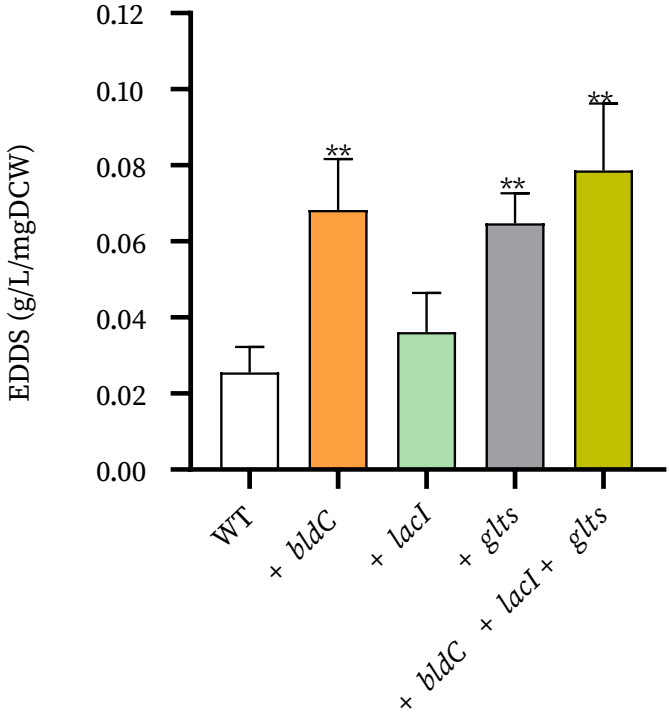

Figure 4.3. **[*S,S*]-EDDS production in *A. japonicum* WT and in different *A. japonicum* mutants. *A. japonicum* (*bldC*), *A. japonicum* (*lacI*), *A. japonicum* (*glts*) and *A. japonicum* (*bldC-lacI-glts*)**. Strains were grown for 120 h in zinc depleted synthetic medium (SM). Error bars show the standard deviation for three biological replicates. Statistical significance were determined using unpaired Student't-test.*p≤0.05, **p≤0.01, ***p≤0.001, ****p≤0.0001.

Discussion

SeMa-Trap is a unique and user-friendly web server that combines genome mining and transcriptomic approaches for the identification of potential target genes to increase the production of BGCs encoding products. With the user-friendly graphical interface of the web server, researchers in the natural product field can easily extract RNA-Seq data without having to navigate complicated command-line tools. However, it is important to note that the scoring system, should not be the only factor considered when selecting target genes. Further analysis, including literature review and consideration of other relevant factors, is necessary to validate the hits obtained through the scoring system.

Although none of the selected genes have been experimentally proven to be directly involved in the biosynthesis of [*S,S*]-EDDS, they may have an impact on the production of this secondary metabolite. The gene *bldC,* along with other *bld* genes, is known to play a critical role in regulating the transition from vegetative to reproductive growth in Streptomyces species by repressing genes essential for cell division and sporulation (Bush *et al.*, 2019). Mutations in *bldC* have been shown to affect sporulation and the production of other secondary metabolites, such as actinorhodin and undecylprodigiosin (Hunt *et al.*, 2005). The pleiotropic regulator LacI can also have varying effects on secondary metabolite biosynthesis depending on the organism and the specific metabolite. For example, overexpression of a LacI-family transcriptional regulator increased the production of antibiotic pigments in *S. coelicolor* but decreased their production in *S. lividans* (Meng *et al.*, 2012). In addition, glutamate synthase, small subunit, catalyzes the reversible reaction from L-glutamate to 2-oxoglutarate, which can be converted to OAA during the TCA cycle. Since OAA is a direct precursor for the biosynthesis of [*S,S*]-EDDS, overexpression of glutamate synthase may have a potential impact on the production of [*S,S*]-EDDS.

Overall, the effectiveness of SeMa-Trap in identifying co-regulated genes in the [*S,S*]-EDDS encoding BGC was demonstrated in this study. After the overexpression of the putative genes *bldC, lacI* and *glts,* the production of [*S,S*]-EDDS increased 3-fold compared to *A. japonicum* WT.

Nucleic Acids Research, 2022 **1**
https://doi.org/10.1093/nar/gkac371

Secondary Metabolite Transcriptomic Pipeline (SeMa-Trap), an expression-based exploration tool for increased secondary metabolite production in bacteria

Mehmet Direnç Mungan [1,2,3], Theresa Anisja Harbig[2], Naybel Hernandez Perez[1], Simone Edenhart[1], Evi Stegmann[1,3], Kay Nieselt[2] and Nadine Ziemert [1,2,3,*]

[1]Interfaculty Institute of Microbiology and Infection Medicine Tübingen (IMIT), University of Tübingen, Auf der Morgenstelle 28, 72076 Tübingen, Germany, [2]Interfaculty Institute for Bioinformatics and Medical Informatics (IBMI), University of Tübingen, 72076 Tübingen, Germany and [3]German Center for Infection Research (DZIF), Partnersite Tübingen, 72076 Tübingen, Germany

Received March 07, 2022; Revised April 20, 2022; Editorial Decision April 27, 2022; Accepted April 29, 2022

ABSTRACT

For decades, natural products have been used as a primary resource in drug discovery pipelines to find new antibiotics, which are mainly produced as secondary metabolites by bacteria. The biosynthesis of these compounds is encoded in co-localized genes termed biosynthetic gene clusters (BGCs). However, BGCs are often not expressed under laboratory conditions. Several genetic manipulation strategies have been developed in order to activate or overexpress silent BGCs. Significant increases in production levels of secondary metabolites were indeed achieved by modifying the expression of genes encoding regulators and transporters, as well as genes involved in resistance or precursor biosynthesis. However, the abundance of genes encoding such functions within bacterial genomes requires prioritization of the most promising ones for genetic manipulation strategies. Here, we introduce the 'Secondary Metabolite Transcriptomic Pipeline' (SeMa-Trap), a user-friendly web-server, available at https://sema-trap.ziemertlab.com. SeMa-Trap facilitates RNA-Seq based transcriptome analyses, finds co-expression patterns between certain genes and BGCs of interest, and helps optimize the design of comparative transcriptomic analyses. Finally, SeMa-Trap provides interactive result pages for each BGC, allowing the easy exploration and comparison of expression patterns. In summary, SeMa-Trap allows a straightforward prioritization of genes that could be targeted via genetic engineering approaches to (over)express BGCs of interest.

GRAPHICAL ABSTRACT

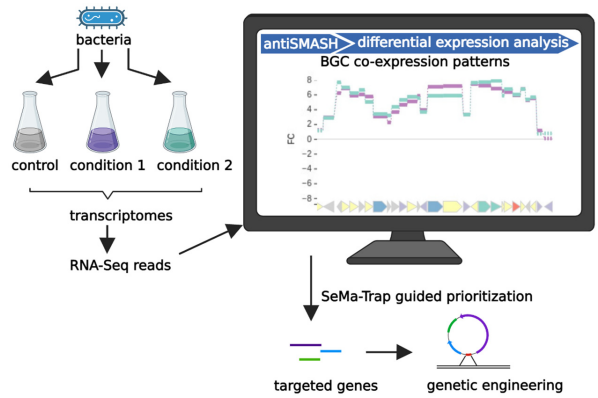

INTRODUCTION

By providing a wide range of biological functions, natural products have been foundational to the survival and evolutionary fitness of various organisms in the tree of life (1). Also known as secondary metabolites (SMs), these compounds are abundantly produced by plants and microorganisms (2). For decades, these molecules have been fueling various industries such as pharmaceutics as antimicrobial agents (3,4). However, the decrease in the discovery rates of novel antibiotics and the parallel increase in resistance towards the existing antibiotics make the identification of new bioactive compounds a task of paramount importance (5). By encoding the enzymes necessary for compound production, biosynthetic gene clusters (BGCs) represent the orga-

*To whom correspondence should be addressed. Tel: +49 7071 2978841; Email: nadine.ziemert@uni-tuebingen.de

nized groups of genes involved in the production of SMs (6). During the last decade an enormous number of genomic sequences have been made available, revolutionizing genome mining efforts in natural product research (7). Based on algorithmic concepts like hidden Markov models (HMMs), highly improved computational tools for BGC prediction such as antiSMASH (8) enable rapid mining of sequenced genomes. By using such tools, thousands of BGCs have been made available to researchers stored in public databases such as MIBiG (9), antiSMASH-DB (10) or The Natural Products Atlas (11). However, from the entire bacterial kingdom, it was recently shown that only 3% of its genomic potential for SMs has been experimentally verified (12). One of the main reasons for this phenomenon is that the expression of the BGCs is often tightly regulated and not observed under laboratory conditions. This non-expressed nature of the BGCs creates a major bottleneck in the identification of bioactive compounds with novel modes of action (13).

To activate silent BGCs and increase the production titers of SMs, several strategies have been devised such as altering the culturing conditions or heterologous expression of the BGCs (14,15). Additionally, genetically modifying global and local regulatory genes can enhance transcription levels of biosynthetic genes (16). Activation or disruption of positive and negative regulators, respectively, has led to the expression of many silent BGCs (17,18). Furthermore, it has been shown that increasing the expression of genes encoding transporters (19), conferring resistance (20), or involved in precursor supply (21) also increases SM production. However, major antibiotic producers like the organisms belonging to the genus *Streptomyces* (22) encode around 7000 genes on average (23). This raises the question: Which ones to genetically modify? Comparative transcriptomic analyses based on RNA-sequencing (RNA-seq) can help decipher the complex pathways that regulate the BGCs of interest and thereby, select the genes to prioritize (hereinafter referred to as target genes) (24,25). This strategy is mostly conducted by comparing the expression levels of BGCs from organisms with genetic variance or from the same strain cultured under different physiological conditions (26,27). The overwhelming number of possible experimental designs make the prioritization of promising culture conditions and target genes crucial for genetic manipulation approaches. To achieve this aim, we developed the 'Secondary Metabolite Transcriptomic Pipeline' (SeMa-Trap). Available at https://sema-trap.ziemertlab.com, SeMa-Trap allows for efficient transcriptome mining of BGCs in bacteria through a user-friendly web interface. The pipeline performs RNA-Seq based transcriptome analysis of BGCs predicted by antiSMASH, compares their fold-changes in various experiments, and allows for promising experimental design and prioritization of the target genes for BGC overexpression. Finally, SeMa-Trap provides interactive result pages for each BGC. This allows easy exploration of BGC expression under certain culturing conditions and the identification of co-regulated genes, which may be located elsewhere in the genome and display potentially interesting functions as defined by the KEGG database (28). Here we provide an overview of the pipeline, highlight the visualization of the interface and demonstrate the efficacy of SeMa-Trap through a case study.

MATERIALS AND METHODS

Workflow

The SeMa-Trap pipeline consists of 4 key steps (Figure 1). The first step is the acquisition of user provided genome and RNA-Seq data. Afterwards, genes involved in BGC expression regulation in the genome (e.g. transporters or regulators, referred to as genes of interest) are annotated, and BGCs are predicted by antiSMASH. BGC annotations in addition to those identified by antiSMASH can also be provided by the user by using the 'Defined clusters' option. To generate reference expression levels, essential housekeeping genes are also identified. In the third step, RNA-Seq analysis is performed to obtain expression levels and fold changes of the genes and BGCs of interest. Finally, results are presented by interactive visualizations and summarizing tables for easy exploration of the expression level changes. All results are kept in the server for 2 months. In addition, they can also be downloaded by saving the results page to the local machine. In case of larger data analysis, local installation and combining SeMa-Trap with in-house analysis pipelines is also possible using Anaconda.

Input options and data acquisition

Input form. SeMa-Trap accepts user provided genomes in GenBank and FASTA format, however, the ideal input is the assembly accession number of the annotated GenBank file since that, in turn, will result in the automatic download of all annotation files from the NCBI FTP server. For efficient housekeeping gene identification, the corresponding taxonomic clade of the organism (e.g. Actinobacteria) should be selected through the 'Reference set' option. If the input genome is not represented by any available reference set, the 'Unknown' option offers HMM models acquired from the Database of Essential Genes (Supplementary Table S1) (29).

RNA-Seq data. For RNA-Seq based data options, allowed input types are run accession numbers from NCBI-SRA or EBI-ENA. Since it is imperative that the reads are downloaded in a fast and reliable fashion, SeMa-Trap utilizes multiple downloading options. IBM Aspera (https://www.ibm.com/products/aspera), a high-speed file transfer system, is the preferred and recommended way of data transfer (https://www.ncbi.nlm.nih.gov/books/NBK242621/). In case of any complications, SeMa-Trap will directly download from FTP servers or using fastq-dump (http://ncbi.github.io/sra-tools/). In case of pre-analyzed RNA-Seq data with other specific tools or parameters, the corresponding 'BAM' formatted files can also be uploaded. Limitations due to the current computational power and the implementation of the server are provided in the Supplementary Methods.

RNA-Seq analysis

Once data acquisition is complete, SeMa-Trap utilizes several tools for analyzing the RNA-Seq data. Firstly, the fastp algorithm (30) is used to filter reads with low quality and for adapter trimming. Afterwards, filtered reads are mapped to

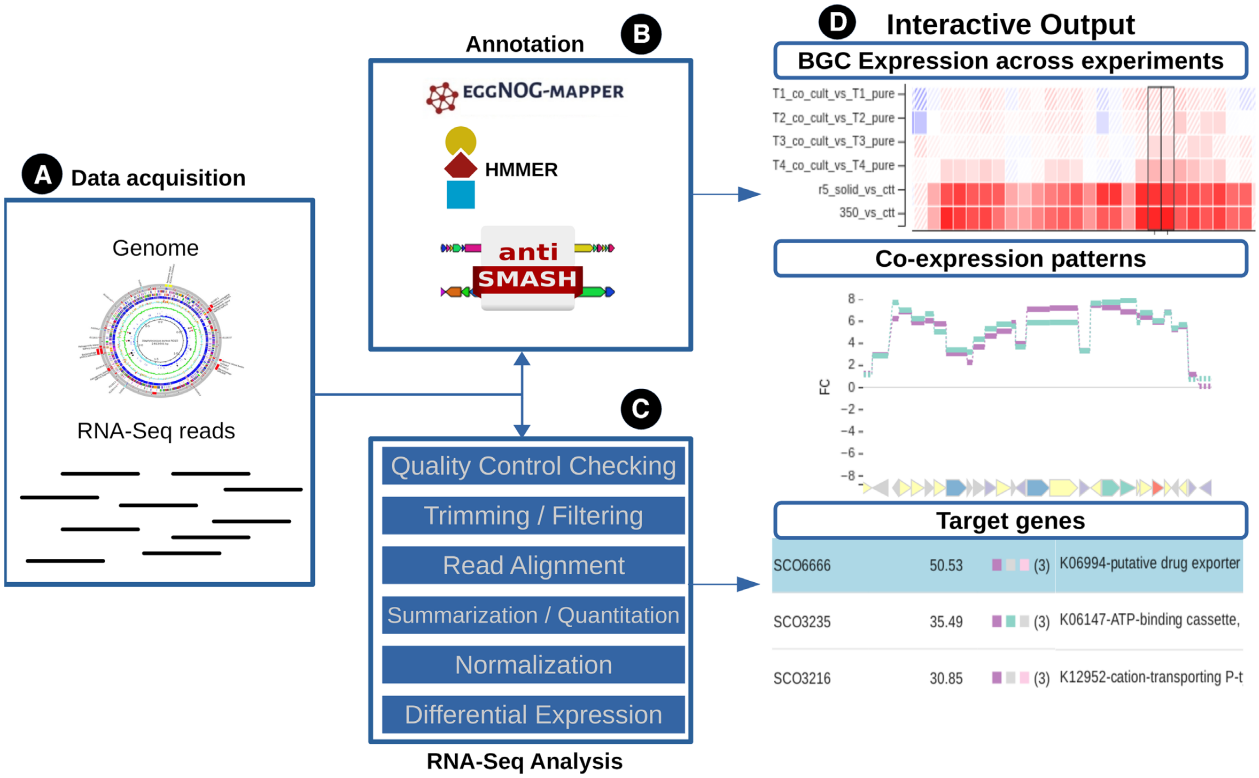

Figure 1. Overall workflow of the SeMa-Trap pipeline. First, the genomic and transcriptomic data provided by the user are acquired from relevant databases (**A**). Next step is the genome-wide annotation of the BGCs, essential housekeeping genes, secondary metabolite specific pathways and genes shown to have an impact on SM production (**B**). Final steps include a complete RNA-Seq analysis (**C**) and the generation of the interactive results (**D**).

the reference genome by Hisat2 (31) and sorted to generate corresponding BAM formatted files via samtools (32). Read count per gene is summarized by featureCounts (33). Finally, gene expression normalization takes place for each gene using the transcript per million (TPM) method described by Wagner et al. (34), and differential expression analysis is performed using DESeq2 (35), as detailed in Supplementary Methods. For the calculation of expression level or fold change of a BGC of interest, average expression of the 'core biosynthetic genes' (annotated by antiSMASH) is taken into account.

Scoring. In order to prioritize target genes, SeMa-Trap uses a scoring function dependent on the gene expression levels throughout the comparative transcriptomic experiments. To calculate such scores, fold changes of the selected BGC and the gene of interest are multiplied and then the calculated numbers from each selected experiment are added together (exemplified in Supplementary Table S2). However, it must be noted that a high score does not necessarily prove an association between a BGC and a gene. It rather points to high expression changes in the different conditions relative to a BGC of interest. Only when using large amounts of expression data, credible associations can be effectively detected (36).

Reference expression level. In order to set meaningful thresholds to label a BGC as 'expressed', SeMa-Trap uses three different average expression levels of specific genes. One of them is the mean expression of housekeeping genes throughout the genome. These genes are annotated by hmmsearch (37) with specific TIGRFAM models (38) unique for each reference set (39,40). The idea here is that on average, a gene defined as 'essential housekeeping gene' should be expressed significantly to be used as a reference for expression (41). However, BGCs can be expressed at lower levels and still produce compounds (42). Since no exact threshold exists to define BGC expression, SeMa-Trap offers separate reference levels such as the mean of non-housekeeping genes or all of the existing genes.

Annotation

Apart from antiSMASH's BGC prediction, the KnownClusterBlast algorithm is also applied to identify the compounds potentially produced by the BGC. If the provided genome is in FASTA format, an initial gene prediction step will take place using Prodigal (43). Since it is shown that certain types of genes actively control BGC expression, an extensive annotation of the genome is essential for prioritizing target genes to manipulate for BGC overexpression. For this purpose, the eggNOG-mapper (44) is used, particularly for the annotation of genes encoding transporters and genes residing in secondary metabolite specific KEGG pathways termed as 'biosynthesis of secondary metabolites' and 'biosynthesis of antibiotics'. Using hmmsearch, genes conferring antibiotic resistance or genes with regulatory functions are further defined via specific HMM models

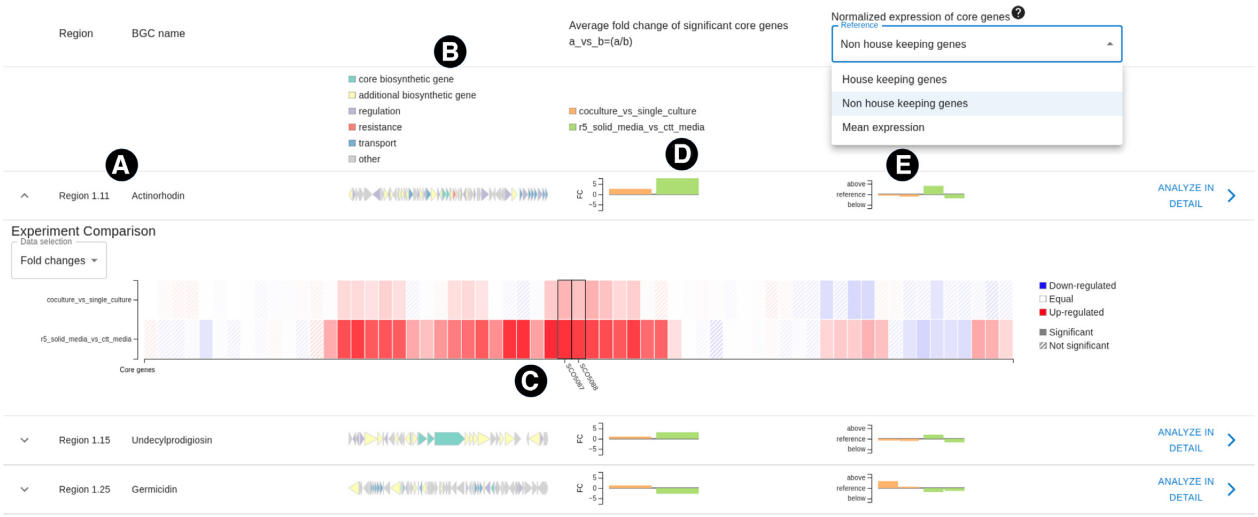

Figure 2. Overview result page of SeMa-Trap run for two comparative transcriptomic experiment designs. (**A**, **B**) The potential compound of the BGC and functional annotations of the genes within, respectively. (**C**) Heatmap of the BGC of interest, displaying each genes fold changes in different experiments. (**D**) Average fold change of the entire BGC, per experiment. (**E**) Expression (TPM) of a BGC relative to the selected, normalized reference expression level.

procured from PFAM (45), Resfams (46) and CARD (47) databases.

RESULTS

Overview

Once the analysis is complete, SeMa-Trap presents the overview of the overall fold changes of predicted BGCs and their expression levels relative to either of the mentioned reference expression levels (Figure 2). Various useful annotations of the genes in the BGCs are presented as well as the corresponding compound of the BGC if it is defined by KnownClusterBlast. Furthermore, a heatmap of the BGC content can be viewed in order to inspect fold changes of genes per experiment. BGCs can be further explored by clicking on the 'Analyze in detail' button.

Case study

A recent study by Lee *et al.* demonstrated the various effects of microbial co-culturing on natural products biosynthesis at the transcriptome level (48). Using six different comparative experimental designs, the authors revealed that competition for iron increases the expression of specific genes leading to actinorhodin overproduction in *Streptomyces coelicolor* A3(2) when co-cultured with *Myxococcus xanthus*. In the following, by analyzing their publicly available RNA-Seq data, we illustrate how SeMa-Trap simplifies the entire analysis.

Visualization options and pathway analysis. The first part of the result page (Figure 3A) offers a range of options such as various displaying options for the presented genes, the selection of specific experiments, and visualization of RNA-Seq results by fold change or TPM based expression level. Furthermore, it is possible to analyze specific pathways more in detail and explore the amount of differentially expressed genes within. In the presented case study, genes involved in the leucine and isoleucine degradation pathways were shown to be overexpressed, which potentially provide precursors for the actinorhodin biosynthesis. Using SeMa-Trap this can easily be highlighted (Figure 3B).

Genome browser. For the investigation of specific genes within the BGC or throughout the rest of the genome, a dynamic genome browser is available. Apart from efficient exploration of gene expression and annotation, the genome browser offers multiple options. Provided that the BGC of interest is significantly expressed, it is possible to set more accurate boundaries for the predicted BGC. Within the antiSMASH defined boundaries of a BGC (Figure 3C), a smaller, continuous succession of genes appears to be co-expressed, suggesting that those are regulated in an operon and represent the actual BGC boundaries.

Target gene prioritization. After thorough investigation, Lee and colleagues identified the SCO6666 gene encoding a transport system alternative to the one in the actinorhodin BGC, which is encoded by the genes SCO5083–5084. Furthermore, they found that the SCO6666 gene highly affected the production of actinorhodin in iron restricted conditions. Such prioritization can be easily made using the SeMa-Trap tables sorted by concordantly and discordantly co-regulated genes including scores (Figure 3D). Selection of the functional category 'Same KEGG annotations as BGC' further simplifies the investigation of the systems alternative to those encoded within the BGC of interest. The 'Combination' column denotes the selected experiments, thus providing information on which genes are co-regulated with the BGC of interest under which conditions.

Proof of principle

As a proof of concept, we used SeMa-Trap to examine the transcriptome data of the actinomycete *Amycolatopsis*

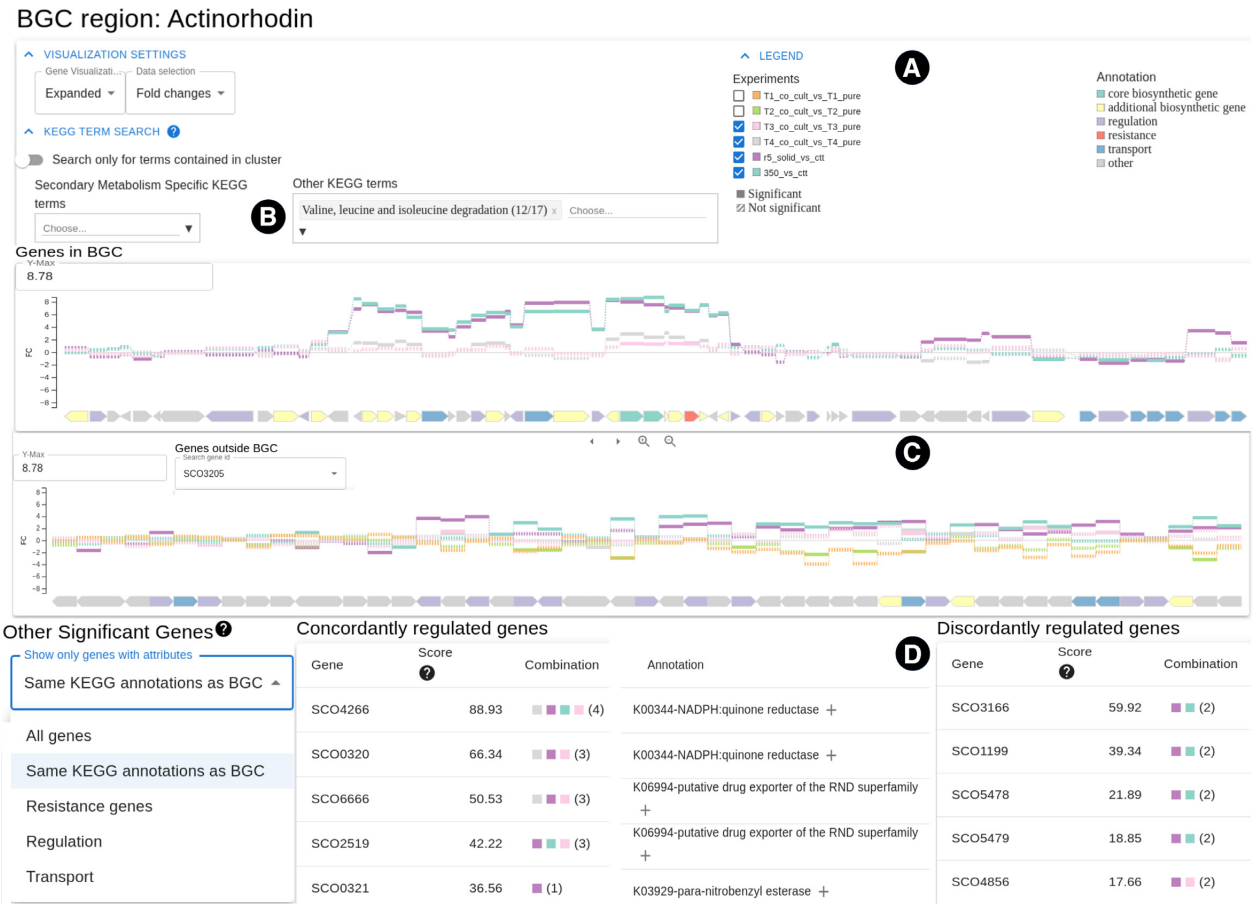

Figure 3. BGC centered results of SeMa-Trap. Initially, color codes for different annotations and multiple visualization settings are presented (**A**). Users can also highlight genes in specific pathways and choose to visualize the results based on the selected experiments (**B**). In section (**C**), two genome browsers are available in order to explore gene expressions from the selected experiments in the predicted cluster and throughout the genome. Finally, genes which are likely impacting the BGC expression based on transcriptomic data can be viewed through an interactive table **(D)**.

japonicum. *A. japonicum* is the producer of the complexing agent [*S,S*]-EDDS (49), a structural isomer of EDTA, which in contrast to EDTA is biodegradable and can replace EDTA in many industrial applications. However, [*S,S*]-EDDS production is inhibited by zinc at concentrations of 2 μM (50). Responsible for this regulation is the zinc uptake regulator *Zur*. To produce [*S,S*]-EDDS even in the presence of zinc the mutant *A. japonicum* Δ*zur* (referred to as zurko) was generated (51). To determine which genes to overexpress to increase [*S,S*]-EDDS production in *A. japonicum*, we performed transcriptomic analysis. For this purpose, RNA-Seq analyses of *A. japonicum* wild type (WT) and *A. japonicum* Δ*zur* cultured in the presence and absence of zinc for 24 h were performed. Thereby, a direct correlation between *zur* gene expression and the [*S,S*]-EDDS biosynthetic genes (BGs) could be observed. In particular, using SeMa-Trap we identified genes that exhibited high co-expression with the [*S,S*]-EDDS BG (concordantly regulated genes) and genes regulated in opposite manner (discordantly regulated genes). Since gene deletion is a multi-step, time-consuming process, we opted for a straightforward approach and overexpressed the targeted genes as a proof of concept. Thereby, we focused on genes with a regulatory function and those connected to secondary metabolism pathways. The target gene *bldC* ('AJAP_RS36645'), with the second highest score in the category 'regulation', encodes a transcriptional regulator of differentiation which controls entry into development and the onset of antibiotic production in *Streptomyces* (52). The *lacI* gene, ('AJAP_RS11995'), encodes a pleiotropic regulator (fifth highest score in the category 'regulation') which enhanced the production of antibiotics in *S. coelicolor* (53). From the pathways connected to secondary metabolism, we selected the glutamate synthase-encoding *glts* ('AJAP_RS11230') gene (with second best score) involved in glutamate biosynthesis. Since glutamate can be converted into L-aspartic acid, one of the precursors for EDDS biosynthesis, this gene was also taken into consideration. None of the selected genes have been experimentally shown to be linked to the [*S,S*]-EDDS production. Simultaneous overexpression of these genes resulted in an increased EDDS production by 3-fold compared to *A. japonicum* WT (Figure 4). Along with the experimental design, detailed methods (Supplementary Tables S3 and S4) and analysis (Supplementary Figures S1 and S2) can be further seen in the Supplementary Data.

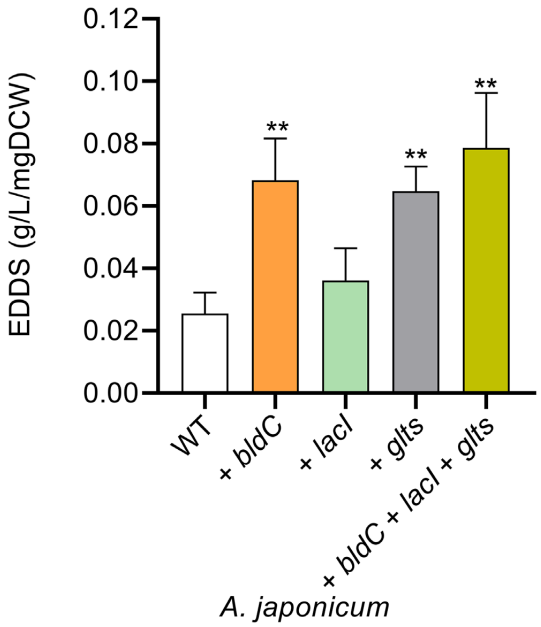

Figure 4. [*S,S*]-EDDS production in *A. japonicum* WT and recombinant strains. Strains were grown for 96 h in zinc depleted synthetic medium (SM). *A. japonicum* wild-type (WT); *A. japonicum* containing an additional copy of the genes *bldC*, *lacI* or glutamate synthase (*glts*), respectively and *A. japonicum* containing an additional copy of the three genes (*bldC* + *lacI* + *glts*).

CONCLUSIONS AND FUTURE PERSPECTIVES

Leveraging on state-of-the-art sequencing techniques, comparative transcriptomic analyses have been continuously used to identify genes that are co-regulated with BGCs of interest and can be manipulated to activate silent BGCs. A variety of tools exists in order to annotate and effectively visualize biological functions of co-regulated genes such as KOBAS (54), conduct RNA-Seq analysis such as ProkSeq (55) or identify BGCs with co-expression data such as CASSIS (56). However, to the best of our knowledge, SeMa-Trap is the only public web server that combines genome mining and transcriptomic approaches for the identification of potential target genes for SM overproduction. The user-friendly graphical interface of the web server allows efficient and easy mining of RNA-Seq data, and was conceived for natural product researchers who are not acquainted with command line tools. Notably, SeMa-Trap also visualizes essential information about the cell response to the production of SMs on a transcriptomic level.

We showed herein that SeMa-Trap greatly facilitates the identification of co-regulated genes as illustrated on the actinorhodin-encoding BGC. However the limitations of the pipeline must be noted. The current scoring system is only designed to sort genes based on their similarity in transcription levels to a BGC of interest. It can not be used as an exclusive method for the selection of target genes. Thus, it is incumbent upon the users to further evaluate the hits returned by SeMa-Trap. For example, in the presented [*S,S*]-EDDS overproduction experiment, our literature search showed that the genes having the best co-expression score were unlikely to play a role in [*S,S*]-EDDS production. Consequently, three of the promising target genes were successfully overexpressed, leading to increased [*S,S*]-EDDS production. Especially when based on a few number of transcriptomic experiments, it becomes more likely that the SeMa-Trap analysis will include false positive target genes in the resulting tables. For future applications, by analyzing large amounts of publicly available RNA-Seq data, we are working on generating associations with certain gene types and classes of BGCs. Through co-expression networks, using statistical methods such as Pearson correlation coefficient, our aim is to reduce the number of false positives (57,58).

In summary, considering the ever-growing need for novel bioactive compounds, we believe that SeMa-Trap will serve as a helpful tool for the natural product community by facilitating the identification of specific co-expression patterns between different types of BGCs and genes with potential regulatory functions. Additionally, such analysis will also improve our ability to define expression thresholds above which the actual production of the encoded compound is observed. Last but not least, knowledge about the global cellular response to SM production may be the starting point to devise alternative strategies to optimize compound production and identify potential resistance mechanisms.

DATA AVAILABILITY

SeMa-Trap is publicly available online at https://sema-trap.ziemertlab.com/ with no access restrictions. All of the source code is available on Bitbucket at https://bitbucket.org/mehmetdirenc/sematrap/. Source code for generating only the interactive HTML output is also available at https://github.com/Integrative-Transcriptomics/bgc-expression-viewer. Transcriptomic data files for EDDS overproduction and presented case study are available in the NCBI Bioproject database under the accession IDs PRJNA809550 and PRJEB25075, respectively.

SUPPLEMENTARY DATA

Supplementary Data are available at NAR Online.

ACKNOWLEDGEMENTS

We thank Dr Libera do Presti for invaluable comments on the manuscript. We also acknowledge Quantitative Biology Center (QBiC) and all SeMa-Trap users for helpful comments and feedback.

FUNDING

N.Z. and M.D.M. acknowledge the German Center for Infection Research [DZIF TTU09.716]; Germany's Excellence Strategy – EXC 2124 [390838134]; N.Z., T.H. and E.S. gratefully acknowledge financial support from the German Research Foundation (DFG) [TRR261, project ID 398967434]; The authors acknowledge the use of de.NBI cloud and the support by the High Performance and Cloud Computing Group at the Zentrum für Datenverarbeitung

of the University of Tübingen through bwHPC and the German Research Foundation (DFG) [INST 37/935-1 FUGG] and the Federal Ministry of Education and Research (BMBF) [031 A535A]. Funding for open access charge: BMBF [DZIF TTU09.716].

Conflict of interest statement. None declared.

REFERENCES

1. Newman,D.J. and Cragg,G.M. (2020) Natural products as sources of new drugs over the nearly four decades from 01/1981 to 09/2019. *J. Nat. Prod.*, **83**, 770–803.
2. Scherlach,K. and Hertweck,C. (2020) Chemical mediators at the bacterial-fungal interface. *Ann. Rev. Microbiol.*, **74**, 267–290.
3. Yan,Y., Liu,Q., Jacobsen,S.E. and Tang,Y. (2018) The impact and prospect of natural product discovery in agriculture: New technologies to explore the diversity of secondary metabolites in plants and microorganisms for applications in agriculture. *EMBO Rep.*, **19**, e46824.
4. Atanasov,A.G., Zotchev,S.B., Dirsch,V.M. and Supuran,C.T. (2021) Natural products in drug discovery: Advances and opportunities. *Nat. Rev. Drug Discov.*, **20**, 200–216.
5. Iwu,C.D., Korsten,L. and Okoh,A.I. (2020) The incidence of antibiotic resistance within and beyond the agricultural ecosystem: a concern for public health. *Microbiologyopen*, **9**, e1035.
6. Ziemert,N., Alanjary,M. and Weber,T. (2016) The evolution of genome mining in microbes—a review. *Nat. Prod. Rep.*, **33**, 988–1005.
7. Medema,M.H., de Rond,T. and Moore,B.S. (2021) Mining genomes to illuminate the specialized chemistry of life. *Nat. Rev. Genet.*, **22**, 553–571.
8. Blin,K., Shaw,S., Kloosterman,A.M., Charlop-Powers,Z., van Wezel,G.P., Medema,M.H. and Weber,T. (2021) antiSMASH 6.0: improving cluster detection and comparison capabilities. *Nucleic Acids Res.*, **49**, W29-W35.
9. Kautsar,S.A., Blin,K., Shaw,S., Navarro-Muñoz,J.C., Terlouw,B.R., van der Hooft,J.J., Van Santen,J.A., Tracanna,V., Suarez Duran,H.G., Pascal Andreu,V. *et al.* (2020) MIBiG 2.0: a repository for biosynthetic gene clusters of known function. *Nucleic Acids Res.*, **48**, D454–D458.
10. Blin,K., Shaw,S., Kautsar,S.A., Medema,M.H. and Weber,T. (2021) The antiSMASH database version 3: increased taxonomic coverage and new query features for modular enzymes. *Nucleic Acids Res.*, **49**, D639–D643.
11. van Santen,J.A., Poynton,E.F., Iskakova,D., McMann,E., Alsup,T.A., Clark,T.N., Fergusson,C.H., Fewer,D.P., Hughes,A.H., McCadden,C.A. *et al.* (2022) The Natural Products Atlas 2.0: a database of microbially-derived natural products. *Nucleic Acids Res.*, **50**, D1317–D1323.
12. Gavriilidou,A., Kautsar,S.A., Zaburannyi,N., Krug,D., Müller,R., Medema,M.H. and Ziemert,N. (2022) Compendium of specialized metabolite biosynthetic diversity encoded in bacterial genomes. *Nature Microbiology*, **7**, 726–735.
13. Chevrette,M.G., Gutiérrez-García,K., Selem-Mojica,N., Aguilar-Martínez,C., Yañez-Olvera,A., Ramos-Aboites,H.E., Hoskisson,P.A. and Barona-Gómez,F. (2020) Evolutionary dynamics of natural product biosynthesis in bacteria. *Nat. Prod. Rep.*, **37**, 566–599.
14. Ambrosino,L., Tangherlini,M., Colantuono,C., Esposito,A., Sangiovanni,M., Miralto,M., Sansone,C. and Chiusano,M.L. (2019) Bioinformatics for marine products: an overview of resources, bottlenecks, and perspectives. *Mar. Drugs*, **17**, 576.
15. Zhang,J.J., Tang,X. and Moore,B.S. (2019) Genetic platforms for heterologous expression of microbial natural products. *Nat. Prod. Rep.*, **36**, 1313–1332.
16. Ochi,K. and Hosaka,T. (2013) New strategies for drug discovery: activation of silent or weakly expressed microbial gene clusters. *App. Microbiol. Biotechnol.*, **97**, 87–98.
17. Beck,C., Gren,T., Ortiz-López,F.J., Jørgensen,T.S., Carretero-Molina,D., Martín Serrano,J., Tormo,J.R., Oves-Costales,D., Kontou,E.E., Mohite,O.S. *et al.* (2021) Activation and identification of a griseusin cluster in *Streptomyces* sp. CA-256286 by employing transcriptional regulators and multi-omics methods. *Molecules*, **26**, 6580.
18. Mingyar,E., Mühling,L., Kulik,A., Winkler,A., Wibberg,D., Kalinowski,J., Blin,K., Weber,T., Wohlleben,W. and Stegmann,E. (2021) A regulator based 'semi-targeted' approach to activate silent biosynthetic gene clusters. *Int. J. Mol. Sci.*, **22**, 7567.
19. Severi,E. and Thomas,G.H. (2019) Antibiotic export: transporters involved in the final step of natural product production. *Microbiology*, **165**, 805–818.
20. Begani,J., Lakhani,J. and Harwani,D. (2018) Current strategies to induce secondary metabolites from microbial biosynthetic cryptic gene clusters. *Ann. Microbiol.*, **68**, 419–432.
21. Wang,W., Li,S., Li,Z., Zhang,J., Fan,K., Tan,G., Ai,G., Lam,S.M., Shui,G., Yang,Z. *et al.* (2020) Harnessing the intracellular triacylglycerols for titer improvement of polyketides in Streptomyces. *Nat. Biotechnol.*, **38**, 76–83.
22. Khadayat,K., Sherpa,D.D., Malla,K.P., Shrestha,S., Rana,N., Marasini,B.P., Khanal,S., Rayamajhee,B., Bhattarai,B.R. and Parajuli,N. (2020) Molecular identification and antimicrobial potential of *Streptomyces* species from Nepalese soil. *Int. J. Microbiol.*, **2020**, 8817467.
23. Lee,N., Kim,W., Hwang,S., Lee,Y., Cho,S., Palsson,B. and Cho,B.-K. (2020) Thirty complete *Streptomyces* genome sequences for mining novel secondary metabolite biosynthetic gene clusters. *Scientific Data*, **7**, 55.
24. Yi,J.S., Kim,M.W., Kim,M., Jeong,Y., Kim,E.-J., Cho,B.-K. and Kim,B.-G. (2017) A novel approach for gene expression optimization through native promoter and 5 UTR combinations based on RNA-seq, ribo-seq, and TSS-seq of *Streptomyces coelicolor*. *ACS Synt. Biol.*, **6**, 555–565.
25. Ferguson,N.L., Peña-Castillo,L., Moore,M.A., Bignell,D.R. and Tahlan,K. (2016) Proteomics analysis of global regulatory cascades involved in clavulanic acid production and morphological development in Streptomyces clavuligerus. *J. Ind. Microbiol. Biotechnol.*, **43**, 537–555.
26. Li,X., Wang,J., Li,S., Ji,J., Wang,W. and Yang,K. (2015) ScbR-and ScbR2-mediated signal transduction networks coordinate complex physiological responses in *Streptomyces coelicolor*. *Sci. Rep.*, **5**, 14831.
27. Ahmed,Y., Rebets,Y., Estévez,M.R., Zapp,J., Myronovskyi,M. and Luzhetskyy,A. (2020) Engineering of *Streptomyces lividans* for heterologous expression of secondary metabolite gene clusters. *Microb. Cell Fact.*, **19**, 5.
28. Kanehisa,M., Furumichi,M., Sato,Y., Ishiguro-Watanabe,M. and Tanabe,M. (2021) KEGG: integrating viruses and cellular organisms. *Nucleic Acids Res.*, **49**, D545–D551.
29. Luo,H., Lin,Y., Gao,F., Zhang,C.-T. and Zhang,R. (2014) DEG 10, an update of the database of essential genes that includes both protein-coding genes and noncoding genomic elements. *Nucleic Acids Res.*, **42**, D574–D580.
30. Chen,S., Zhou,Y., Chen,Y. and Gu,J. (2018) fastp: an ultra-fast all-in-one FASTQ preprocessor. *Bioinformatics*, **34**, i884–i890.
31. Kim,D., Paggi,J.M., Park,C., Bennett,C. and Salzberg,S.L. (2019) Graph-based genome alignment and genotyping with HISAT2 and HISAT-genotype. *Nat. Biotechnol.*, **37**, 907–915.
32. Danecek,P., Bonfield,J.K., Liddle,J., Marshall,J., Ohan,V., Pollard,M.O., Whitwham,A., Keane,T., McCarthy,S.A., Davies,R.M. *et al.* (2021) Twelve years of SAMtools and BCFtools. *Gigascience*, **10**, giab008.
33. Liao,Y., Smyth,G.K. and Shi,W. (2014) featureCounts: an efficient general purpose program for assigning sequence reads to genomic features. *Bioinformatics*, **30**, 923–930.
34. Wagner,G.P., Kin,K. and Lynch,V.J. (2012) Measurement of mRNA abundance using RNA-seq data: RPKM measure is inconsistent among samples. *Theor. Biosci.*, **131**, 281–285.
35. Love,M.I., Huber,W. and Anders,S. (2014) Moderated estimation of fold change and dispersion for RNA-seq data with DESeq2. *Genome Biol.*, **15**, 550.
36. Kwon,M.J., Steiniger,C., Cairns,T.C., Wisecaver,J.H., Lind,A.L., Pohl,C., Regner,C., Rokas,A. and Meyer,V. (2021) Beyond the biosynthetic gene cluster paradigm: genome-wide coexpression networks connect clustered and unclustered transcription factors to secondary metabolic pathways. *Microbiol. Spect.*, **9**, e00898-21.
37. Eddy,S.R. (2011) Accelerated profile HMM searches. *PLoS Comput. Biol.*, **7**, e1002195.

38. Haft,D.H., Selengut,J.D., Richter,R.A., Harkins,D., Basu,M.K. and Beck,E. (2012) TIGRFAMs and genome properties in 2013. *Nucleic Acids Res.*, **41**, D387–D395.
39. Alanjary,M., Kronmiller,B., Adamek,M., Blin,K., Weber,T., Huson,D., Philmus,B. and Ziemert,N. (2017) The Antibiotic Resistant Target Seeker (ARTS), an exploration engine for antibiotic cluster prioritization and novel drug target discovery. *Nucleic Acids Res.*, **45**, W42–W48.
40. Mungan,M.D., Alanjary,M., Blin,K., Weber,T., Medema,M.H. and Ziemert,N. (2020) ARTS 2.0: feature updates and expansion of the Antibiotic Resistant Target Seeker for comparative genome mining. *Nucleic Acids Res.*, **48**, W546–W552.
41. Moureu,S., Caradec,T., Trivelli,X., Drobecq,H., Beury,D., Bouquet,P., Caboche,S., Desmecht,E., Maurier,F., Muharram,G. *et al.* (2021) Rubrolone production by *Dactylosporangium vinaceum*: biosynthesis, modulation and possible biological function. *Appl. Microbiol. Biotechnol.*, **105**, 5541–5551.
42. Amos,G.C., Awakawa,T., Tuttle,R.N., Letzel,A.-C., Kim,M.C., Kudo,Y., Fenical,W., Moore,B.S. and Jensen,P.R. (2017) Comparative transcriptomics as a guide to natural product discovery and biosynthetic gene cluster functionality. *Proc. Natl. Acad. Sci. U.S.A.*, **114**, E11121–E11130.
43. Hyatt,D., Chen,G.-L., LoCascio,P.F., Land,M.L., Larimer,F.W. and Hauser,L.J. (2010) Prodigal: prokaryotic gene recognition and translation initiation site identification. *BMC Bioinformatics*, **11**, 119.
44. Cantalapiedra,C.P., Hernández-Plaza,A., Letunic,I., Bork,P. and Huerta-Cepas,J. (2021) eggNOG-mapper v2: functional annotation, orthology assignments, and domain prediction at the metagenomic scale. *Mol. Biol. Evol.*, **38**, 5825–5829.
45. Mistry,J., Chuguransky,S., Williams,L., Qureshi,M., Salazar,G.A., Sonnhammer,E.L., Tosatto,S.C., Paladin,L., Raj,S., Richardson,L.J. *et al.* (2021) Pfam: the protein families database in 2021. *Nucleic Acids Res.*, **49**, D412–D419.
46. Gibson,M.K., Forsberg,K.J. and Dantas,G. (2015) Improved annotation of antibiotic resistance determinants reveals microbial resistomes cluster by ecology. *ISME J.*, **9**, 207–216.
47. Alcock,B.P., Raphenya,A.R., Lau,T.T., Tsang,K.K., Bouchard,M., Edalatmand,A., Huynh,W., Nguyen,A.-L.V., Cheng,A.A., Liu,S. *et al.* (2020) CARD 2020: antibiotic resistome surveillance with the comprehensive antibiotic resistance database. *Nucleic Acids Res.*, **48**, D517–D525.
48. Lee,N., Kim,W., Chung,J., Lee,Y., Cho,S., Jang,K.-S., Kim,S.C., Palsson,B. and Cho,B.-K. (2020) Iron competition triggers antibiotic biosynthesis in *Streptomyces coelicolor* during coculture with *Myxococcus xanthus*. *ISME J.*, **14**, 1111–1124.
49. Nishikiori,T., Okuyama,A., Naganawa,H., Takita,T., Hamada,M., Takeuchi,T., Aoyagi,T. and and Umezawa,H. (1984) Production by actinomycetes of (*S,S*)-N,N'-ethylenediamine-disuccinic acid, an inhibitor of phospholipase C.. *J. Antibiot. (Tokyo)*, **37**, 426–427.
50. Zwicker,N., Theobald,U., Zähner,H. and Fiedler,H. (1997) Optimization of fermentation conditions for the production of ethylene-diamine-disuccinic acid by *Amycolatopsis orientalis*. *J. Ind. Microbiol. Biotechnol.*, **19**, 280–285.
51. Spohn,M., Wohlleben,W. and Stegmann,E. (2016) Elucidation of the zinc-dependent regulation in *Amycolatopsisjaponicum* enabled the identification of the ethylenediamine-disuccinate (*S,S*-EDDS) genes. *Environ. Microbiol.*, **18**, 1249–1263.
52. Schumacher,M.A., den Hengst,C.D., Bush,M.J., Le,T., Tran,N.T., Chandra,G., Zeng,W., Travis,B., Brennan,R.G. and Buttner,M.J. (2018) The MerR-like protein BldC binds DNA direct repeats as cooperative multimers to regulate *Streptomyces* development. *Nat. Commun.*, **9**, 1139.
53. Meng,L., Yang,S.H., Kim,T.-J. and Suh,J.-W. (2012) Effects of two putative LacI-family transcriptional regulators, SCO4158 and SCO7554, on antibiotic pigment production of *Streptomyces coelicolor* and *Streptomyces lividans*. *J. Kor. Soc. Appl. Biol. Chem.*, **55**, 737–741.
54. Bu,D., Luo,H., Huo,P., Wang,Z., Zhang,S., He,Z., Wu,Y., Zhao,L., Liu,J., Guo,J. *et al.* (2021) KOBAS-i: intelligent prioritization and exploratory visualization of biological functions for gene enrichment analysis. *Nucleic Acids Res.*, **49**, W317–W325.
55. Mahmud,A.F., Delhomme,N., Nandi,S. and Fällman,M. (2021) ProkSeq for complete analysis of RNA-seq data from prokaryotes. *Bioinformatics*, **37**, 126–128.
56. Wolf,T., Shelest,V., Nath,N. and Shelest,E. (2016) CASSIS and SMIPS: promoter-based prediction of secondary metabolite gene clusters in eukaryotic genomes. *Bioinformatics*, **32**, 1138–1143.
57. Andersen,M.R., Nielsen,J.B., Klitgaard,A., Petersen,L.M., Zachariasen,M., Hansen,T.J., Blicher,L.H., Gotfredsen,C.H., Larsen,T.O., Nielsen,K.F. *et al.* (2013) Accurate prediction of secondary metabolite gene clusters in filamentous fungi. *Proc. Nat. Acad. Sci. U.S.A.*, **110**, E99–E107.
58. Liesecke,F., Daudu,D., Dugé de Bernonville,R., Besseau,S., Clastre,M., Courdavault,V., De Craene,J.-O., Crèche,J., Giglioli-Guivarc'h,N., Glévarec,G. *et al.* (2018) Ranking genome-wide correlation measurements improves microarray and RNA-seq based global and targeted co-expression networks. *Sci. Rep.*, **8**, 10885.

Chapter 5

Supplementary Information

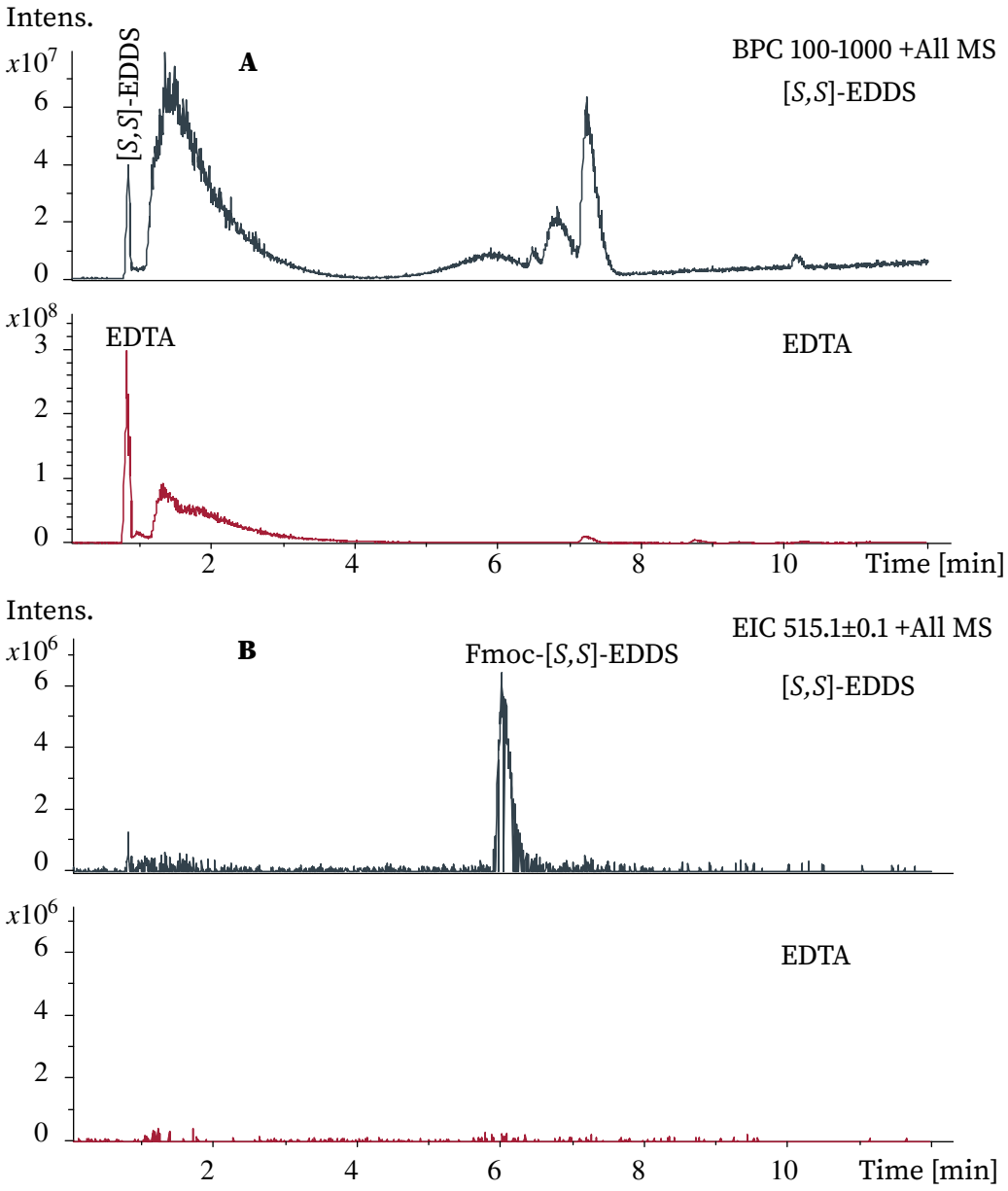

Figure S1. **HPLC-MS chromatograms of [*S,S*]-EDDS and EDTA treated with Fmoc-Cl**. (A) Based peak chromatogram (BPC) of [S,S]-EDDS (in black) and EDTA (in red). (B) Extracted ion chromatogram (EIC) for Fmoc-[*S,S*]-EDDS (in black), showing a peak with *m/z* of 515.1 $[M+H]^+$ and EDTA buffer mixed with Fmoc-Cl (control) (in red)

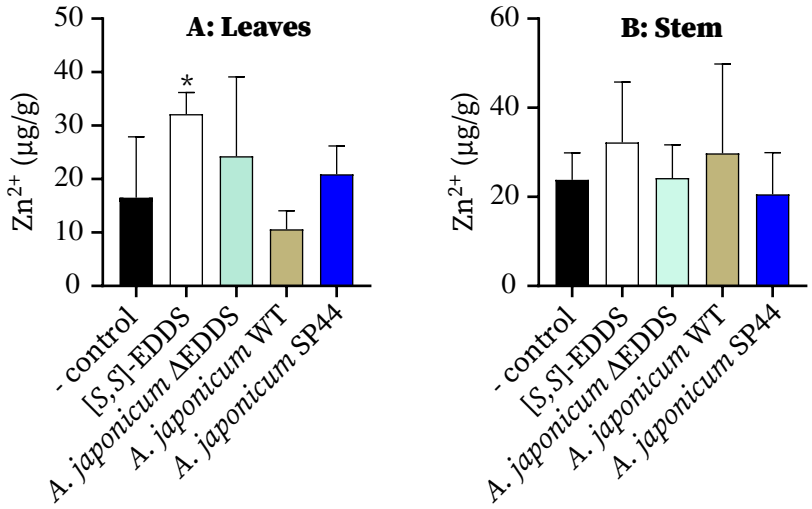

Figure S2. **Zn^{2+} content in *Phaseolus vulgaris* cv. Black pole 21 days post treatments.**. Measurements were performed with samples obtained from the leaves, stem, and roots 21 days post treatments (DPT). Error bars indicate the mean and SD of 5 replicates. Statistical significance (*p<0.05,) was determined by unpaired Student´s test.

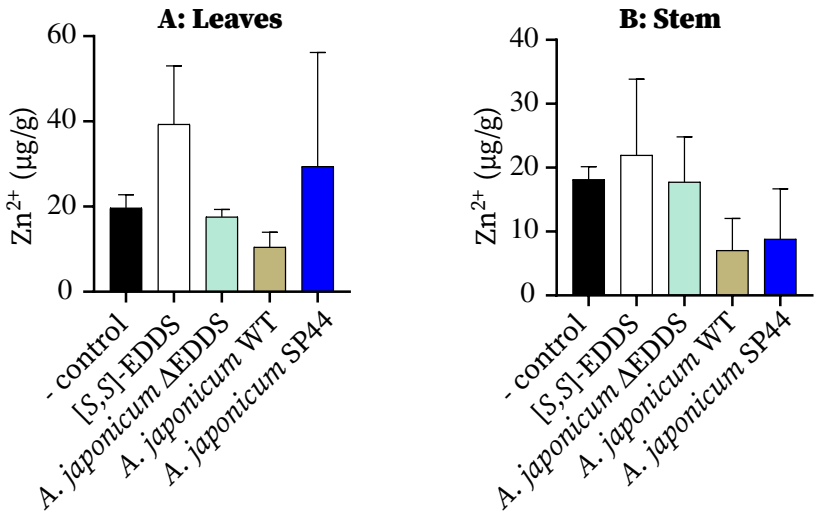

Figure S3. **Zn^{2+} content in *Phaseolus vulgaris* cv. Black pole 24 days post treatments**. Measurements were performed with samples obtained from the leaves, stem, and roots 24 days post treatments (DPT). Error bars indicate the mean and SD of 5 replicates. Statistical significance was determined by unpaired Student´s test.

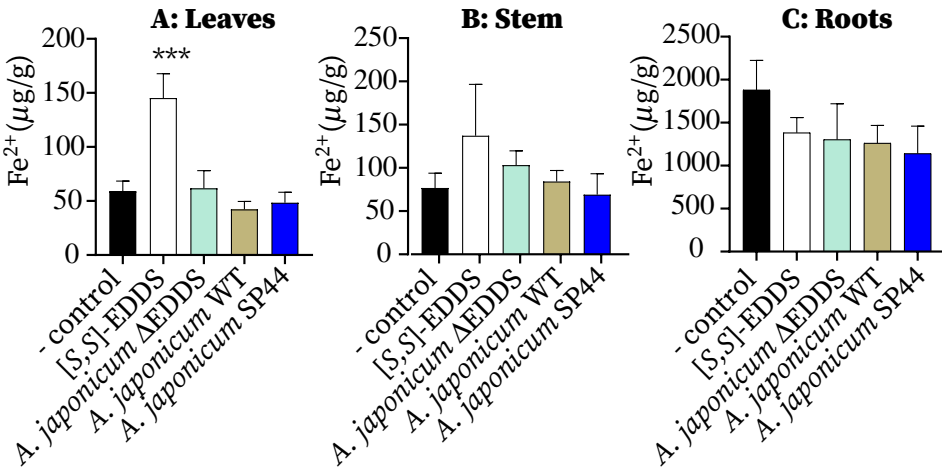

Figure S4. **Fe^{2+} content in *Phaseolus vulgaris* cv. Black pole 7 days post treatments.** Measurements were performed with samples obtained from the leaves, stem, and roots 7 days post treatments (DPT). Error bars indicate the mean and SD of 5 replicates. Statistical significance (***p<0.001,) was determined by unpaired Student´s test.

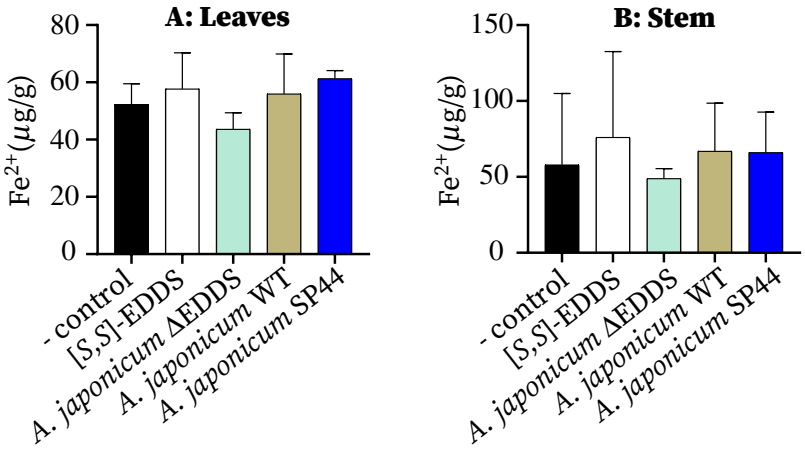

Figure S5. **Fe^{2+} content in *Phaseolus vulgaris* cv. Black pole 21 days post treatments** . Measurements were performed with samples obtained from the leaves, stem, and roots 21 days post treatments (DPT). Error bars indicate the mean and SD of 5 replicates. Statistical significance was determined by unpaired Student´s test.

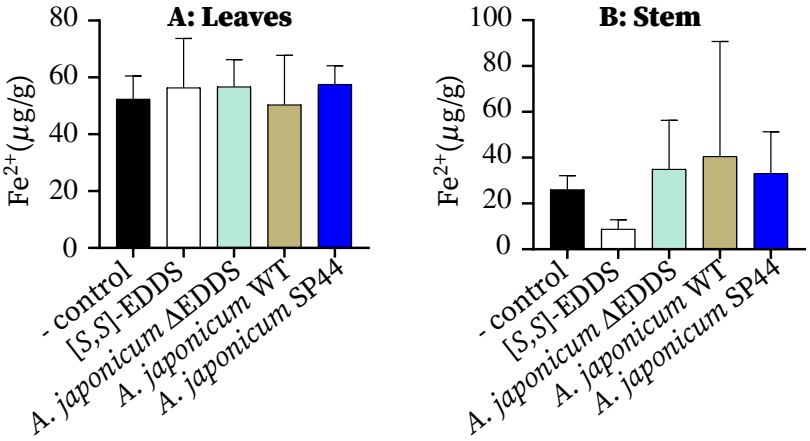

Figure S6. **Fe^{2+} content in *Phaseolus vulgaris* cv. Black pole 24 days post treatments**. Measurements were performed with samples obtained from the leaves, stem, and roots 24 days after the treatments. Error bars indicate the mean and SD of 5 replicates. Statistical significance was determined by unpaired Student´s test

.

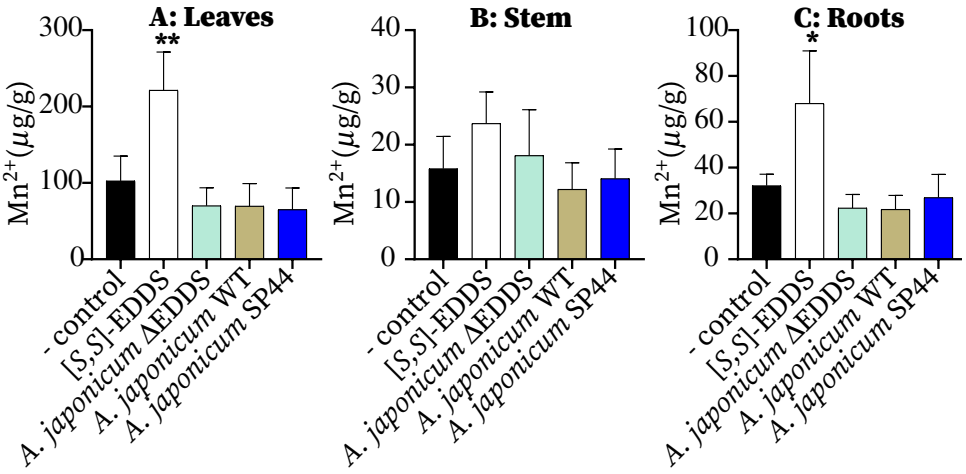

Figure S7. **Mn^{2+} content in *Phaseolus vulgaris* cv. Black pole 7 days post treatments**. Measurements were performed with samples obtained from the leaves, stem, and roots 7 days after the treatments. Error bars indicate the mean and SD of 5 replicates. Statistical significance (*p<0.05, **p<0.01) was determined by unpaired Student´s test.

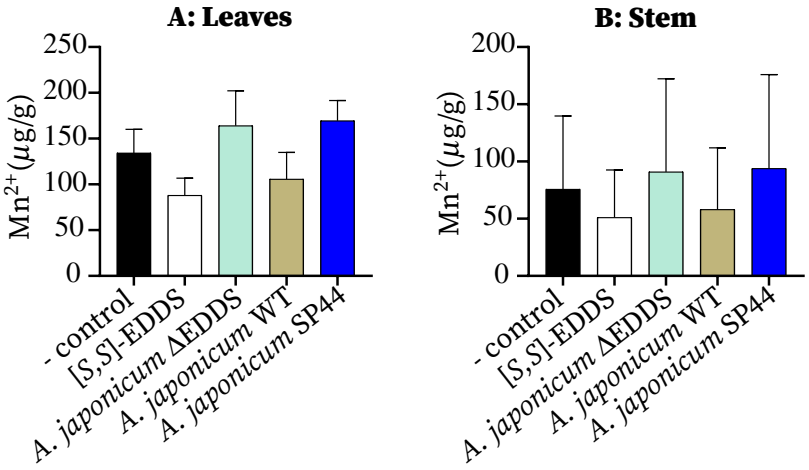

Figure S8. **Mn^{2+} content in *Phaseolus vulgaris* cv. Black pole 21v days post treatments**. Measurements were performed with samples obtained from the leaves, stem, and roots 21 days after the treatments. Error bars indicate the mean and SD of 5 replicates. Statistical significance was determined by unpaired Student´s test.

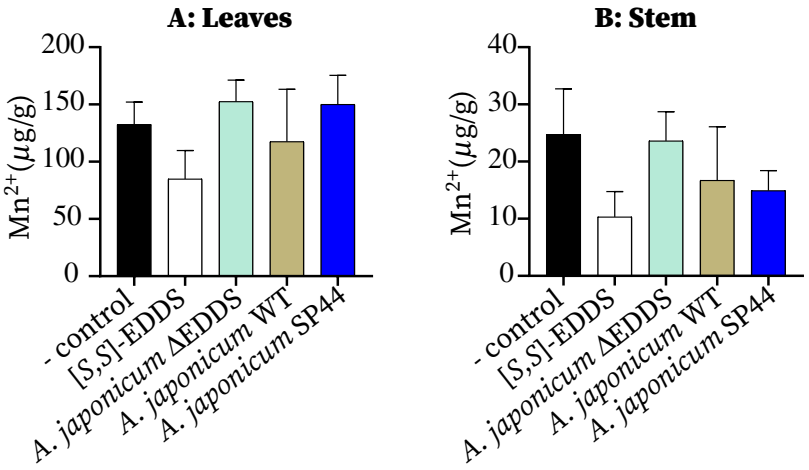

Figure S9. **Mn^{2+} content in *Phaseolus vulgaris* cv. Black pole 24 days post treatments**. Measurements were performed with samples obtained from the leaves, stem, and roots 24 days after the treatments. Error bars indicate the mean and SD of 5 replicates. Statistical significance was determined by unpaired Student´s test.

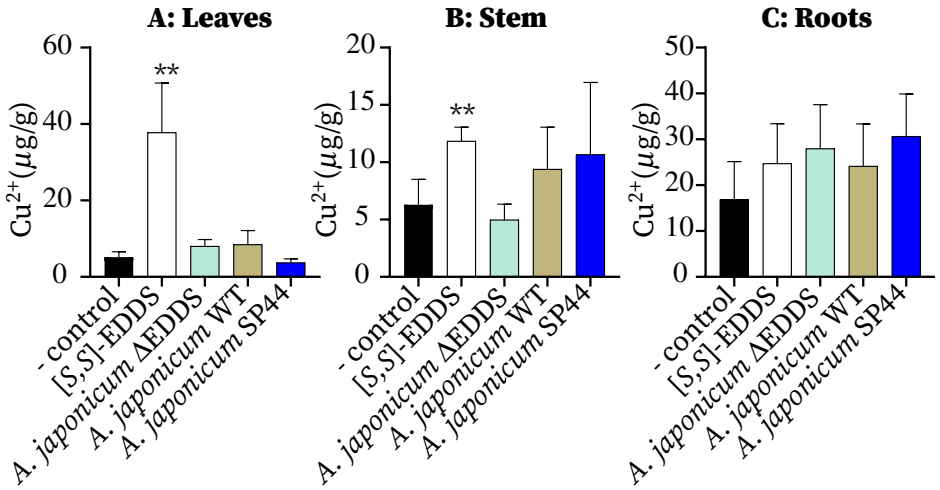

Figure S10. **Cu^{2+} content in *Phaseolus vulgaris* cv. Black pole 7 days post treatments**. Measurements were performed with samples obtained from the leaves, stem, and roots 7 days after the treatments. Error bars indicate the mean and SD of 5 replicates. Statistical significance(**p<0.01) was determined by unpaired Student´s test.

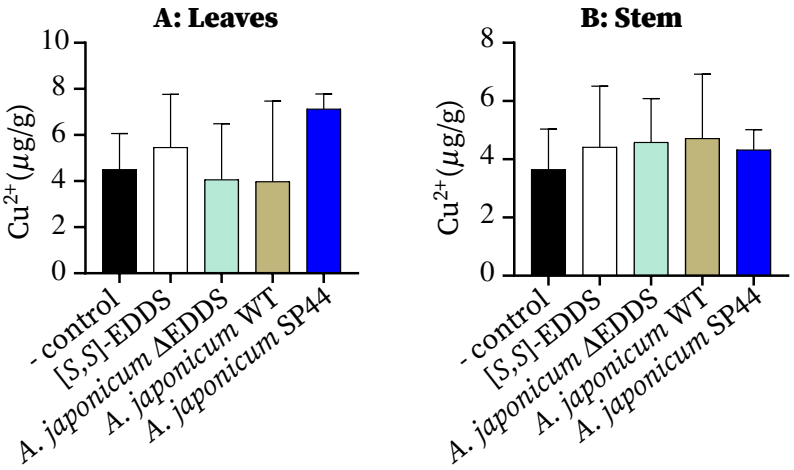

Figure S11. **Cu^{2+} content in *Phaseolus vulgaris* cv. Black pole 21 days post treatments**. Measurements were performed with samples obtained from the leaves, stem, and roots 21 days after the treatments. Error bars indicate the mean and SD of 5 replicates. Statistical significance was determined by unpaired Student´s test.

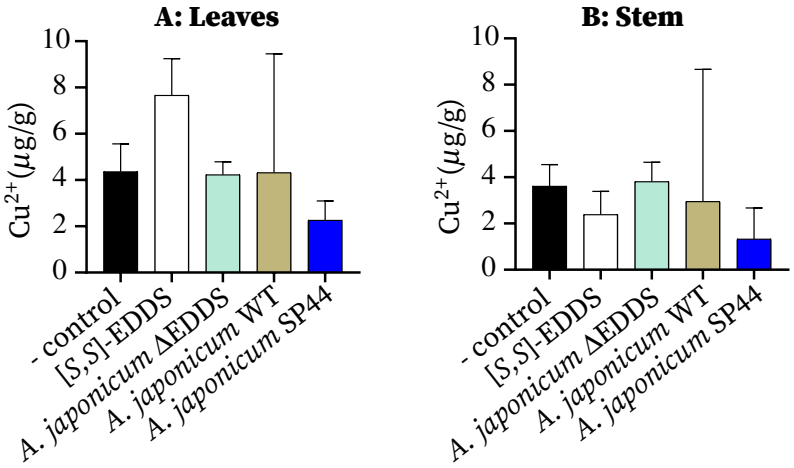

Figure S12. **Cu^{2+} content in *Phaseolus vulgaris* cv. Black pole 24 days post treatments**. Measurements were performed with samples obtained from the leaves, stem, and roots 24 days after the treatments. Error bars indicate the mean and SD of 5 replicates. Statistical significance was determined by unpaired Student´s test.

```
Chelativorans   41   PYDSQIHRAHVVMLTEQGILTVEESATILSGLAQVDELAAT--------DGSLRTYLPYE   92
A. japonicum    38   PYDIAGSRAHARVLRKAGLLTEDELTGMLAALDTLAQDVASGAFTPTVADEDVHTAL-ER   96

Chelativorans   93   AALKRTIGSVAGKMHIGRSRNDLANAGKRMFLRDQLLRTIEAVIGYREAVVHKAADHLDT  152
A. japonicum    97   GLLERAGTELGGKLRAGRSRNDQVATLFRMWLRDAARRVVAGTLGVVDALVSQAKRHPDA  156

Chelativorans  153   VMVVYTQRKEAQPITLGHYLMAISENLAKNLDRYRELYARINLCPLGAAATAGTGWPLNR  212
A. japonicum   157   ILPGRTHLQHAQPVLLAHHLLAHGQSLLRDVTRLRDWDARTAESPYGSGALAGSSLGLDP  216

Chelativorans  213   DRTSALLGFDGLVVNSIEGVAGWDHVAEHAFVNAVFLSGLSRLASEIQLWSTDEYQVAEL  272
A. japonicum   217   EAVAEELGFDTSVENSIDGTASRDFVAEFAFDVAMLAVNLSRIAEEVIIWNTAEFGYVTL  276

Chelativorans  273   DASFAGTSSIMPQKKNPDSLERSRKAAFAAMGPLVGILTSLNAIEYQYSAARVE-LEP--  329
A. japonicum   277   DDAWATGSSIMPQKKNPDVAELTRGKAGRLIGNLTGLLATLKAQPLAYNRDLQEDKEPVF  336

Chelativorans  330   RSIDALIAATHAMTGVVRTLHPNKERMRQYAAENYSTMTDLTDMLVRRVGIDYREAHEIV  389
A. japonicum   337   DSVEQLELLFPAIAGMLETLTFHTDRLAELAPAGFTLATDIAEWLVRQ-GVPFRVAHEAA  395

Chelativorans  390   AHVVITAIEKGIKANKIGLDLVQEAAVAQTGAGINVSADDIKDALDPWQNVLRREGKGMP  449
A. japonicum   396   GESVRVAEARG-----VGLDELTDEEFEKINPALTPA---VREVLTVEGSVSSRNARGGT  447

Chelativorans  450   APMSVKASIDDAMAELHKDRAWLA  473
A. japonicum   448   APERVAEQRDRLVARVAEHRTWLG  471
```

Figure S13. **Sequence alignment of EDDS lyases from *Chelativorans sp.*BNC1 *A. japonicum*.** Both proteins share 33% sequence identity

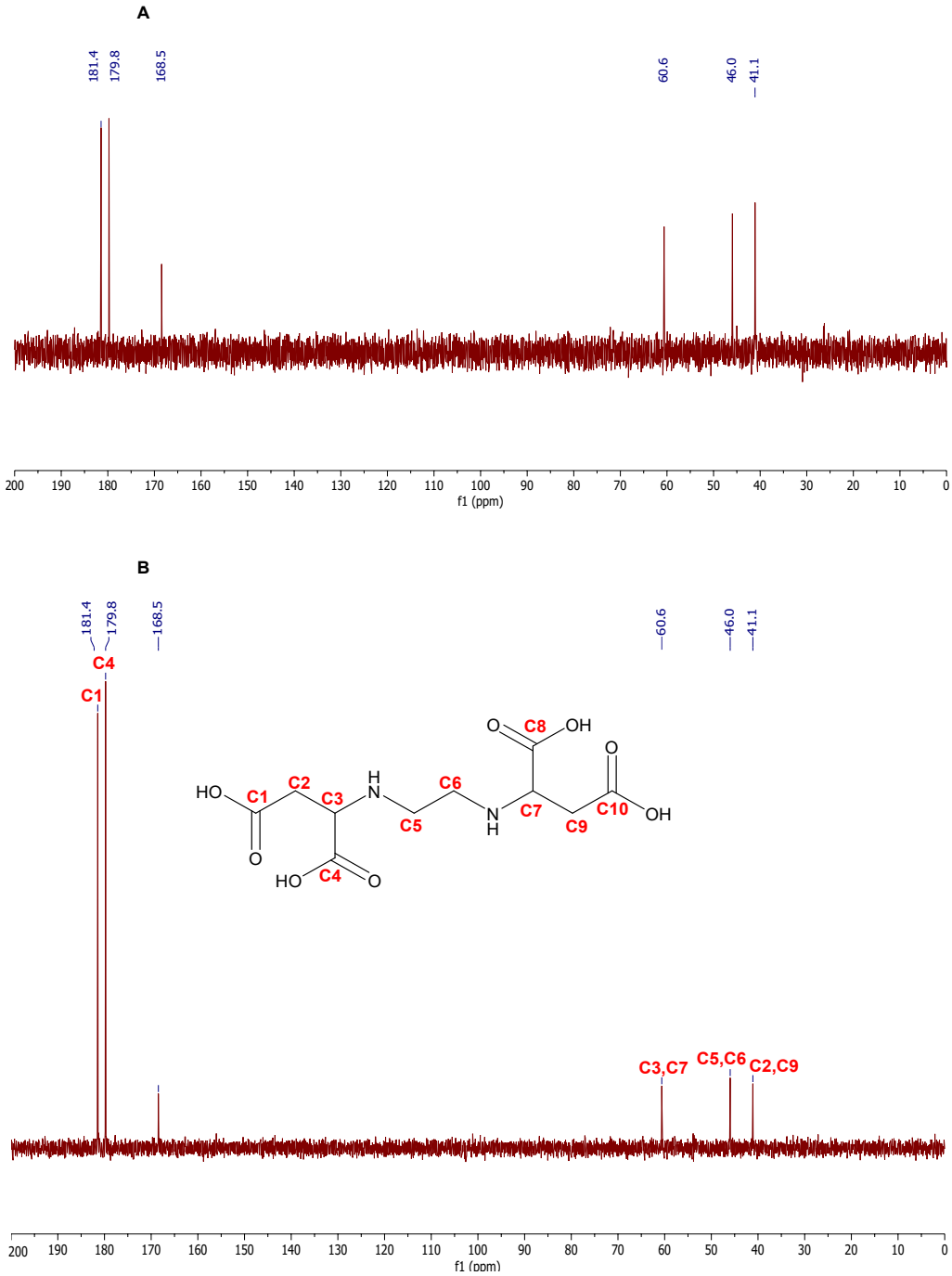

Figure S14. **^{13}C NMR spectra of [S,S]-EDDS**. (A) [*S,S*]-EDDS isolated from *A. japonicum* OP2 culture without feeding (B) [S,S]-EDDS isolated from *A. japonicum* OP2 culture fed with 1,4-^{13}C-^{15}N L-aspartic acid (NaOD, 400 MHz).

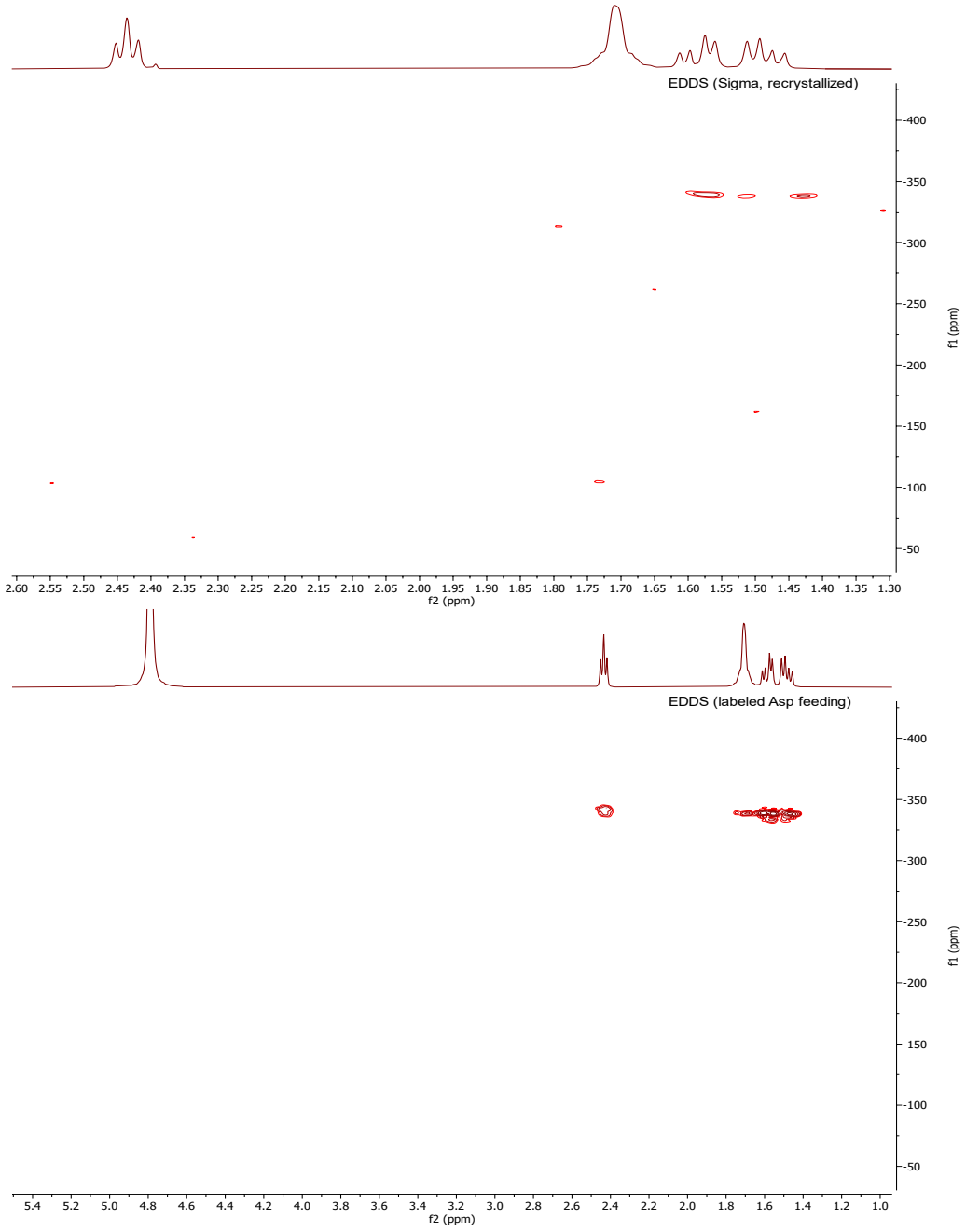

Figure S15. **^{1}H-^{15}N HMBC spectra of [*S,S*]-EDDS** (A) Isolated from *A. japonicum* OP2 without feeding (B) Isolated from *A. japonicum* OP2 culture fed with 1,4-^{13}C-^{15}N L-aspartic acid (NaOD, 400 MHz).

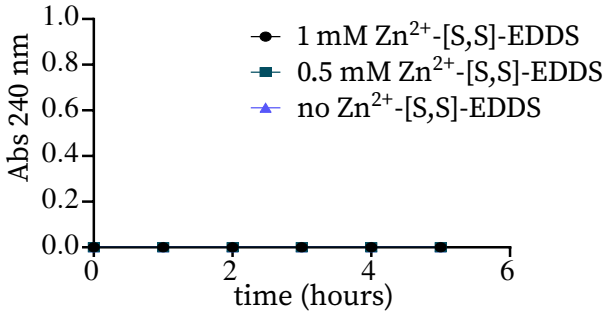

Figure S16. **Enzymatic reaction of the arginosuccinate lyase of *A. japonicum* (Asl_{Aj}) using Zn^{2+}-[*S,S*]-EDDS as substrate**. Spectrophotometric measurement at 240nm to detect the formation of fumarate during a reaction catalyzed by 10µM Asl_{Aj} and Zn^{2+}-[*S,S*]-EDDS ((0.5mM or 1mM) in Tris-HCL buffer (pH 8.0). As negative control, a reaction containing 10μM Asl_{Aj} in Tris-HCL buffer (pH 8.0)

.

Organism	Homologous protein AesA/AesC	Similarity % (AesA/AesC)	enzymes	Related product	References
S. mutabilis subs. capreolus ATCC 23892	CmnK/CmnB	22/33	ornithine cyclodeaminase/ cysteine synthase	capreomycin	Felnagle et al. 2007
Streptomyces sp. ATCC 11861	VioK/VioB	25/32	ornithine cyclodeaminase/ cysteine synthase	viomycin	Thomas et al. 2003
Staphylococcus aureus	SbnB/SbnA	22/30	ornithine cyclodeaminase/ cysteine synthase	Staphyloferrin B	Beasley et al. 2011b
Streptomyces albulus PD-1	NjxB/NjxA	31/34	ornithine cyclodeaminase/ cysteine synthase	poly (L-diaminopropionic acid) PDAP	Xu et al. 2015

Figure S17. **List of similarity between AesA/AesC proteins known to be related to L-DAPP biosynthesis.**

Region	Type	From	To	Most similar known cluster		Similarity
Region 1	ectoine	397,859	408,248	ectoine	Other	100%
Region 2	redox-cofactor	1,116,848	1,138,882	lankacidin C	NRP+Polyketide	20%
Region 3	aminopolycarboxylic-acid	1,683,656	1,697,031	[S,S]-EDDS	Other	100%
Region 4	NRPS-like	1,879,470	1,922,420	desulfoclethramycin/clethramycin	Other	8%
Region 5	thiopeptide	2,004,849	2,027,556			
Region 6	NRPS , T1PKS	2,465,162	2,608,773	ECO-0501	Polyketide	85%
Region 7	NAPAA	2,983,948	3,017,393	ε-Poly-L-lysine	NRP	100%
Region 8	hglE-KS , T1PKS	3,188,983	3,277,402	hexacosalactone A	Other	9%
Region 9	lanthipeptide-class-ii	3,305,052	3,327,095			
Region 10	other , NRPS-like , NRPS	3,388,054	3,458,655	maduropeptin	Polyketide:Iterative type I polyketide+Polyketide:Enediyne type I polyketide	34%
Region 11	lanthipeptide-class-ii	3,852,107	3,874,977			
Region 12	terpene	3,926,045	3,946,778	2-methylisoborneol	Terpene	100%
Region 13	NAPAA	3,953,382	3,987,446	depsibosamycin B/depsibosamycin C/depsibosamycin D	NRP	9%
Region 14	NRPS , PKS-like	4,069,506	4,185,857	azicemicin B	Polyketide	11%
Region 15	NRPS , NRP-metallophore	4,379,513	4,441,441	albachelin	NRP	100%
Region 16	NRP-metallophore , NRPS	4,530,446	4,589,590	mirubactin	NRP	78%
Region 17	T1PKS	4,714,233	4,758,888	sanglifehrin A	NRP+Polyketide	4%
Region 18	NRPS-like , NRPS , T1PKS	4,855,276	4,926,566	theonellamide	NRP+Polyketide	21%
Region 19	T1PKS , hglE-KS	5,121,670	5,172,126	hexacosalactone A	Other	11%
Region 20	terpene	5,279,353	5,299,034	leucomycin	Polyketide	3%
Region 21	terpene	5,831,581	5,851,176	isorenieratene	Terpene	42%
Region 22	T1PKS , thiopeptide , LAP	6,416,171	6,486,484	amycolamycin A/amycolamycin B	Polyketide	31%
Region 23	T3PKS , NRPS-like , NRPS	6,800,521	6,897,743	ristomycin A	Saccharide+NRP:Glycopeptide	100%
Region 24	NRPS-like , T1PKS	6,902,710	6,949,003	polyoxypeptin	NRP+Polyketide	10%
Region 25	arylpolyene	7,062,949	7,104,100	kinamycin	Polyketide	5%
Region 26	other , PKS-like , amglyccycl	7,571,659	7,619,730	cetoniacytone A	Other:Cyclitol	38%
Region 27	lanthipeptide-class-iii	8,042,656	8,065,199	Ery-9/Ery-6/Ery-8/Ery-7/Ery-5/Ery-4/Ery-3	RiPP:Lanthipeptide	100%
Region 28	terpene	8,232,022	8,254,163	geosmin	Terpene	100%
Region 29	CDPS	8,296,964	8,317,650			

Figure S18. **antiSMASH analysis of *A. japonicum*. Region 3 corresponds to the aminopolycarboxylic acid [S,S]-EDDS**. Biosynthesis mechanisms differs from NRPS or NIS pathways typical for siderophore bioynthesis.Region 15 and 16 correspond to the metalophores albachelin and mirubactin, respectivelly.

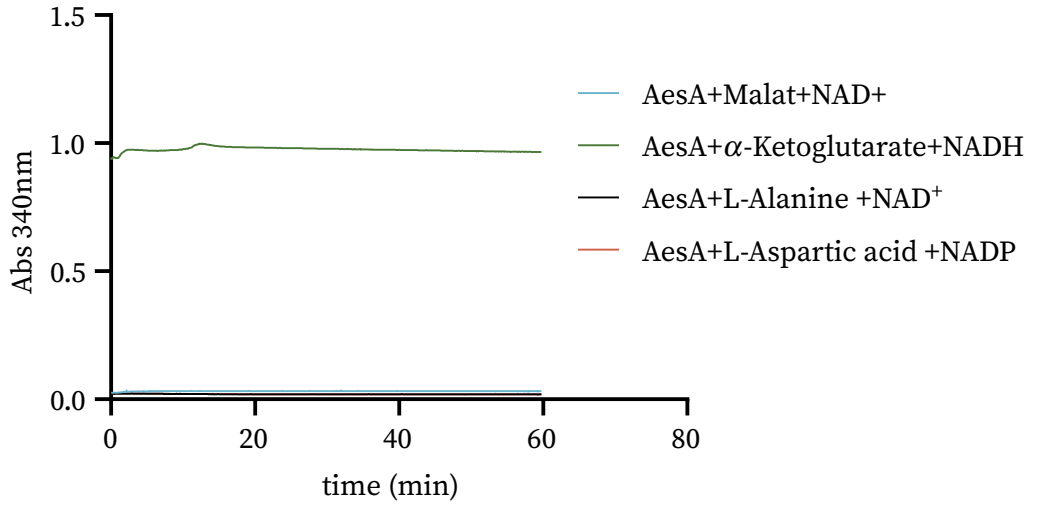

Figure S19. **Biochemical analysis of AesA according to (Wang *et al.*, 2022)**. Analysis of AesA using putative substrates. Spectrophotometric measurement (340nm) of AesA reaction over time. The decrease in absorbance at 340 nm indicates the consumption of NADH in the reaction

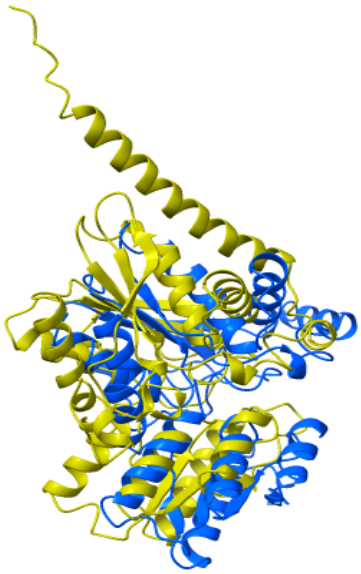

Figure S20. **Structure prediction of AesC protein by AlphaFold (ColabFold v1.5.2)**. The structure is colored based on the confidence metric (pLDDT) provided by Alphafold analysis; from blue (high confidence) to red (low confidence).

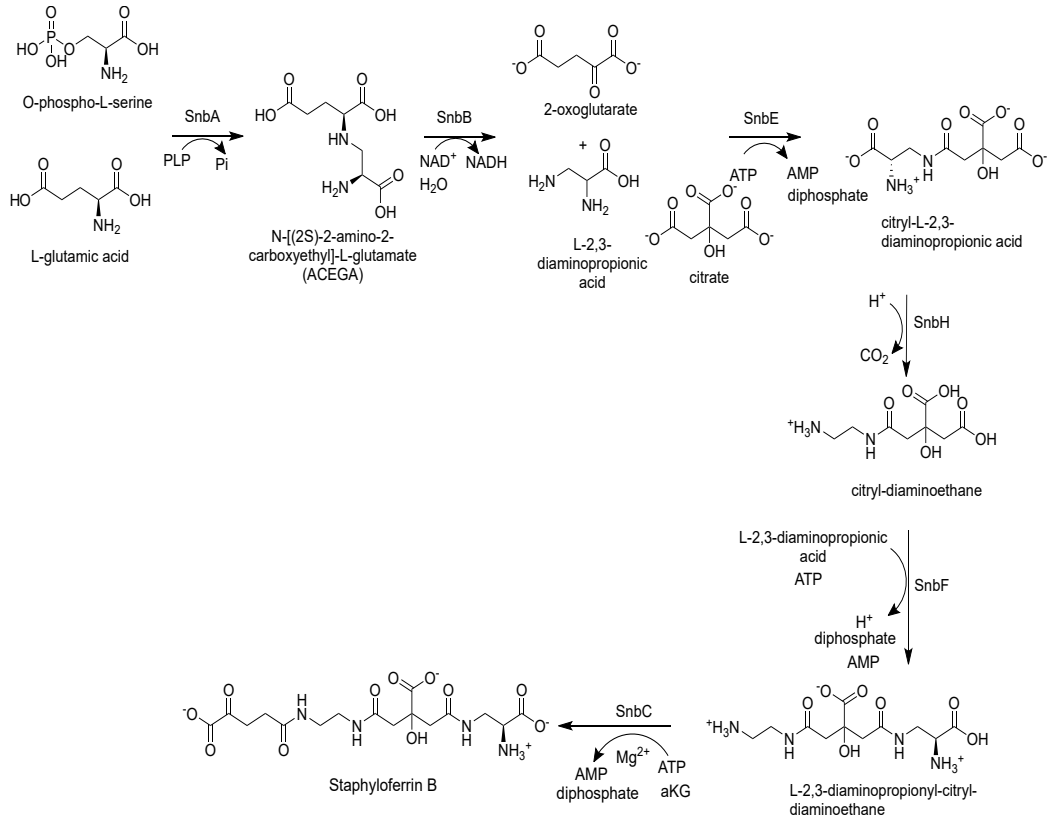

Figure S21. **Staphylofferin B biosynthetic pathway (Cheung *et al.*, 2009; Kobylarz *et al.*, 2014)**

Bibliography

Albarracín, V. H., Winik, B., Kothe, E., Amoroso, M. J., and Abate, C. M. (2008). Copper bioaccumulation by the actinobacterium amycolatopsis sp. ab0. *Journal of basic microbiology*, **48**(5), 323–330.

Álvarez-Fernández, A., Pérez-Sanz, A., and Lucena, J. J. (2001). Evaluation of effect of washing procedures on mineral analysis of orange and peach leaves sprayed with seaweed extracts enriched with iron. *Communications in Soil Science and Plant Analysis*, **32**(1-2), 157–170.

Ammendola, S., Pasquali, P., Pistoia, C., Petrucci, P., Petrarca, P., Rotilio, G., and Battistoni, A. (2007). High-affinity zn2+ uptake system znuabc is required for bacterial zinc homeostasis in intracellular environments and contributes to the virulence of salmonella enterica. *Infection and immunity*, **75**(12), 5867–5876.

Andreini, C., Bertini, I., Cavallaro, G., Holliday, G. L., and Thornton, J. M. (2008). Metal ions in biological catalysis: from enzyme databases to general principles. *Journal of biological inorganic chemistry : JBIC : a publication of the Society of Biological Inorganic Chemistry*, **13**(8), 1205–1218.

Andrews, S. C., Robinson, A. K., and Rodríguez-Quiñones, F. (2003). Bacterial iron homeostasis. *FEMS microbiology reviews*, **27**(2-3), 215–237.

Beasley, F. C., Cheung, J., and Heinrichs, D. E. (2011). Mutation of l-2,3-diaminopropionic acid synthase genes blocks staphyloferrin b synthesis in staphylococcus aureus. *BMC microbiology*, **11**, 199.

Bindraban, P. S., Dimkpa, C. O., Angle, S., and Rabbinge, R. (2018). Unlocking the multiple public good services from balanced fertilizers. *Food Security*, **10**(2), 273–285.

Blin, K., Medema, M. H., Kazempour, D., Fischbach, M. A., Breitling, R., Takano, E., and Weber, T. (2013). antismash 2.0–a versatile platform for genome mining of secondary metabolite producers. *Nucleic acids research*, **41**(Web Server issue), W204–12.

Blin, K., Shaw, S., Kloosterman, A. M., Charlop-Powers, Z., van Wezel, G. P., Medema, M. H., and Weber, T. (2021). antismash 6.0: improving cluster detection and comparison capabilities. *Nucleic acids research*, **49**(W1), W29–W35.

Blindauer, C. A. (2015). Advances in the molecular understanding of biological zinc transport. *Chemical communications (Cambridge, England)*, **51**(22), 4544–4563.

Bonner, M. R. and Alavanja, M. C. R. (2017). Pesticides, human health, and food security. *Food and Energy Security*, **6**(3), 89–93.

Bush, M. J., Chandra, G., Al-Bassam, M. M., Findlay, K. C., and Buttner, M. J. (2019). Bldc delays entry into development to produce a sustained period of vegetative growth in streptomyces venezuelae. *mBio*, **10**(1).

Cai, Z., Chen, Q., Wang, H., He, Y., Wang, W., Zhao, X., and Ye, Q. (2012). Degradation of the novel herbicide zj0273 by amycolatopsis sp. m3-1 isolated from soil. *Applied microbiology and biotechnology*, **96**(5), 1371–1379.

Cantalapiedra, C. P., Hernández-Plaza, A., Letunic, I., Bork, P., and Huerta-Cepas, J. (2021). eggnog-mapper v2: Functional annotation, orthology assignments, and domain prediction at the metagenomic scale. *Molecular biology and evolution*, **38**(12), 5825–5829.

Capdevila, D. A., Wang, J., and Giedroc, D. P. (2016). Bacterial strategies to maintain zinc metallostasis at the host-pathogen interface. *The Journal of biological chemistry*, **291**(40), 20858–20868.

Carpino, L. A. and Han, G. Y. (1972). 9-fluorenylmethoxycarbonyl amino-protecting group. *Journal of Organic Chemistry*, **37**, 3404–3409.

Carter, J. H. n., Du Bus, R. H., Dyer, J. R., Floyd, J. C., Rice, K. C., and Shaw, P. D. (1974). Biosynthesis of viomycin. i. origin of alpha, beta-diaminopropionic acid and serine. *Biochemistry*, **13**(6), 1221–1227.

Cebulla, I. (1995). *Gewinnung komplexbildender Substanzen mittels Amycolatopsis orientalis*. Doctoral thesis.

Cerasi, M., Liu, J. Z., Ammendola, S., Poe, A. J., Petrarca, P., Pesciaroli, M., Pasquali, P., Raffatellu, M., and Battistoni, A. (2014). The zupt transporter plays an important role in zinc homeostasis and contributes to salmonella enterica virulence. *Metallomics : integrated biometal science*, **6**(4), 845–853.

Chen, L., Liu, T., and Ma, C. (2010). Metal complexation and biodegradation of edta and s,s-edds: a density functional theory study. *The journal of physical chemistry. A*, **114**(1), 443–454.

Cheung, J., Beasley, F. C., Liu, S., Lajoie, G. A., and Heinrichs, D. E. (2009). Molecular characterization of staphyloferrin b biosynthesis in staphylococcus aureus. *Molecular microbiology*, **74**(3), 594–608.

Choi, S. and Bird, A. J. (2014). Zinc'ing sensibly: controlling zinc homeostasis at the transcriptional level. *Metallomics : integrated biometal science*, **6**(7), 1198–1215.

Choi, S.-H., Lee, K.-L., Shin, J.-H., Cho, Y.-B., Cha, S.-S., and Roe, J.-H. (2017). Zinc-dependent regulation of zinc import and export genes by zur. *Nature communications*, **8**, 15812.

Cummings, D. A., Snelling, A. I., and Puri, A. W. (2021). Methylotroph natural product identification by inverse stable isotopic labeling. *bioRxiv*.

Edenhart, S., Denneler, M., Spohn, M., Doskocil, E., Kavšček, M., Amon, T., Kosec, G., Smole, J., Bardl, B., Biermann, M., Roth, M., Wohlleben, W., and Stegmann, E. (2020). Metabolic engineering of amycolatopsis japonicum for optimized production of s,s-edds, a biodegradable chelator. *Metabolic engineering*, **60**, 148–156.

Fasusi, O. A., Cruz, C., and Babalola, O. O. (2021). Agricultural sustainability: Microbial biofertilizers in rhizosphere management. *Agriculture*, **11**(2), 163.

Felnagle, E. A., Rondon, M. R., Berti, A. D., Crosby, H. A., and Thomas, M. G. (2007). Identification of the biosynthetic gene cluster and an additional gene for resistance to the antituberculosis drug capreomycin. *Applied and environmental microbiology*, **73**(13), 4162–4170.

Fleige, C., Hansen, G., Kroll, J., and Steinbüchel, A. (2013). Investigation of the amycolatopsis sp. strain atcc 39116 vanillin dehydrogenase and its impact on the biotechnical production of vanillin. *Applied and environmental microbiology*, **79**(1), 81–90.

Flett, F., Mersinias, V., and Smith, C. P. (1997). High efficiency intergeneric conjugal transfer of plasmid DNA from Escherichia coli to methyl DNA-restricting streptomycetes. *FEMS Microbiology Letters*, **155**(2), 223–229.

Foster, A. W., Osman, D., and Robinson, N. J. (2014). Metal preferences and metallation. *Journal of Biological Chemistry*, **289**(41), 28095–28103.

Gadkari, D., Mörsdorf, G., and Meyer, O. (1992). Chemolithoautotrophic assimilation of dinitrogen by streptomyces thermoautotrophicus ubt1: identification of an unusual n2-fixing system. *Journal of bacteriology*, **174**(21), 6840–6843.

Gibson, F. and Magrath, D. I. (1969). The isolation and characterization of a hydroxamic acid (aerobactin) formed by aerobacter aerogenes 62-i. *Biochimica et biophysica acta*, **192**(2), 175–184.

Goodfellow, M., Brown, A. B., Cai, J., Chun, J., and Collins, M. D. (1997). Amycolatopsis japonicum sp. nov., an actinomycete producing (s,s)-n,n'-ethylenediaminedisuccinic acid. *Systematic and Applied Microbiology*, **20**(1), 78–84.

Grass, G., Wong, M. D., Rosen, B. P., Smith, R. L., and Rensing, C. (2002). Zupt is a zn(ii) uptake system in escherichia coli. *Journal of bacteriology*, **184**(3), 864–866.

Grim, K. P., San Francisco, B., Radin, J. N., Brazel, E. B., Kelliher, J. L., Párraga Solórzano, P. K., Kim, P. C., McDevitt, C. A., and Kehl-Fie, T. E. (2017). The metallophore staphylopine enables staphylococcus aureus to compete with the host for zinc and overcome nutritional immunity. *mBio*, **8**(5).

Hani, E. K. and Chan, V. L. (1994). Cloning, characterization, and nucleotide sequence analysis of the argh gene from campylobacter jejuni tgh9011 encoding argininosuccinate lyase. *Journal of bacteriology*, **176**(7), 1865–1871.

Hantke, K. (2001). Bacterial zinc transporters and regulators. *Biometals : an international journal on the role of metal ions in biology, biochemistry, and medicine*, **14**(3-4), 239–249.

Hantke, K. (2005). Bacterial zinc uptake and regulators. *Current opinion in microbiology*, **8**(2), 196–202.

Ho, P. C. (2005). Hplc of amines as 9-fluorenyimethyl chloroformate derivatives. In I. Molnár-Perl, editor, *Quantitation of amino acids and amines by chromatography*, volume 70 of *Journal of chromatography*, pages 471–501. Elsevier, Amsterdam and Boston.

Hong, H.-J., Hutchings, M. I., Hill, L. M., and Buttner, M. J. (2005). The role of the novel fem protein vank in vancomycin resistance in streptomyces coelicolor. *The Journal of biological chemistry*, **280**(13), 13055–13061.

Hough, E., Hansen, L. K., Birknes, B., Jynge, K., Hansen, S., Hordvik, A., Little, C., Dodson, E., and Derewenda, Z. (1989). High-resolution (1.5 å) crystal structure of phospholipase c from bacillus cereus. *Nature*, **338**(6213), 357–360.

Hughes, C. C. (2021). Chemical labeling strategies for small molecule natural product detection and isolation. *Natural product reports*, **38**(9), 1684–1705.

Hunt, A. C., Servín-González, L., Kelemen, G. H., and Buttner, M. J. (2005). The bldc developmental locus of streptomyces coelicolor encodes a member of a family of small dna-binding proteins related to the dna-binding domains of the merr family. *Journal of bacteriology*, **187**(2), 716–728.

Irving, H. and Williams, R. J. P. (1953). 637. the stability of transition-metal complexes. *Journal of the Chemical Society (Resumed)*, page 3192.

Jones, P. W. and Williams, D. R. (2002). Chemical speciation simulation used to assess the efficiency of environment-friendly edta alternatives for use in the pulp and paper industry. *Inorganica Chimica Acta*, **339**, 41–50.

Jumper, J., Evans, R., Pritzel, A., Green, T., Figurnov, M., Ronneberger, O., Tunyasuvunakool, K., Bates, R., Žídek, A., Potapenko, A., Bridgland, A., Meyer, C., Kohl, S. A. A., Ballard, A. J., Cowie, A., Romera-Paredes, B., Nikolov, S., Jain, R., Adler, J., Back, T., Petersen, S., Reiman, D., Clancy, E., Zielinski, M., Steinegger, M., Pacholska, M., Berghammer, T., Bodenstein, S., Silver, D., Vinyals, O., Senior, A. W., Kavukcuoglu, K., Kohli, P., and Hassabis, D. (2021). Highly accurate protein structure prediction with alphafold. *Nature*, **596**(7873), 583–589.

Kallifidas, D., Pascoe, B., Owen, G. A., Strain-Damerell, C. M., Hong, H.-J., and Paget, M. S. B. (2010). The zinc-responsive regulator zur controls expression of the coelibactin gene cluster in streptomyces coelicolor. *Journal of bacteriology*, **192**(2), 608–611.

Kandari, D., Joshi, H., and Bhatnagar, R. (2021). Zur: Zinc-sensing transcriptional regulator in a diverse set of bacterial species. *Pathogens*, **10**(3).

Kezerian, C. and Ramsey, W. (1964). Bis-addiction products and methods of reparing same. *Patent U.S 3158635*.

Kieser, T., Bibb, M., Buttner, M., Chater, K., and Hopwood, D. (2000). *Practical streptomyces genetics*. John Innes Centre, Norwich, England.

Knepper, T. P. (2003). Synthetic chelating agents and compounds exhibiting complexing properties in the aquatic environment. *TrAC Trends in Analytical Chemistry*, **22**(10), 708–724.

Kobylarz, M. J., Grigg, J. C., Takayama, S.-i. J., Rai, D. K., Heinrichs, D. E., and Murphy, M. E. P. (2014). Synthesis of l-2,3-diaminopropionic acid, a siderophore and antibiotic precursor. *Chemistry & biology*, **21**(3), 379–388.

Kobylarz, M. J., Grigg, J. C., Liu, Y., Lee, M. S. F., Heinrichs, D. E., and Murphy, M. E. P. (2016). Deciphering the substrate specificity of sbna, the enzyme catalyzing the first step in staphyloferrin b biosynthesis. *Biochemistry*, **55**(6), 927–939.

Kodani, S., Komaki, H., Suzuki, M., Hemmi, H., and Ohnishi-Kameyama, M. (2015). Isolation and structure determination of new siderophore albachelin from amycolatopsis alba. *Biometals : an international journal on the role of metal ions in biology, biochemistry, and medicine*, **28**(2), 381–389.

Kour, D., Rana, K. L., Yadav, A. N., Yadav, N., Kumar, M., Kumar, V., Vyas, P., Dhaliwal, H. S., and Saxena, A. K. (2020). Microbial biofertilizers: Bioresources and eco-friendly technologies for agricultural and environmental sustainability. *Biocatalysis and Agricultural Biotechnology*, **23**, 101487.

Lechevalier, M. P., PRAUSER, H., LABEDA, D. P., and RUAN, J.-S. (1986). Two new genera of nocardioform actinomycetes: Amycolata gen. nov. and amycolatopsis gen. nov. *International Journal of Systematic Bacteriology*, **36**(1), 29–37.

Lee, S. Y., Kim, H. U., Park, J. H., Park, J. M., and Kim, T. Y. (2009). Metabolic engineering of microorganisms: general strategies and drug production. *Drug discovery today*, **14**(1-2), 78–88.

Lhospice, S., Gomez, N. O., Ouerdane, L., Brutesco, C., Ghssein, G., Hajjar, C., Liratni, A., Wang, S., Richaud, P., Bleves, S., Ball, G., Borezée-Durant, E., Lobinski, R., Pignol, D., Arnoux, P., and Voulhoux, R. (2017). Pseudomonas aeruginosa zinc uptake in chelating environment is primarily mediated by the metallophore pseudopaline. *Scientific reports*, **7**(1), 17132.

López-Rayo, S., Correas, C., and Lucena, J. J. (2012). Novel chelating agents as manganese and zinc fertilisers: characterisation, theoretical speciation and stability in solution. *Chemical Speciation & Bioavailability*, **24**(3), 147–158.

López-Rayo, S., Nadal, P., and Lucena, J. J. (2015). Reactivity and effectiveness of traditional and novel ligands for multi-micronutrient fertilization in a calcareous soil. *Frontiers in plant science*, **6**, 752.

López-Rayo, S., Nadal, P., and Lucena, J. J. (2016). Novel chelating agents for iron, manganese, zinc, and copper mixed fertilization in high ph soil-less cultures. *Journal of the science of food and agriculture*, **96**(4), 1111–1120.

López-Rayo, S., Sanchis-Pérez, I., Ferreira, C. M. H., and Lucena, J. J. (2019). S,s-edds/fe: A new chelate for the environmentally sustainable correction of iron chlorosis in calcareous soil. *The Science of the total environment*, **647**, 1508–1517.

Luo, C., Shen, Z., Li, X., and Baker, A. J. M. (2006). Enhanced phytoextraction of pb and other metals from artificially contaminated soils through the combined application of edta and edds. *Chemosphere*, **63**(10), 1773–1784.

MacNeil, D. J., Gewain, K. M., Ruby, C. L., Dezeny, G., Gibbons, P. H., and MacNeil, T. (1992). Analysis of streptomyces avermitilis genes required for avermectin biosynthesis utilizing a novel integration vector. *Gene*, **111**(1), 61–68.

Maret, W. (2019). The redox biology of redox-inert zinc ions. *Free radical biology & medicine*, **134**, 311–326.

Marschner, P. (2012). Marschner's mineral nutrition of higher plants: Third edition.

Mastropasqua, M. C., D'Orazio, M., Cerasi, M., Pacello, F., Gismondi, A., Canini, A., Canuti, L., Consalvo, A., Ciavardelli, D., Chirullo, B., Pasquali, P., and Battistoni, A. (2017). Growth of pseudomonas aeruginosa in zinc poor environments is promoted by a nicotianamine-related metallophore. *Molecular microbiology*, **106**(4), 543–561.

McCormick, M. H., McGuire, J. M., Pittenger, G. E., Pittenger, R. C., and Stark, W. M. (1955). Vancomycin, a new antibiotic. i. chemical and biologic properties. *Antibiotics annual*, **3**, 606–611.

Meers, E., Ruttens, A., Hopgood, M. J., Samson, D., and Tack, F. M. G. (2005). Comparison of edta and edds as potential soil amendments for enhanced phytoextraction of heavy metals. *Chemosphere*, **58**(8), 1011–1022.

Meng, L., Yang, S. H., Kim, T.-J., and Suh, J.-W. (2012). Effects of two putative laci-family transcriptional regulators, sco4158 and sco7554, on antibiotic pigment production of streptomyces coelicolor and streptomyces lividans. *Journal of the Korean Society for Applied Biological Chemistry*, **55**(6), 737–741.

Menges, R., Muth, G., Wohlleben, W., and Stegmann, E. (2007). The abc transporter tba of amycolatopsis balhimycina is required for efficient export of the glycopeptide antibiotic balhimycin. *Applied microbiology and biotechnology*, **77**(1), 125–134.

Mishra A, S. A. (2017). Biochemical characterization of argininosuccinate lyase from m. tuberculosis: significance of a c-terminal cysteine in catalysis and thermal stability.

Mizunashi, W. (2001). Protein having ethylenediamine-n,n′- disuccinic acid: Ethylenediamine lyase acitivity and gene encoding the same. u.s. patent.

Morey, J. R., Kehl-Fie, T. E., and Rappe, M. S. (2020). Bioinformatic mapping of opine-like zincophore biosynthesis in bacteria. *mSystems*, **5**(4), e00554–20.

Muchmore, D. C., McIntosh, L. P., Russell, C. B., Anderson, D. E., and Dahlquist, F. W. (1989). [3] expression and nitrogen-15 labeling of proteins for proton and nitrogen-15 nuclear magnetic resonance. In *Nuclear Magnetic Resonance Part B Structure and Mechanism*, volume 177 of *Methods in Enzymology*, pages 44–73. Academic Press.

Mungan, M. D., Harbig, T. A., Perez, N. H., Edenhart, S., Stegmann, E., Nieselt, K., and Ziemert, N. (2022). Secondary metabolite transcriptomic pipeline (sema-trap), an expression-based exploration tool for increased secondary metabolite production in bacteria. *Nucleic acids research*.

Neal, J.A., and Rose, N.J. (1968). Stereospecific ligands and their complexes. i. a cobalt (iii) complex of ethylenediaminedisuccinic acid. *Inorganic Chemistry*, **7**, 2405–&.

Neilands, J. B. (1995). Siderophores: Structure and function of microbial iron transport compounds. *Journal of Biological Chemistry*, **270**(45), 26723–26726.

Nikos Alexandratos and Jelle Bruinsma - FAO (2012). World agriculture towards 2030/2050: the 2012 revision.

Nishida, H. and Tokiwa, Y. (1993). Distribution of poly(ß-hydroxybutyrate) and poly(-caprolactone)aerobic degrading microorganisms in different environments. *Journal of Environmental Polymer Degradation*, **1**(3), 227–233.

Nishikiori, T., Okuyama, A., Naganawa, H., Takita, T., Hamada, M., Takeuchi, T., Aoyagi, T., and and Umezawa, H. (1984). Production by actinomycetes of (s,s)-n,n'-ethylenediamine-disuccinic acid, an inhibitor of phospholipase c. *J Antibiot (Tokyo)*, **37**, 426–427.

Noll, M., Petrukhin, K., and Lutsenko, S. (1998). Identification of a novel transcription regulator from proteus mirabilis, pmtr, revealed a possible role of yjai protein in balancing zinc in escherichia coli. *Journal of Biological Chemistry*, **273**(33), 21393–21401.

Nowack, B. and VanBriesen, J. M. (2005). Chelating agents in the environment. In B. Nowack, editor, *Biogeochemistry of chelating agents*, volume 910 of *National meeting of the American Chemical Society*, pages 1–18. Oxford Univ. Press, Oxford.

Outten, C. E. and O'Halloran, T. V. (2001). Femtomolar sensitivity of metalloregulatory proteins controlling zinc homeostasis. *Science (New York, N.Y.)*, **292**(5526), 2488–2492.

Parte, A. C., Sardà Carbasse, J., Meier-Kolthoff, J. P., Reimer, L. C., and Göker, M. (2020). List of prokaryotic names with standing in nomenclature (lpsn) moves to the dsmz. *International Journal of Systematic and Evolutionary Microbiology*, **70**(11), 5607–5612.

Patzer, S. I. and Hantke, K. (1998). The znuabc high-affinity zinc uptake system and its regulator zur in escherichia coli. *Molecular microbiology*, **28**(6), 1199–1210.

Patzer, S. I. and Hantke, K. (2000). The zinc-responsive regulator zur and its control of the znu gene cluster encoding the znuabc zinc uptake system in escherichia coli. *Journal of Biological Chemistry*, **275**(32), 24321–24332.

Pérez-Montaño, F., Alías-Villegas, C., Bellogín, R. A., del Cerro, P., Espuny, M. R., Jiménez-Guerrero, I., López-Baena, F. J., Ollero, F. J., and Cubo, T. (2014). Plant growth promotion in cereal and leguminous agricultural important plants: from microorganism capacities to crop production. *Microbiological research*, **169**(5-6), 325–336.

Poddar, H., de Villiers, J., Zhang, J., Puthan Veetil, V., Raj, H., Thunnissen, A.-M. W. H., and Poelarends, G. J. (2018). Structural basis for the catalytic mechanism of ethylenediamine- n, n'-disuccinic acid lyase, a carbon-nitrogen bond-forming enzyme with a broad substrate scope. *Biochemistry*, **57**(26), 3752–3763.

Pollack, J. R., Ames, B. N., and Neilands, J. B. (1970). Iron transport in salmonella typhimurium: mutants blocked in the biosynthesis of enterobactin. *Journal of bacteriology*, **104**(2), 635–639.

Pranamuda, H., Tokiwa, Y., and Tanaka, H. (1997). Polylactide degradation by an amycolatopsis sp. *Applied and environmental microbiology*, **63**(4), 1637–1640.

Rai, V., Fisher, N., Duckworth, O. W., and Baars, O. (2020). Extraction and detection of structurally diverse siderophores in soil. *Frontiers in microbiology*, **11**, 581508.

Ramsaywak, P. C., Labbé, G., Siemann, S., Dmitrienko, G. I., and Guillemette, J. (2004). Molecular cloning, expression, purification, and characterization of fructose 1,6-bisphosphate aldolase from mycobacterium tuberculosis—a novel class ii a tetramer. *Protein Expression and Purification*, **37**(1), 220–228.

Robson, A. D., editor (1993). *Zinc in Soils and Plants*. Springer Netherlands, Dordrecht.

Saeed, M. and Fox, R. L. (1977). Relation between suspension ph and zinc solubility in acid and calcareous soils. *Soil Science*, pages 124, 199–204.

Saifullah, Meers, E., Qadir, M., de Caritat, P., Tack, F., Du Laing, G., and Zia, M. (2009). Edta-assisted pb phytoextraction. *Chemosphere*, **74**(10), 1279–1291.

Sambrook, J., Fritsch, E., and Maniatis, T. (1989). *Molecular cloning: a laboratory manual, 2nd ed. Cold Spring Harbor Laboratory, Cold Spring Harbor, NY*.

Sandstead, H. H. (2013). Human zinc deficiency: discovery to initial translation. *Advances in Nutrition*, **4**(1), 76–81.

Sastre Toraño, J. and Guchelaar, H. J. (1998). Quantitative determination of the macrolide antibiotics erythromycin, roxithromycin,. *Journal of chromatography. B, Biomedical sciences and applications*, **720**(1-2), 89–97.

Satroutdinov, A. D., Dedyukhina, E. G., Chistyakova, T. I., Witschel, M., Minkevich, I. G., Eroshin, V. K., and Egli, T. (2000). Degradation of metal−edta complexes by resting cells of the bacterial strain dsm 9103. *Environmental science & technology*, **34**(9), 1715–1720.

Schapiro, J. M., Libby, S. J., and Fang, F. C. (2003). Inhibition of bacterial dna replication by zinc mobilization during nitrosative stress. *Proceedings of the National Academy of Sciences of the United States of America*, **100**(14), 8496–8501.

Schowanek, D. R. (1997). Biodegradation of edds.

Schröder, I., Vadas, A., Johnson, E., Lim, S., and Monbouquette, H. G. (2004). A novel archaeal alanine dehydrogenase homologous to ornithine cyclodeaminase and mu-crystallin. *Journal of bacteriology*, **186**(22), 7680–7689.

Sensi, P., MARGALITH, P., and TIMBAL, M. T. (1959). Rifomycin, a new antibiotic; preliminary report. *Il Farmaco; edizione scientifica*, **14**(2), 146–147.

Seyedsayamdost, M. R., Traxler, M. F., Zheng, S.-L., Kolter, R., and Clardy, J. (2011). Structure and biosynthesis of amychelin, an unusual mixed-ligand siderophore from amycolatopsis sp. aa4. *Journal of the American Chemical Society*, **133**(30), 11434—11437.

Shin, J.-H., Oh, S.-Y., Kim, S.-J., and Roe, J.-H. (2007). The zinc-responsive regulator zur controls a zinc uptake system and some ribosomal proteins in streptomyces coelicolor a3(2). *Journal of bacteriology*, **189**(11), 4070–4077.

Shuab, R., Lone, R., Naidu, J., Sharma, V., and Imtiyaz, S. (2014). Benefits of inoculation of arbuscular mycorrhizal fungi on growth and development of onion (allium cepa) plant.

Soltanpour, P. N. and Schwab, A. P. (1977). A new soil test for simultaneous extraction of macro– and micro–nutrients in alkaline soils. *Communications in Soil Science and Plant Analysis*, **8**(3), 195–207.

Spohn, M., Kirchner, N., Kulik, A., Jochim, A., Wolf, F., Muenzer, P., Borst, O., Gross, H., Wohlleben, W., and Stegmann, E. (2014). Overproduction of ristomycin a by activation of a silent gene cluster in amycolatopsis japonicum mg417-cf17. *Antimicrobial agents and chemotherapy*, **58**(10), 6185–6196.

Spohn, M., Wohlleben, W., and Stegmann, E. (2016). Elucidation of the zinc-dependent regulation in amycolatopsis japonicum enabled the identification of the ethylenediamine-disuccinate (s,s-edds) genes. *Environmental microbiology*, **18**(4), 1249–1263.

Stegmann, E. (1999). *Molekulargenetische und biochemische Untersuchungen der EDDS-Produktion in Amycolatopsis japonicum MG417-CF17*. PhD dissertation, Eberhard-Karls-Universität Tübingen.

Stegmann, E., Pelzer, S., Wilken, K., and Wohlleben, W. (2001). Development of three different gene cloning systems for genetic investigation of the new species amycolatopsis japonicum mg417-cf17, the ethylenediaminedisuccinic acid producer. *Journal of biotechnology*, **92**(2), 195–204.

Takahashi, R., Fujimoto, N., Suzuki, M., and Endo, T. (1997). Biodegradabilities of Ethylenediamine-N,N-disuccinic Acid (EDDS) and Other Chelating Agents. *Bioscience, Biotechnology, and Biochemistry*, **61**(11), 1957–1959.

Takahashi-Íñiguez, T., Aburto-Rodríguez, N., Vilchis-González, A. L., and Flores, M. E. (2016). Function, kinetic properties, crystallization, and regulation of microbial malate dehydrogenase. *Journal of Zhejiang University-SCIENCE B*, **17**(4), 247–261.

Tandy, S., Schulin, R., Suter, M. J. F., and Nowack, B. (2005). Determination of s,s'-ethylenediamine disuccinic acid (edds) by high performance liquid chromatography after derivatization with fmoc. *Journal of chromatography. A*, **1077**(1), 37–43.

Tandy, S., Ammann, A., Schulin, R., and Nowack, B. (2006). Biodegradation and speciation of residual ss-ethylenediaminedisuccinic acid (edds) in soil solution left after soil washing. *Environmental pollution (Barking, Essex : 1987)*, **142**(2), 191–199.

Thomas, M. G., Chan, Y. A., and Ozanick, S. G. (2003). Deciphering tuberactinomycin biosynthesis: isolation, sequencing, and annotation of the viomycin biosynthetic gene cluster. *Antimicrobial agents and chemotherapy*, **47**(9), 2823–2830.

Thomas P. Knepper ,Johannes Driemler, Anke Maes, Jutta Müller,Darius Soßdorf (2001). Einträge synthetischer komplexbildner in die gewässer: Umweltforschungsplan des bundesministeriums für umwelt, naturschutz und reaktorsicherheit.

Trehan, S. P. and Sekhon, G. S. (1977). Effect of clay, organic matter and caco3 content on zinc adsorption by soils. *Plant and Soil*, **46**(2), 329–336.

van Kleef, M. A. and Duine, J. A. (1988). L-tyrosine is the precursor of pqq biosynthesis in hyphomicrobium x. *FEBS letters*, **237**(1-2), 91–97.

Vandevivere, P. C., Saveyn, H., Verstraete, W., Feijtel, T. C., and Schowanek, D. R. (2001). Biodegradation of metal-s,s-edds complexes. *Environmental science & technology*, **35**(9), 1765–1770.

Vansuyt, G., Robin, A., Briat, J.-F., Curie, C., and Lemanceau, P. (2007). Iron acquisition from fe-pyoverdine by arabidopsis thaliana. *Molecular plant-microbe interactions : MPMI*, **20**(4), 441–447.

Veesenmeyer, J. L., Hauser, A. R., Lisboa, T., and Rello, J. (2009). Pseudomonas aeruginosa virulence and therapy: evolving translational strategies. *Critical care medicine*, **37**(5), 1777–1786.

Wang, M. and Gould, S. J. (1993). Biosynthesis of capreomycin. 2. incorporation of l-serine, l-alanine, and l-2,3-diaminopropionic acid. *The Journal of Organic Chemistry*, **58**(19), 5176–5180.

Wang, M., Niikura, H., He, H.-Y., Daniel-Ivad, P., and Ryan, K. S. (2020). Biosynthesis of the n-n-bond-containing compound l-alanosine. *Angewandte Chemie (International ed. in English)*, **59**(10), 3881–3885.

Wang, Y., Lu, Y., Lu, J., Yang, Z.-N., and Yang, Z. (2022). Research progress on the biosynthesis and bioproduction of the biodegradable chelating agent (s,s)-edds. *Process Biochemistry*, **116**, 38–48.

Wen, J., Stacey, S. P., McLaughlin, M. J., and Kirby, J. K. (2009). Biodegradation of rhamnolipid, edta and citric acid in cadmium and zinc contaminated soils. *Soil Biology and Biochemistry*, **41**(10), 2214–2221.

Whitburn, J. S., Wilkinson, S. D., and Williams, D. R. (1999). Chemical speciation of ethylenediamine-n,n- disuccinic acid (edds) and its metal complexes in solution. *Chemical Speciation and Bioavailability*, **11**, 85–93.

Willett, A. I. and Rittmann, B. E. (2003). Slow complexation kinetics for ferric iron and edta complexes make edta non-biodegradable. *Biodegradation*, **14**(2), 105–121.

Witschel, M. and Egli, T. (1997). Purification and characterization of a lyase from the edta-degrading bacterial strain dsm 9103 that catalyzes the splitting of s,s-ethylenediaminedisuccinate, a structural isomer of edta. *Biodegradation*, **8**(6), 419–428.

Wu, Q., Deering, R., Zhang, G., Wang, B., Li, X., Sun, J., Chen, J., Zhang, H., Rowley, D., and Wang, H. (2018). Albisporachelin, a new hydroxamate type siderophore from the deep ocean sediment-derived actinomycete amycolatopsis albispora wp1t. *Marine Drugs*, **16**(6), 199.

Xu, Z., Sun, Z., Li, S., Xu, Z., Cao, C., Xu, Z., Feng, X., and Xu, H. (2015). Systematic unravelling of the biosynthesis of poly (l-diaminopropionic acid) in streptomyces albulus pd-1. *Scientific reports*, **5**, 17400.

Zhao, B., Moody, S. C., Hider, R. C., Lei, L., Kelly, S. L., Waterman, M. R., and Lamb, D. C. (2012). Structural analysis of cytochrome p450 105n1 involved in the biosynthesis of the zincophore, coelibactin. *International journal of molecular sciences*, **13**(7), 8500–8513.

Zhao, C., Song, C., Luo, Y., Yu, Z., and Sun, M. (2008). L-2,3-diaminopropionate: one of the building blocks for the biosynthesis of zwittermicin a in bacillus thuringiensis subsp. kurstaki strain ybt-1520. *FEBS letters*, **582**(20), 3125–3131.

Zhuge, B., Fang, H. Y., Yu, H., Rao, Z. M., Shen, W., Song, J., and Zhuge, J. (2008). Bioconversion of lovastatin to a novel statin by amycolatopsis sp. *Applied microbiology and biotechnology*, **79**(2), 209–216.

Zwicker, N., Theobald, U., Zähner, H., and Fiedler, H. (1997). Optimization of fermentation conditions for the production of ethylene-diamine-disuccinic acid by amycolatopsis orientalis. *J Ind Microbiol Biotechnol*, **19**, 280–285.